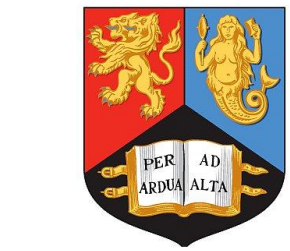

UNIVERSITY OF BIRMINGHAM

Project 1: TOWARDS A PROPHYLACTIC EPSTEIN BARR VIRUS (EBV) VACCINE TO PREVENT EBV-ASSOCIATED MALIGNANCIES AND INFECTIOUS MONONUCLEOSIS

and

Project 2: ANALYSING THE TRANSCRIPTIONAL RESPONSE TO HISTONE DEACETYLASE INHIBITORS TREATMENT IN NORMAL AND CANCER CELL LINES

by

TEJA BAJT

A combined research thesis submitted to the University of Birmingham as part of the requirement for the degree of MASTER OF RESEARCH in Molecular and Cellular Biology.

College of Life and Environmental Sciences
School of Biosciences
University of Birmingham
September 2013

Summary

The combined thesis submitted for award of the Master of Research in Molecular and Cellular Biology consists of two projects.

The first project with the title “towards a prophylactic Epstein Barr Virus (EBV) vaccine to prevent EBV-associated malignancies and infectious mononucleosis” aim was to investigate T cell responses in healthy EBV-seropositive donors to two EBV structural proteins MCP, encoded by BcLF1, and LTP, encoded by BPLF1. The results of first project showed that EBV proteins MCP and LTP are a good vaccine candidates.

The second project with the title “analysing the transcriptional response to histone deacetylase inhibitors treatment in normal and cancer cell lines” aim was to analyse the transcriptional response to histone deacetylase inhibitor valproic acid (VPA) treatment in normal and cancer cell lines. The results of second project showed that VPA is not as toxic to normal cells as other chemotherapeutic agents and is a promising candidate for advanced epigenetic chemotherapy.

UNIVERSITY OF BIRMINGHAM

PROJECT 1: TOWARDS A PROPHYLACTIC EPSTEIN BARR VIRUS (EBV) VACCINE TO PREVENT EBV-ASSOCIATED MALIGNANCIES AND INFECTIOUS MONONUCLEOSIS

BY

TEJA BAJT

This project is submitted in partial fulfilment of the requirements for the award of the MRes in Molecular and Cellular Biology.

Supervisor: Dr James E Turner

School of Cancer Sciences
University of Birmingham
March 2013

Abstract

Epstein Barr virus (EBV) is one of the eight human herpesviruses that infects >90% of the population. Most people are infected as infants without any symptoms however, when people get EBV later in life, 70% of people develop infectious mononucleosis (IM). EBV is also associated with several malignancies and in 2008 there were approximately 200,000 new cases of EBV-associated cancers worldwide.

The first generation of EBV vaccines targeted the glycoprotein gp350. While the vaccines bolstered immunity, preventing the IM symptoms, people still became EBV-seropositive. A second generation of vaccines will now target EBV structural proteins. As the MCP, encoded by BcLF1, and LTP, encoded by BPLF1, are large and abundant structural proteins expressed very early on in infection, they are potential vaccine candidates.

The combined results from three prediction algorithms were used to identify peptide sequences from MCP and LTP containing an HLA-A*02 or HLA-B*07 T cell epitope and IFN-y responses from nine EBV-seropositive donors were examined.

Ex-vivo IFN-y responses were small whereas, *in-vitro* responses expanded. Responses were seen from either the CD4+ or CD8+ T cell pool dependent on peptide pool and donor. HLA-C*06 restricted CD8+ T cell clones were established from one representative donor. CD4+ T cell clones from one representative donors have shown recognition of lytic LCLs being of great importance in controlling the EBV infection. The EBV structural proteins MCP and LTP are frequent targets of T cells in healthy individuals and may be important targets for future EBV vaccines.

Acknowledgements

I would firstly like to thank my primary supervisor Dr James E Turner and secondary supervisor Dr Graham S Taylor for giving me the opportunity to work with them and for their guidance, support and advices. I would also like to thank Dr James E Turner for all his support in the thesis writing. All their help and advices have been highly valued all through the project.

I would also like to thank Laura Quinn, Luke Williams, Alison Leese, Gordon Ryan and Jill Brooks who also provided much help in the lab. A big thank you also to everyone else from the T cell group. Thank you for welcoming me into your group.

Last but not least, I would like to thank my family and Danijel for their unconditional support. Without them being always there for me I would not achieve this.

Abbreviations

BCA	Bicinchoninic acid
BSA	Bovine Serum Albumin
CD	Cluster of differentiation
dH_20	Distilled water
EBV	Epstein-Barr virus
EDTA	Ethylene-diamine-tetra-acetic acid
ELISA	Enzyme-linked immunosorbent assay
ELISPOT	Enzyme-linked immunosorbent spot
EtBr	Ethidium bromide
FCS	Fetal Calf Serum
IL-2	Interleukin-2
IL-7	Interleukin-7
IFN-y	Interferon-y
LB	Luria-Bertain media
LSM	Lymphocyte Separation Media
MACS	Magnetic-Activated Cell Separation buffer
MLA	Monkey Leukocyte Antigen
PBMCs	Peripheral Blood Mononuclear Cells
PBS	Phosphate-Buffered Saline
PCR	Polymerase Chain Reaction
RPMI	Roswell Park Memorial Institute media
TAE	Tris-acetate-EDTA buffer

List of Contents

List of Figures and Tables

1. Introduction

1.1. Overview

Throughout evolution, viruses have acquired various characteristics to infect and survive within their hosts. To protect against infection, or to counteract disease following virus acquisition, host immunity developed. The human immune system consists of relatively simple defences, such as the skin, and stomach acid, and more complex defences, including specialised cells that destroy pathogens. Despite these defences, humans and other animals can become infected with viruses. Some viruses are able to evade immune-surveillance and persist asymptomatically after primary infection in a state of dormancy, also known as latency. This is a common characteristic of one family of viruses, the human herpesviruses. Herpesviruses cause a wide range of diseases including certain malignancies. The two herpesviruses most strongly associated with cancer, referred to as tumour-associated viruses or oncoviruses, are Epstein-Barr virus (EBV) and Kaposi's sarcoma-associated herpesvirus (KSHV) (Butt and Miggin, 2012, Schiller and Lowy, 2010). In 2008, there were 12.7 million of new cases of cancer worldwide (Jemal et al., 2011) and it is estimated that approximately 2 million of these cases were caused by infection. Indeed, 10% of all cancers are associated by EBV infection alone (de Martel et al., 2012, Cohen et al., 2011). Preventing infection with oncoviruses is therefore of great importance, and following the success of successful vaccines targeting tumour viruses in the past (e.g., Hepatitis B Virus and Human Papilloma Virus) there is significant interest in developing a prophylactic EBV-vaccine. This project examined whether EBV structural proteins, that are potentially good vaccine targets due to their size and abundance on EBV-infected cells, elicit frequent immune responses in healthy individuals. The results of this project provide new insight into potential EBV-vaccine candidates.

1.2. Immune system

1.2.1. Innate immunity

The human body is protected against pathogens by several mechanisms. First, the skin acts as a physical barrier and deters microbes in several ways, such as having an acidic pH (pH 5.5), having a high salt content, regularly shedding cells, and harbouring antimicrobial peptides (Percival et al., 2012). Epithelial surfaces in the gut and lungs also have protective functions. The gastric acid (hydrochloric acid; HCl) in the stomach is of very low pH (approximately 1.7 up to 5.0 during digestion) and inactivates or kills pathogens directly (Birk et al., 2012). These mechanical/chemical barriers aim to prevent pathogens from entering the body, however, if this first line of protection fails, then other secondary mechanisms exist.

Pathogens can be recognised by cells of innate immune system that protect the human body in the first few days of infection. These cells include phagocytic tissue residing cells such as macrophages and dendritic cells, and mobile cells such as neutrophils, eosinophils and monocytes. Invading pathogens are recognised by pattern-recognition receptors (PRRs) on phagocytes (e.g., macrophages). For example, toll-like receptors (TLRs) are capable of detecting bacteria and viruses in extracellular spaces as well as in the intracellular compartments of the cell. Once the pathogen has been recognised by tissue residing macrophages, these cells secrete chemokines. As a result, neutrophils migrate to the site of infection and secret cytokines, such as interleukin-1 (IL-1), interleukin-12 (IL-12), interleukin-6 (IL-6), interferon-α (IFN-α), interferon-β (IFN-β), tumour necrosis factor-α (TNF-α) etc. Cytokines are soluble signalling molecules that attract inflammatory cells of both the innate and adaptive immune system (Zepp, 2010, Moser and Leo, 2010, Alberts et al., 2007, Janeway et al., 1999). Some pathogens (e.g., bacteria) can be cleared by the innate immune system, however in the case of virus infection, it is necessary to employ the adaptive arm of the immune system.

1.2.2. Adaptive immunity

There are several distinct properties that are characteristic of the adaptive immune system especially when referring to the T cells. First, cells of the adaptive immune system can recognise antigens as "self-antigens" or "non-self antigens". Non-self antigens represent peptides derived from invading pathogens, or other foreign material. Immune cells with autoreactive receptors recognising "self-antigens" are eliminated by negative selection in the thymus. Second, the adaptive immune system is able to detect intracellular pathogens, such as viruses. The cells of the adaptive immune system survey molecules expressed on the surface of body cells, and will recognise any foreign antigen that is presented. Third, after infection has been resolved, the adaptive immune system establishes a state of "immunological memory". Thus, if re-infection occurs with the same pathogen, a much faster and more vigorous immune response takes place in an attempt to eliminate re-infection (Moser and Leo, 2010, Zepp, 2010).

The effector cells of the adaptive immune system are specialised haematopoietic cells (lymphocytes) of which there are several sub-types. Lymphocytes are derived from lymphoid progenitor cells and differentiate into B lymphocytes (B cells), T lymphocytes (T cells) and natural killer cells (NK). Upon activation naïve B cells differentiate into plasma cells which secrete antibodies (molecules that can kill or identify pathogens) and memory B cells which ensure a rapid immune response upon a second exposure to the same pathogen. Naïve T cells upon activation differentiate into cytotoxic T cells that destroy infected cells, and helper T cells that stimulate other cells such as B cells, macrophages etc. There are two subsets of T cells distinguished by their cell surface molecules (i.e. cluster of differentiation; CD). Cytotoxic T cells express CD8 and helper T cells express CD4 surface molecules (Moser and Leo, 2010, Janeway et al., 1999, Wang et al., 2013a).

The adaptive immune system is composed of primary (e.g., thymus and bone marrow) and secondary (e.g., lymph nodes and spleen) lymphoid organs. In bone marrow B cells

and T cells are generated but only B cells mature in bone marrow whereas, T cells migrate and mature in thymus. Mature B and T cells migrate through blood stream into secondary lymphoid organs (Moser and Leo, 2010).

Viruses replicate inside cells, and use host cellular machinery to produce virus-derived proteins. Infected cells express (and sometimes release) these proteins or peptides (referred to as antigens) that can be recognised by lymphocytes. B cells have B cell antigen receptor (BCR) that is capable of recognising soluble antigen. When activated, B cells secrete antibodies, also referred to as immunoglobulins, which bind to antigen in blood or lymph and facilitate its destruction by phagocytes in a process known as opsonisation. Antibodies bound to cell surface antigens can activate a series of proteins found in blood (the complement system; part of innate immunity) inducing cell lysis and destruction of the target. Antibody binding can also sometimes directly neutralize pathogen, preventing further infection (Moser and Leo, 2010). There are several classes of antibodies, also referred to as immunoglobulins. IgM antibodies are secreted during primary responses and IgG are secreted later on in infection. Other immunoglobulin sub-classes exist, including IgA that is found in secretions on muscosal membranes, IgE that is associated with allergic responses and IgD which is co-expressed with IgM on surface of mature B cells and is suggested to be a transmembrane antigen receptor (Chen and Cerutti, 2011, Moser and Leo, 2010). As explained later, the goal of vaccination is often to increase the number of neutralising antibodies preventing viruses to infect the cell.

T cells are able to identify virus-derived peptides expressed on infected cells, or peptides characteristic of changes within self cells, such as malignant transformation. T cells have a T cell receptor (TCR) that is unable to recognise soluble antigen. Pathogen derived proteins in infected cells are degraded into small peptides and presented on a cell surface by transmembrane presenting molecules known as human leukocyte antigen (HLA), or major histocompatibility complexes (MHC) (Moser and Leo, 2010, Patronov and Doytchinova, 2013). In the cytosol, proteins are degraded into small, 9 – 11 amino acid long peptides, and presented on the cell surface to CD8+ T cells by MHC

class I molecules in an MHC class I/peptide complex. Professional antigen presenting cells (i.e., dendritic cells; DCs) present longer peptides usually 15 – 24 amino acids long (Zavala-Ruiz et al., 2004) by MHC class II molecules in MHC class II/peptide complexes recognised by CD4+ T cells. Upon recognition of antigenic peptides, CD8+ T cells become activated and can directly kill target cells through several mechanisms. Upon binding with a target cell, T cells secrete perforin, a pore-forming protein that punches holes in the membranes of the infected cells. The T cell then releases proteases (e.g., granzyme-A) that can enter the cell though the pores, and by degradation of intracellular proteins, trigger apoptosis causing rapid death of an infected cell (Moser and Leo, 2010, Flesch et al., 2012). CD8+ T cells are also able to induce cell death through other pathways, including interaction between the Fas-ligand on T cells with the Fas-receptor on target cells (Moser and Leo, 2010, Patronov and Doytchinova, 2013, van Lier et al., 2003). Harnessing both the innate and adaptive immune system to fight against disease causing pathogens through vaccination is therefore of a great importance.

1.3. Vaccination against viruses

In the past century vaccination has saved millions of lives by reducing the incidence of many infectious diseases including diphtheria, mumps, and measles (Zepp, 2010, Rappuoli et al., 2011). Due to advances in scientific understanding, vaccination is not only used to prevent infectious disease, but is also used to provide therapy for other diseases such as cancer (Rappuoli et al., 2011, Zepp, 2010).

All vaccines present an antigen to the immune system and initiate an immune response. Prophylactic or preventative vaccines are administered prior to pathogen exposure and aim to prevent infection and therefore disease. Some vaccines can be administered after exposure to the pathogen. These so-called post-exposure-prophylactic vaccines aim to counteract the infection before it takes hold, and therefore limit disease (Patronov and Doytchinova, 2013, Wu et al., 2010). Therapeutic vaccines are used for the treatment of malignancies by boosting immune responses

and the aim is to destroy tumour cells expressing tumour-associated antigens (TAA) (Dougan and Dranoff, 2012, Wang et al., 2013b).

There are several vaccine formulations. Inactivated vaccines contain virus particles that have been altered by high temperature or chemicals, and thus the virus loses the ability to replicate. The vaccine however can still provoke large immune responses. Live attenuated vaccines contain virus particles with low levels of virulence. These viruses are selected by passaging the virus in multiple rounds of cell culture, or growing it in cells from a different species, so that the ability of the virus to infect human cells is reduced. The virus is however able to replicate, and therefore provides a source of antigen until it is eventually eliminated by the immune system. Subunit vaccines provoke immune responses without introducing infectious virus. One example of a subunit vaccine is the hepatitis B vaccine that contains the surface antigen HBsAg that is normally expressed by infected cells (Shouval, 2003, Schiller and Lowy, 2010). Virus-like particles (VLP) vaccines contain viral proteins without viral nucleic acid, thus are non-pathogenic as the virus cannot replicate. The most recent advance in vaccinology exploits DNA vaccines containing genetically engineered virus DNA that is incorporated into body cells. Thus, virus proteins are produced by the cell and expressed on the cell surface. A gene encoding a previously identified immunodominant B cell and/or T cell antigen is usually chosen as antigen (Patronov and Doytchinova, 2013). For example, the DNA vaccine described by Hui et al., 2013 consisted of Modified Vaccinia Ankara Virus vector with an insert of EBV viral genes encoding two EBV proteins known to be expressed by EBV-associated tumour cells.

Vaccinations are often administered intradermally, intramuscularly or subcutaneously (Combadiere and Liard, 2011). Other delivery methods are used (e.g., oral vaccination with polio) and other vaccine routes are currently being developed, including intranasal vaccination (Rose et al., 2012), aerosol vaccination (Giudice and Campbell, 2006), transcutaneous or transdermal vaccination (Giudice and Campbell, 2006, Combadiere and Liard, 2011), rectal and vaginal vaccination (Neutra and Kozlowski, 2006, Yu and Vajdy, 2010).

1.4. Herpesviruses

Herpesviruses are enveloped viruses containing a double-stranded DNA genome (Wu et al., 2010, Meyding-Lamadé and Strank, 2012, Gilden et al., 2007). The family *Herpesviridae* consists of three subfamilies *Alphaherpesvirinae, Betaherpesvirinae* and *Gammaherpesvirinae.* Eight herpes viruses have been formally classified: herpes simplex virus type 1 (HSV-1), herpes simplex virus type 2 (HSV-2), varicella zoster virus (VZV or HSV-3), Epstein-Barr virus (EBV or HHV-4), cytomegalovirus (CMV or HHV-5), human herpesvirus type 6 (HHV-6), human herpesvirus type 7 (HHV-7) and Kaposi's Sarcoma-associated herpesvirus (KSHV or HHV-8) (Table 1) (Davison, 2011, Adams and Carstens, 2012, Taylor and Blackbourn, 2011, Meyding-Lamadé and Strank, 2012, Gilden et al., 2007). Recently, it has been suggested that HHV-6 should be split into two distinct viruses – type 6A and type 6B (Davison, 2011) (see table 1).

Herpesviruses typically exhibit very few hallmarks of infection. Primary infection usually occurs in childhood and often passes with no symptoms (Gilden et al., 2007). Herpes viruses have two distinct life cycles or phases. In the lytic phase, the virus is actively replicating causing lysis of infected cells and infecting other cells or organisms. In the case of saliva transmitted herpesviruses (e.g. EBV) infectious virus particles are released into saliva enabling infection of another naïve host upon close contact. When the infection is brought under control, the virus shifts into a latent phase, characterised by few or no symptoms of disease. During this latent phase, the virus successfully evades the immune system using a variety of strategies (Wu et al., 2010).

There are several different mechanisms by which herpesviruses evade immune recognition such as restriction of gene expression, down regulating MHC class I expression and production of cytokines (e.g. interleukin-10 – an anti-inflammatory cytokine) (Banks and Rouse, 1992). Herpesviruses have the ability to re-activate after latency and realise viral particles causing lysis of infected cells and infection of non-infected cells. This phase is called lytic replication (Wu et al., 2010, Meyding-Lamadé and Strank, 2012, Gilden et al., 2007, Davison, 2011). The two phases - latency and lytic

replication are continuous processes, and herpesviruses therefore can infect their hosts persistently for life (Wu et al., 2010).

Although herpesviruses exist within hosts for a lifetime, the infection is usually asymptomatic and the majority of infected people will never develop a virus-associated disease. However, some herpes viruses can cause life-threatening diseases in immune-compromised individuals such as HIV-positive individuals, transplant patients on immunosuppressive therapy and individuals with x-linked lymphoproliferative disease (Wu et al., 2010, Hislop et al., 2007, Kutok and Wang, 2006). However, some healthy individuals can develop herpes viruses associated malignancies as two herpesviruses (EBV and KSHV) are already classified as agents carcinogenic to humans (Taylor and Blackbourn, 2011).

Table 1: Human Herpesviruses (HHV) characteristics

Type	*Full name*	*Site of Latency*	*Means of Spread*	*Disease after primary infection*	*Associated diseases*
HHV-1	Herpes simplex virus-1 (HSV-1)	Sensory nerve ganglia	Close contact (sexually transmitted disease)	Painful skin or mucosal lesions	Oral lesions (cold sores)
HHV-2	Herpes simplex virus-2 (HSV-2)	Sensory nerve ganglia	Close contact (sexually transmitted disease)	Genital lesions	Genital lesions
HHV-3	Varicella zoster virus (VZV)	Sensory nerve ganglia (cranial nerve)	Respiratory and close contact	Varicella (chickenpox)	Herpes zoster (shingles)
HHV-4	Epstein-Barr virus (EBV)	B cells, endothelial and epithelial cells	Close contact (saliva), transfusions, tissue transplant, and congenital	Infectious mononucleosis	Several malignancies
HHV-5	Cytomegalovirus (CMV)	Bone marrow progenitor cells and myeloid cells	Saliva	Infectious mononucleosis like symptomes	CMV disease, CMV retinitis, CMV - gastroenteritis
HHV-6	Roseolovirus, Herpes lymphotropic virus	Monocytes and macrophages	Close contact, saliva	Roseola (sixth disease)	Unknown
HHV-7	Human herpesvirus-7	Monocytes, lymphocytes and salivary glands	Close contact, saliva	Roseola (sixth disease), Exanthema subitum	Unknown
HHV-8	Kaposi's sarcoma-associated herpesvirus (KSHV)	B cells	Close contact, saliva	Unknown	Kaposi's sarcoma, Castleman's disease, primary effusion lymphomas

Information summarised from (Davison, 2011, Gilden et al., 2007, Hislop et al., 2007, Schiffer and Corey, 2013, Taylor and Blackbourn, 2011, Viner et al., 2012, Wu et al., 2010).

1.5. Epstein-Barr virus (EBV)

EBV is a herpesvirus of the gamma subfamily and is also known as human herpes virus-4 (HHV-4) (Kutok and Wang, 2006, Wu et al., 2010). There are two major types of EBV, type A or EBV-1 with highest prevalence in the West and type B or EBV-2 with highest prevalence in Africa. Although other data suggests that both types coexist equally in the same human population (Straus et al., 1993) and individuals can be infected with multiple strains and/or types. However, it is not established whether reinfection with multiple strains occurs over time or if individuals acquire multiple strains at primary infection (Sitki-Green et al., 2003, Tierney et al., 2006). EBV is transmitted by saliva and has a high infectious rate as over 90% of human population is infected. Infection usually occurs in early childhood and passes asymptomatically. If primary infection occurs later in life individuals can develop infectious mononucleosis (IM) with symptoms such as sore throat, fatigue, fever, pharyngitis etc. (Cohen et al., 2011, Cohen, 2000, Kutok and Wang, 2006, Straus et al., 1993, Luzuriaga and Sullivan, 2010). The EBV genome is linear double-stranded DNA with approximately 184,000 base pairs (Straus et al., 1993, Kutok and Wang, 2006, Luzuriaga and Sullivan, 2010) encoding approximately 100 viral proteins (Straus et al., 1993, Cohen, 2000). The EBV genome is enveloped within capsid and viral tegument alongside viral envelope (see figure 2) (Kutok and Wang, 2006, Cohen, 2000). Capsid and viral tegument contain many proteins such as glycoprotein 350 (gp350) which is the target of neutralising antibodies. EBV is associated with several conditions.

1.5.1. Infectious mononucleosis (IM)

Symptoms of IM often occur after an incubation period of 30 to 50 days after the first exposure to EBV (Luzuriaga and Sullivan, 2010). IM is a sign of primary EBV infection (Luzuriaga and Sullivan, 2010) and usually affects adolescents or young adults in their first three decades of life (Cohen, 2000, Luzuriaga and Sullivan, 2010). Diagnosis is based on triade of clinical symptoms such as fever, pharyngitiy and adenopathy.

Laboratory findings usually show atypical lymphocytes (Luzuriaga and Sullivan, 2010, Straus et al., 1993, Kutok and Wang, 2006, Cohen, 2000). Symptoms can persist for few weeks however fatigue can persist for 6 months or even longer. The majority of patients entirely recuperate after 2-3 months (Luzuriaga and Sullivan, 2010). After symptoms have resolved lytic infection proteins can be found in blood even a year after IM and proteins associated with latent infection persist for life time with recurrent shifts to lytic infection without clinical symptoms (Luzuriaga and Sullivan, 2010).

1.5.2. EBV-associated diseases

EBV is associated with several other diseases besides infectious mononucleosis. EBV was the first virus linked to human cancer. The link between EBV and human cancer was discovered with identification of EBV virion in cells of Burkitt lymphoma (Michelow et al., 2012). The diseases associated with EBV are Hodgkin lymphomas, non-Hodgkin lymphomas, posttransplant lymphoproliferative disorder (PTLD), pyothorax-associated lymphomas, nasopraryngeal carcinomas, smooth muscle tumours, follicular dendritic cell tumours, Burkitt lymphomas, and gastric carcinomas (Michelow et al., 2012, Straus et al., 1993, Long et al., 2011, Taylor and Blackbourn, 2011, Kutok and Wang, 2006). In 2008 there was approximately 200,000 new cases (10%) of EBV associated malignancies worldwide of which there was approximately, 13,200 new cases of Hodgkin lymphomas, 6,300 new cases of Burkitt lymphomas in Africa and approximately 60,000 new cases of nasopharyngeal carcinomas attributed to EBV (de Martel et al., 2012). Gastric carcinoma is most common EBV-associated malignancy as there are 1 million new cases per year worldwide and estimated 90,000 cases are EBV-associated (Cohen et al., 2011). EBV infection has also been associated with autoimmune diseases such as systemic lupus erythematosus, rheumatoid arthritis and multiple sclerosis (Lossius et al., 2012, Draborg et al., 2012, Tselis, 2012, Croia et al., 2012).

1.6. Mechanisms of EBV infection and virus protein expression

The internalization of EBV viral capsid or nucleoprotein core into the host cell is the most important step in viral infection (Shaw et al., 2010). Upon transmission to a naïve host, the virus replicates in cells of oropharynx (probably epithelial cells) (Hislop et al., 2007). After infection of a cell (usually by a single virion), EBV DNA changes from being linear to circular episomal DNA (Kutok and Wang, 2006) although, such circularisation is specific to memory B cells, and therefore does not happen in normal infection of epithelial cells. Infection of B cells is activated by attachment of glycoprotein 350/220 (gp350/220) to B cell surface molecule CD21. After attachment, the virus is internalised and engulfed in cytoplasmic vesicle. The glycoprotein 42 (gp42) binds to the HLA class II receptor. (Shaw et al., 2010, Kutok and Wang, 2006). Another route of infection can occur by attachment of gp350/220 to B cell surface molecule CD35 also causing persistent infection as in infection through CD21 (Ogembo et al., 2013). The EBV genes BZLF1 and BRLF1 trigger the shift from latent to lytic cycle enabling virus shedding and lifelong persisting infection in the host (Kutok and Wang, 2006, Hislop et al., 2007). After primary infection, lytic cycle proteins are expressed and can be divided into three groups: immediate early (IE) proteins, early (E) proteins and late (L) proteins. After lytic cycle latency occurs and latent peptides are expressed (see figure 1) (Hislop et al., 2007).

As already described in section 1.5 EBV consists of envelope, tegument, capsid and viral DNA. The EBV genes probably encode six capsid proteins (Henson et al., 2009), five envelope proteins and ten tegument proteins. Among the envelope glycoproteins such as gp42, gB, gL, gH, is the glycoprotein gp350 the most dominant and the largest EBV envelope glycoprotein with 350 kDa (Johannsen et al., 2004). Therefore gp350 has received attention as a target for vaccination (Cohen et al., 2013).

The research presented in this thesis is focused on two EBV proteins that are already present on the incoming virion. The major capsid protein (MCP), encoded by the gene BcLF1, (Henson et al., 2009) and the large tegument protein (LTP), encoded by the

gene BPLF1 (Schmaus et al., 2004, Whitehurst et al., 2012) (see figure 2). The EBV capsid proteins are encoded by six genes, one being BcLF1, which by mass, is the largest of all six capsid proteins (155 kDa) (Henson et al., 2009, Johannsen et al., 2004). In the normal lytic cycle, the BcLF1 gene is expressed in the late phase (Adhikary et al., 2007). Data from Prang et al., 1997 shows that the BcLF1 gene can be detected at primary infection when IM symptoms occur but cannot be detected in healthy EBV-seropositive people, who are likely to be in a state of latency. Thus, BcLF1 is an attractive vaccine candidate due its existence on the incoming virion, as well as relatively early expression in the lytic cycle. The second protein examined in this thesis is the LTP encoded by BPLF1. This is one of the ten tegument proteins, and is by mass, the largest of all EBV tegument proteins at 350 kDa (Johannsen et al., 2004). BPLF1 is also expressed in the late phase of the lytic cycle, but is also present on the incoming virion, making it another potentially attractive vaccine target (Schmaus et al., 2004, Whitehurst et al., 2012). BPLF1 specific antibodies can be detected at primary infection with EBV, in people with EBV reactivation, in EBV-positive tumours and in more than half of EBV-seropositive healthy people (Schmaus et al., 2004). It has also been suggested that inhibition of the BPLF1 can cause inhibit EBV replication (Gastaldello et al., 2010).

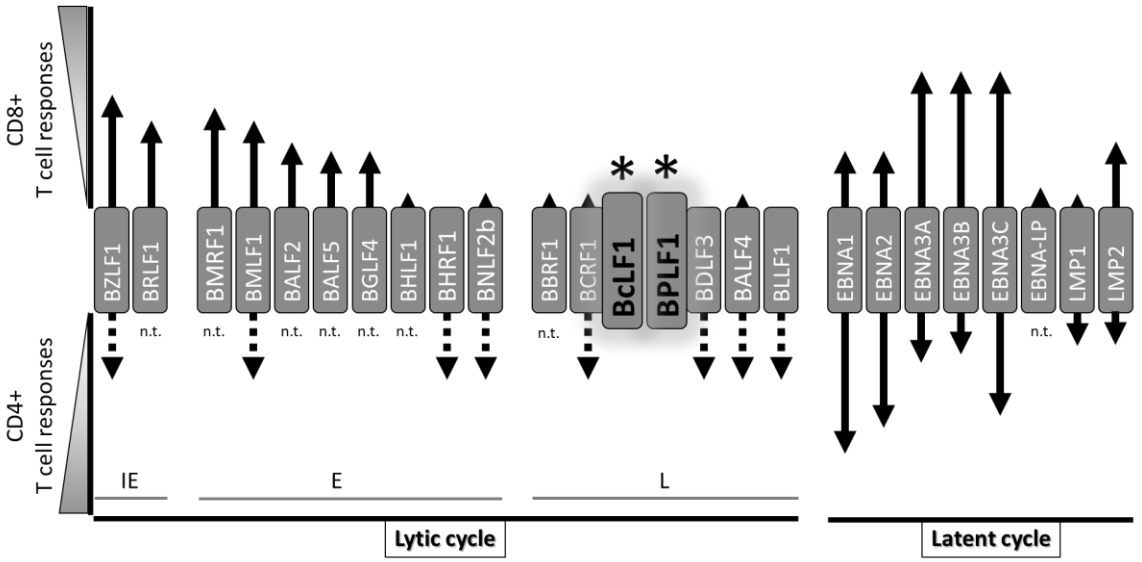

Figure 1: Diagram of EBV proteins in EBV-seropositive healthy people. Proteins are presented as immediate early (IE) proteins, early (E) proteins and late (L) proteins of the lytic cycle and the proteins of latent cycle with relative immunodominance for CD8+ and CD4+ T cell responses. Dotted arrows denote CD4+ T cell responses where their relative immunodominance is not yet determined. Proteins denoted as n.t. were not tested. The two asterisks (*) denote two genes (BcLF1 and BPLF1) encoding proteins to which responses were investigated in this project. Figure adapted from (Hislop et al., 2007).

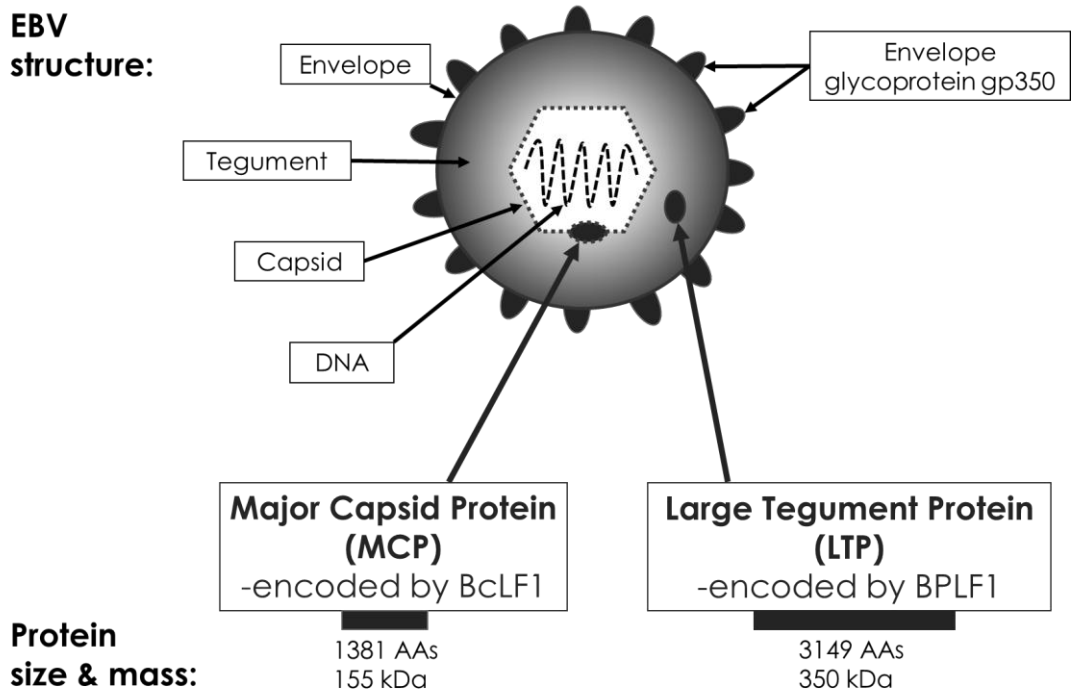

Figure 2: The EBV structure. EBV consists of an envelope, with the most dominant glycoprotein gp350, a tegument, a capsid and DNA. The major capsid protein (MCP), encoded by BcLF1, and large tegument protein (LTP), encoded by BPLF1, are denoted with protein size and mass. Figure adapted from (Draborg et al., 2012).

1.7. EBV vaccines and immunotherapies

The majority of human population is infected with EBV but most people never develop EBV-associated diseases. However, there are also certain risk groups of people who can develop EBV-associated diseases, such as transplant recipients, HIV positive individuals, and individuals living in parts of the world with high incidence of Burkitt lymphoma and nasopharyngeal carcinoma (Cohen, 2000, Wu et al., 2010, Cohen et al., 2013). Two forms of EBV vaccines are being developed. Prophylactic vaccines aim to prevent EBV infection, and might prevent IM and reduce the incidence of cancers associated with EBV (Long et al., 2011, Schiller and Lowy, 2010, Münz and Moormann, 2008). Therapeutic EBV vaccines aim to enhance natural immunity and reduce the risk of EBV-associated malignancies. These vaccines would be administrated after primary EBV infection (Wu et al., 2010, Cohen et al., 2011). Therapeutic EBV vaccines can also be used as immunotherapies for treatment of EBV-associated malignancies as clinical trial data has shown a resolution of lesions in nasopharyngeal carcinoma (NPC) and Hodgkin lymphoma patients (HL) in patients administered with an EBV vaccine (Cohen et al., 2011). In NPC patients, a phase II clinical trial was conducted to assess the infusion of EBV-specific cytotoxic T lymphocytes (EBV-CTL) targeting the latent membrane protein 2 (LMP2) because LPM2 is a protein expressed on majority of NPC tumours. The results showed a two-fold expansion of LMP2 specific T cells two weeks after infusion returning to normal levels six weeks later. Expansion and responses were measured with enzyme-linked immunosorbent spot (ELISPOT) assay (Louis et al., 2010).

1.8. Human EBV vaccine trials

Several EBV vaccine trials have been conducted. The majority of vaccines tested focused on stimulating neutralising antibodies to glycoprotein 350 (gp 350) – a protein important for B cell infection with EBV. In one phase II clinical trial, 181 EBV-seronegative young adults aged 16 to 25 years were given a recombinant gp350

vaccine. The responses to vaccine were assessed by measuring anti-gp350 antibodies by gp350 enzyme-linked immunosorbent assay (ELISA). The vaccine was protective against IM in 78% of people but did prevent EBV infection. Interestingly, 8/9 individuals in the non-vaccinated control group developed IM on primary infection (Sokal et al., 2007).

Another trial which was the first vaccine trial in humans using recombinant vaccinia virus also exploiting gp350 was conducted on nine EBV-seronegative infants who were immunized with vaccinia virus expressing gp350/220. The vaccine protected infants from infection for the duration of the study (16 months) as 6/9 vaccinated infants remained EBV-seronegative, compared to 10/10 in the non-vaccinated control group (Gu et al., 1995). After the completion of the trial EBV-seronegative infants were not followed up, thus the, long term effectiveness of the vaccine is not known. However, the results of this trial suggest that live viral vectors can offer better protection against EBV, compared to sub-unit vaccines, potentially because both humoral and cellular immunity are targeted (Cohen et al., 2011).

A recent phase I trial of a therapeutic vaccine examined MVA expressing tumour antigens EBNA1 and LMP2 that are expressed on most NPC tumours. The trial was conducted on patients in NPC remission to determine the safe and immunogenic dose. The data showed a clear increase in IFN-y production by EBV specific T cells measured by ELISPOT assay in comparison to control antigens not included in the vaccine (EBNA3A and an influenza antigen) showing no increase in response after vaccination. The trial showed that this particular vaccine is safe and immunogenic and further trials should be conducted understand the clinical effects (Hui et al., 2013).

A phase I trial using single synthetic HLA-B*0801 restricted CD8+ T cell epitope was conducted on fourteen EBV-seronegative individuals from age of 18 to 50. The results showed that the vaccine was well tolerated and expanded the numbers of EBV-specific T cells within two weeks of vaccination. These EBV-specific T cells produced IFN-y in response to peptide and destroyed targets. Five out of ten vaccinated volunteers

became EBV-seropositive, and two out of four volunteers in control group became EBV-seropositive. Thus, while the efficacy of a single epitope T cell vaccine remain unclear, this data shows that a strong T cell response can be elicited by vaccination (Elliott et al., 2008).

1.9. The ideal EBV vaccine

The ideal EBV vaccine would prevent primary EBV infection and therefore prevent the development of EBV-associated malignancies. Potential vaccine targets are large proteins that are abundantly expressed very early on in primary infection allowing the immune system to recognise infection and respond by destroying the newly infected cells. Potential vaccines might combine novel targets with glycoprotein gp350, considering this is the target of neutralising antibodies. Despite the efficacy of live and live attenuated vaccines this is probably not an option for vaccinating against EBV, considering that EBV is an oncovirus that establish lifelong latent infection, and might increase the risk of cancer.

1.10. Summary, overview and aims of this thesis.

Part one of this thesis is split into two sections, cell biology and molecular biology. The aim of cell biology part of the project was to examine T cell responses to two EBV structural proteins MCP (BcLF1) and LTP (BPLF1) which have not been extensively investigated before in EBV-seropositive healthy individuals

The data obtained and presented in this thesis shows that individuals exhibit frequent responses, derived from both the CD8+ and CD4+ T cell pool, to EBV structural proteins. The major aims of this thesis were to:

1. Examine whether healthy individuals exhibit T cell responses to the EBV structural proteins BcLF1 (MCP) and BPLF1 (LTP).
2. Examine whether these responses can be expanded *in vitro*.

3. Examine whether these responses were from the CD4+ or CD8+ T cell pool.
4. Establish T cell clones specific for the MCP and LT from a representative donor
5. To determine the HLA-type of these clones
6. To begin experiments to show that the MCP and LTP might be good vaccine candidates

The aim of molecular biology part of the project was to produce a tool to so that T cell responses to whole protein antigens encoded by BcLF1 and BPLF1 genes could be established in individuals, avoiding complications over HLA-type. The BcLF1 gene had already been inserted into an appropriate vector before this project started. Therefore, to achieve our aim the BPLF1 had to be inserted into a vector. In order to examine the CD4+ T cell responses invariant chain had to be inserted into the vector.

Therefore, the aims were:

1. To amplify BPLF1 protein gene by PCR.
2. To insert invariant chain into pENTR1A vector.
3. To insert BPLF1 gene into pENTR1A vector.

2. Materials and Methods

2.1. Reagents

Reagent in text	Formulation
10% RPMI	RPMI (Sigma Life sciences, USA), 10% main batch FCS (PAA laboratories GmbH, Austria), 1% streptomycin and penicillin (Invitrogen)
10% B cell RPMI	RPMI, 10% main batch B cell FCS (Biosera, South America Origin), 1% streptomycin and penicillin
1% RPMI HUS	RPMI, 1% Human Serum (TCS Biosciences Ltd, UK), 1% streptomycin and penicillin
50x TAE buffer	For 500 ml: 121 g Tris base in 250 ml dH_2O, 28,6 ml acetic acid, 50 ml 0,5 M EDTA pH 8,0 and dH_2O to 500 ml
1x TAE buffer	50x TAE, 1960 ml dH_2O and 40 µl EtBr (10 mg/ml)
IL-7 media	RPMI, 10% B cell FCS, 1% streptomycin and penicillin, 5 µl IL-7 (Peprotech)
IL-2 media	RPMI, 10% B cell FCS), 1% streptomycin and penicillin, IL-2 50 IU/ml (Peprotech)
Lymphocyte separation medium	PAA laboratories GmbH, Austria
MACS buffer	Distilled water, PBS (Oxoid Ltd, UK), BSA, EDTA
Freezing mix	70% RPMI, 20% main batch FCS, 10% DMSO

Other reagents	Source
IFN-γ ELISPOT	Mabtech, Sweden
Anti-CD4 beads	Invitrogen Dynal AS, Norway
DNA Molecular Weight Marker X	Roche applied science
Expand Long Template PCR System	Roche applied science
Phusion High-Fidelity PCR Kit	New England BioLabs, UK
QIAprep spin miniprep Kit	QIAGEN, Sussex, UK
QIAquick Gel Extraction Kit	QIAGEN, Sussex, UK

2.2. Methods

2.3. Cell Biology Techniques

2.3.1. T cell epitope prediction

Amino acid sequences of the EBV major capsid protein (MCP) encoded by BcLF1 and the large tegument protein (LTP) encoded by BPLF1 were obtained from the National Center for Biotechnology Information (NCBI) database. HLA-A*02 or HLA-B*07 restricted CD8+ T cell epitopes (9-mers) were predicted using three prediction programmes available online Syfpeithi (Rammensee et al., 1999), BIMAS (Parker et al., 1994) and the Immune Epitope Database (IEDB) (Salimi et al., 2012). The top 2% of epitopes predicted by Syfpeithi were compared with the top 20 epitopes predicted by BIMAS and the top 20 epitopes predicted by IEDB. The 9-mer epitopes were extended into 20-mers to allow for potential recognition by CD4+ T cells. For BcLF1 there were sixteen peptides predicted and for BPLF1 there were twenty-five peptides predicted and synthesised by AltaBiosciences (Birmingham, UK) (table 2).

2.3.2. Bicinchoninic (BCA) assay

Protein concentration of synthesised peptides was determined by the bicinchoninic assay (Pierce Biotechnology, USA) (Smith et al., 1985). Briefly, the BCA assay combines the reduction of Cu^{2+} to Cu^{+1} by peptide (the biuret reaction) with the colorimetric detection of the cuprous cation (Cu^{+1}) using bicinchoninic acid. Standards (125µg/ml up to 2000 µg/ml), samples and a blank (DMSO only) were added to a 96 well plate. BCA working reagent was added, wells mixed, and the plate was incubated at 37°C for 30 min. Absorbance was measured at 560 nm using a micro-plate reader (Bio-rad, model 680).

2.3.3. T cell epitope peptide pools

Predicted T cell epitopes (peptides) were organised into peptide pools shown below and used in assays at a concentration 2 µg/ml (see table 2).

Table 2: T cell epitope peptide pools

Gene	***Protein***	***Expressed in***	***HLA restriction***	***Pool***	***20-mer***
BcLF1	Major capsid protein (MCP)	Late lytic cycle	**A2**	1	YIIEEVAPVRRILKFGNKVV
					LEQPCSFLQEAFPALSASSR
					ALIDEFMSVKQTHAPIHYGH
				2	SQYVRSRLSEMVAAVSGESV
					ALERGLINTVLSVKLRHAPP
					SRASTSMFIGTPNVSRREAR
				3	KCGLPTEDFLHPSNYDLLRL
					QPRVPISAAVIKLGNHAVAV
					SMYRKIYGELIALEQALMRL
			B7	4	HPRLHTPAHTLNSLNAAPAP
					SPRGRAACVVSCENYNQEVA
					QTHAPIHYGHYIIEEVAPVR
				5	NGTLLRDPRTYLAGMTNVNG
					NAIQYVRFLETALAVSCVNT
					HRRPNHMNVLVIVDEFYDNK
					LSVKLRHAPPMFILQTLADP
BPLF1	Large tegument protein (LTP)	Late lytic cycle	**A2**	6	DTIQQIVRSKKYLMNILKSI
					GAKMLAEIPQLAESDDGKFD
					HSTLKETAAAVNLLPGLLAV
					SLTQILAAMLLGITRVRRER
				7	LRTILDDIEAMLGLAGVASA
					QSGILKGHEM AQLTDVPSSV
					SDQTTLLWNTPSVVTQFLSI
					ALWPHPEFLGLVHNQSTARA
				8	MMALLVGTHPAYAAAFLGAP
					CFAPEALQQLWHSLRPLEGP
					TLSQASRVLSRFVSQLRRKL
					AVWLRELLTEARAAKPKEAR
			B7	9	QIPIPLPQAAPSNPKIPLTT
					FVKHPLTNNLPLLITISAPP
					SRDEAPDDELRSLLPSPPKA
					SVTPSPRLPLQIPIPLPQAA
				10	TGWGNGAPTRRAQFLAAAGP
					RAQFLAAAGPAKYAGTLWLE
					YDATITGQAPEDALRLLSGL
					KPGQSTGGIAPTPSAASLTT
				11	GSTSGDLVVP SGSPSSLSTA
					PQSPLLEKVAPGRPRDWLSP
					KEAPPSAASQLPKMPKCKDS
					DPGEAPSGFPIPQAPALGSG
					AESEASGPPSPQSPLLEKVA

2.3.4. T cell epitope control peptides

Peptides derived from several EBV proteins, known to elicit a response in donors based on previous experiments (data not shown), were used as positive controls at a final concentration of 2 μg/ml (see table 3).

Table 3: T cell epitope control peptides

Protein	*Cycle*	*HLA-restriction*	*Epitope sequence*	*Epitope abbreviation*
EBNA1	Latent	B35.01	HPVGEADYFEY	HPV
EBNA3A	Latent	B7	RPPIFIRRL	RPP
EBNA3A	Latent	B8	FLRGRAYGL	FLR
EBNA3C	Latent	B7	QPRAPIRPI	QPR
LMP2	Latent	A2	CLGGLLTMV	CLG
BRLF1	Lytic	A2	YVLDHLIVV	YVL
BZLF1	Lytic	B35.01	EPLPQGQLTAY	EPL

2.3.5. Blood sample collection

Blood was collected into lithium heparin vacutainers from nine EBV-seropositive healthy donors via venepuncture of a forearm vein. Blood was collected following ethical approval given by South Birmingham Research Ethics Committee (reference: 07/Q2702/24).

2.3.6. Blood sample processing

Peripheral blood mononuclear cells (PBMCs) were isolated from blood using density gradient centrifugation. Blood was diluted 1:1 with plain RPMI and carefully layered upon lymphocyte separation media (LSM). Tubes were centrifuged at $600 \times g$ for 30 min at room temperature (no brake). Lymphocytes were harvested from the interface

between plasma and LSM. Cells were washed twice in plain RPMI by centrifuging at $750 \times g$ for 10 min and $600 \times g$ for 5 min (low brake) at room temperature. Cells were re-suspended in 10% RPMI and counted using a haemocytometer.

2.3.7. Thawing cells

Cells were thawed in a 37°C water bath and slowly re-suspended in 10% RPMI using the drip-by-drip method. Cells were washed twice in 10% RPMI at $400 \times g$ for 5 min (low break). Cells were re-suspended in 10% RPMI and counted using a haemocytometer.

2.3.8. Freezing cells

Cells in 10% RPMI were centrifuged at $600 \times g$ for 5 min, re-suspended in freezing mix, and transferred to a cryovial. Vials were frozen at −1°C/min to −80°C using a freezing container (Mr Frosty, Nalgene). Cells were moved to −196°C within 24 hours.

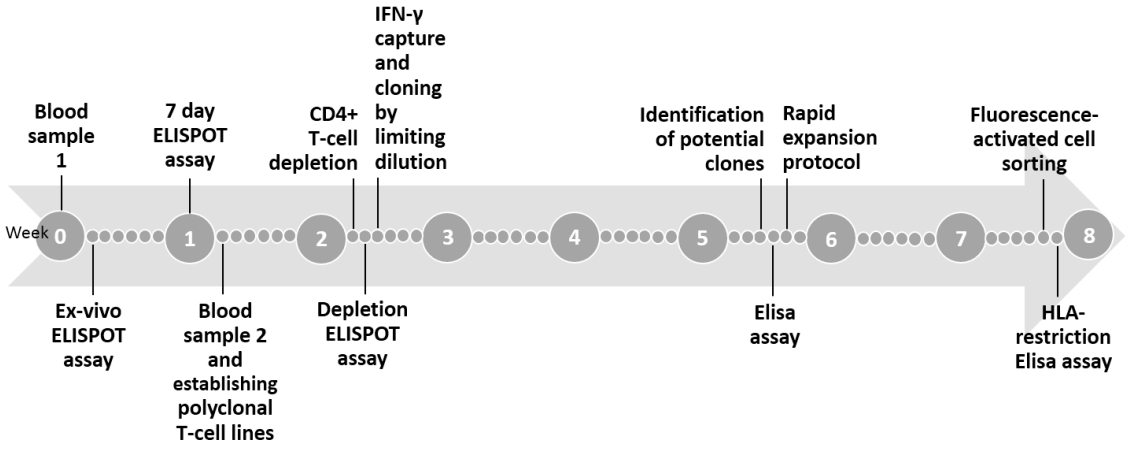

Figure 3: Schematic diagram of cell biology experiments time course. After collection and processing of blood sample obtaining PBMCs first, "*ex-vivo* ELISPOT assay" was performed alongside preparation of cells for 7 day culture for "7 day ELISPOT assay". After obtaining the results of both ELISPOT assays blood sample from the same donor was taken again to "establish polyclonal T cell lines". Alongside culturing T cells "CD4+ T cell depletion" was performed and the next day "depletion ELISPOT assay". The next day "IFN-γ capture and cloning by limiting dilution" was performed from polyclonal T cell lines. Potential clones were incubated at 37°C for approximately 3 weeks and identified. Identified potential clones were screened using "Elisa assay" and if positive for selected peptide pool clones were expanded by "rapid expansion protocol". After two weeks of incubation at 37°C T cell clones were identified by "fluorescence activated cell sorting" and HLA restriction was performed by Elisa assay the next day.

2.3.9. *Ex-vivo* ELISPOT assay

T cell responses to predicted T cell epitopes were assessed using IFN-γ ELISPOT. PVDF-membrane plates were treated with 70% ethanol in sterile distilled water for 30 sec. Treated plates were washed twice with filtered PBS. Plates were coated with anti-human IFN-γ antibody 1-DIK) at concentration of 7.5 µg/ml. Plates were incubated at room temperature for 3 hours. Plates were washed four times with filtered PBS and blocked with 10% RPMI. Plates were incubated at room temperature for 1 hour. Lymphocytes were added at 250,000 cells/well in duplicate. Predicted and control peptides were added at a concentration of 2 µg/ml per well. A negative control (10% RPMI media) was included in all assays. Plates were incubated overnight at 37°C. After 12-16 hours, plates were washed with 0.05% Tween/PBS eight times. The secondary antibody (Anti-human IFN-γ 7-B6-1-biotin) was added at concentration of 1µg/ml. Plates were incubated for 3 hours at room temperature. Plates were washed with 0.05% Tween/PBS solution eight times. Third antibody (Streptavidin-Alkaline Phosphatase) at ratio of 1:1000 was added and plates incubated for 1 hour and 30 min at room temperature. Plates were washed with 0.05% Tween/PBS solution eight times and filtered PBS three times. Substrate (TMB) was added and plates left to develop for 45 min. Colour development was stopped by rinsing plates with tap water. Plates were read on ELISPOT reader (Aid ELISPOT Reader). Spots were expressed relative to 1 million cells.

2.3.10. 7 day (*in-vitro*) ELISPOT assay

PBMCs were plated out in round bottom 96 well plates containing 10% RPMI in an identical format to the ex-vivo ELISPOT assay. Peptides were added to well in duplicate at 2 µg/ml. Plates were incubated for 7 days. After 7 days cells were washed four times in 10% RPMI by centrifuging at $750 \times g$ for 5 min (low break) at room temperature. Cells were re-suspended in 10% RPMI and transferred on to PVDF-membrane plates. One of the duplicate wells was stimulated with peptide, whereas the parallel well served as a negative control to give an indication of background IFN-γ. T cell responses

to predicted T cell epitopes were assessed using IFN-γ ELISPOT as described above in *ex-vivo* ELISPOT assay section. Plates were read on ELISPOT reader (Aid ELISPOT Reader). Spots were expressed relative to 1 million cells.

2.3.11. Establishing polyclonal T cell lines

PBMCs were counted using a haemocytometer. From a starting number of 5×10^6 cells, one third of cells were pulsed with peptide for for 2 hours at 37°C. The remaining cells were left in media at 37°C. After incubation, peptide-pulsed cells were washed by centrifuging at $600 \times g$ for 5 min at room temperature and combined with non-peptide pulsed cells. Cells were re-suspended in media containing IL-7 and plated out onto 24 well plates at 1.5×10^6 cells/well. After two days IL-2 was added at 50 IU/ml.

2.3.12. CD4+ T cell depletion

By examining results from the *ex-vivo* and 7 day ELISOT assays, peptide pools stimulating a response in donors were defined. To determine which subset of T cells responded to predicted T cell epitopes, CD4+ T cell depletion was performed to separate CD4+ and CD8+ T cells which we then examined for IFN-γ responses. Polyclonal T cell lines were established, and after 7 days, cells were washed three times with media at $600 \times g$ for 5 min at room temperature and counted using a haemocytometer. Anti-CD4 beads were washed twice in RPMI and added to cells at concentration of 4 beads per CD4+ T cell, assuming that CD4+ T cells represent 2/3 of the total cell count. Beads were incubated with cells at 4°C for 30 min. The CD4+ fraction was isolated using a magnet (Invitrogen Dynal AS, Norway) and the CD4-negative fraction was transferred to a new tube. The CD4+ fraction was re-suspended in media and transferred into a 24 well plate and left for 4 hours at 37°C to allow beads to detach from cells. The CD4+ fraction (minus beads) were collected as the non-adherent fraction of cells were transferred into new tubes and washed once with media at $400 \times g$ for 5 min at room temperature. Cells were re-suspended in media,

counted and plated out onto PVDF-membrane plates. Cells were assessed by IFN-γ production by ELISPOT as described in section 2.3.9.

2.3.13. IFN-γ capture prior to cloning by limiting dilution

A polyclonal T cell line was established from a representative donor using the peptide pool known to elicit a large IFN-γ response. Antigen specific cells from a polyclonal T cell line were enriched using an IFN-γ secretion and capture kit (Miltenyi Biotec Ltd., UK). Polyclonal T cell lines were pulsed with peptides at concentration of 2µg/ml for 3 hours. Polyclonal T cells were washed in MACS buffer at $600 \times g$ for 5 min at 4°C and re-suspended in cold media (5% RPMI HS). IFN-γ catch reagent was added and incubated for 10 min on ice. Warm media was added and cells were incubated at 37°C for 45 min on rotator to allow for IFN-γ secretion. After incubation cells were placed on ice for 3 min and then topped up with cold MACS buffer. Cells were centrifuged at $400 \times g$ for 5 min at 4°C and re-suspended in 80µl cold MACS buffer. Anti-IFN-γ PE was added and incubated on ice for 10 min. Cells were centrifuged at $400 \times g$ for 5 min at 4°C and re-suspended in cold MACS buffer. Anti-PE beads were added and incubated on ice for 15 min. Cold MACS buffer was added. Cells were centrifuged at $400 \times g$ for 5 min at 4°C and re-suspended in cold MACS buffer. Magnetic columns were washed with MACS buffer. Cells with magnetic beads were added into magnetic columns placed in magnet. Columns were taken out of the magnet and washed with MACS. IFN-γ positive cells were centrifuged at $400 \times g$ for 5 min at 4°C.

2.3.14. Cloning by limiting dilution

IFN-γ positive cells were re-suspended in media. Lymphocytes were isolated from apheresis cones (National Blood Service, Birmingham, UK) using density gradient centrifugation as described in section (numbers). Lymphocytes from three apheresis cones were mixed and pulsed with 10µg/ml of PHA for 1 hour at 37°C. Cells were then washed twice at $600 \times g$ for 5 min at room temperature. Lymphocytes were gamma-

irradiated with 40 Gy and washed 3-4 times at $600 \times g$ for 5 min at room temperature. IFN-γ positive cells at concentration of either 0.3 cell/well or 1 cell/well were combined with buffy cells at (100,000 buffy cells/well). Anti-CD3 (clone OKT3) was added at a concentration of 30 ng/ml. These preparations were added to round bottom plates at 100 µl per well. After 2 days 100 µl MLA with IL-2 was added into each well and potential T cell clones were incubated at 37°C for 3 weeks.

2.3.15. Identification of potential clones

After 3 weeks round bottom cloning plates were visually screened for potential clones. Approximately 50 µl from potential clones were transferred onto round bottom 96 well plates and washed four times at $750 \times g$ for 5 min and re-suspended in media. Potential clones were split in duplicates peptide pulsing one well at concentration of 2 µg/ml and adding media to second well as negative control. Plates were incubated overnight at 37°C. Responses from potential T cell clones to predicted T cell epitopes were assessed using IFN-γ ELISA.

2.3.16. ELISA

Responses from potential T cell clones to predicted T cell epitopes were assessed using ELISA assay. Maxisorb plates were treated with primary IFN-γ antibody (Pharmingen anti-human IFN-γ 18891D, Thermo scientific, USA) at concentration of 0.777 µg/ml and incubated overnight at 37°C. Treated plates were blocked with blocking buffer and incubated for 1 hour and 30 min at room temperature. Plates were washed in 0.05% Tween/PBS solution five times. Onto the plates IFN-γ standards were added at concentration of 4000, 2000, 1000, 500, 250, 125, 62.5, 31.25 and zero pg/ml, and samples. Plates were incubated for 3 hours at room temperature. Plates were washed in 0.05% Tween/PBS solution five times. Secondary IFN-γ antibody (Pharmingen biotinylated anti-human IFN-γ 188902D, Thermo scientific, USA) was added at concentration of 0.375 µg/ml and plates were incubated for 1 hour at room

temperature. Plates were washed in 0.05% Tween/PBS solution six times. Extra-avidin peroxidase was added diluted in 1% BSA/PBS/0.05% Tween/PBS solution in dilution factor 1:1000 and plates were incubated for 30 min at room temperature. Plates were washed in 0.05% Tween/PBS solution eight times. Tetramethylbenzidine (TMB) substrate was added and plates were left to develop for 30 min at room temperature. Reaction was stopped with HCl/dH_2O solution. Plates were read at 450 nm on microplate reader (Bio-rad, model 680).

2.3.17. Rapid expansion protocol (REP)

T cell clones that responded to peptide were transferred from cloning plates into 24 well plates and expanded using the rapid expansion protocol (REP). Lymphocytes from three apheresis cones were prepared as described in section 2.3.14. Autologous lymphoblastoid cell line (LCL) were pulsed with 2 µg/ml of peptide for 1 hour at 37°C and gamma-irradiated with 40 Gy. In order to expand T cell clones mixture was prepared containing 1 million lymphocytes, 100,000 LCLs with monkey leukocyte antigen (MLA) and IL-2. T cell clones were added into wells and incubated at 37°C.

2.3.18. Characterisation of T cell clones: Flow cytometry

T cell clones were transferred into tubes containing MACS buffer and centrifuged at $250 \times g$ for 5 min and re-suspended in MACS buffer. T cell clones were incubated with the following monoclonal antibodies for 20 min at room temperature; CD8 FITC, CD4 APC, CD3 APC-cy7 (Pharmingen, San Diego, USA) and washed and re-suspended in MACS buffer. Cell preparations were read on a flow cytometer (BD FACS CANTO II, BD Biosciences) collecting 10,000 gated lymphocytes. The flow cytometer was regularly calibrated using Calibrite beads (BD Biosciences, San Jose, USA) and compensation adjustments were made using single labelled antibody tubes. Data were analysed using FlowJo7 (Tree Star, Inc., Ashland, OR). The lymphocyte population was gated on the forward *versus* side-scatter. Viable cells were gated on the basis of 7-

aminoactinomycin D (7-AAD) viability dye exclusion and examined for CD3 and CD4 or CD8 expression.

2.3.19. Characterisation of CD8+ T cell clones: HLA class-I restriction

Aliquots of clones 56 and 58 were washed twice in media at $600 \times g$ for 5 min at room temperature and cells were counted. Approximately 2500 CD8+ T cells were transferred into duplicate wells of a round bottom 96-well plate. T cells were incubated overnight with media (negative control), peptide-pulsed autologous LCLs, or a panel of peptide-pulsed LCLs from donors. LCLs were selected to match the HLA class-I type of clones at one or two alleles. LCLs were incubated with 2 µg/ml of the relevant peptide pool for 1 hour at 37°C and washed four times in media at $600 \times g$ for 5 min at room temperature, and approximately 25,000 LCLs added to T cells. Plates were incubated at 37°C overnight. After approximately 18 hours, media was carefully removed and assayed for IFN-γ by ELISA.

2.3.20. Characterisation of CD4+ T cell clones: recognition of lytic LCLs

Prior to establishing whether clones were CD4+ or CD8+ by flow cytometry, initial screening experiments (not included in this thesis) showed that clones responded to peptide-pulsed LCLs from a number of laboratory donors. Once it was established clone 28 was CD4+, these cells were used to examine whether BcLF1-specific T cells recognised lytic LCLs derived from donor LCLs known to elicit a response. It was not within the scope of this thesis to undertake a full HLA class-II restriction. An aliquot of clone 28 was washed twice in media at $600 \times g$ for 5 min at room temperature and cells were counted. Approximately 2500 CD4+ T cell clones were transferred into duplicate wells of a round bottom 96-well plate. T cells were incubated overnight with either media (negative control), BZLF1 knock out LCLs, B95.8 LCLs (10% lytic), B95.8 LCLs pulsed with peptide pool 5, or peptide pool 5 alone. LCLs used for lytic recognition were provided by a colleague, and were previously shown to be lytic by BZLF1 staining and flow cytometry (data not shown). LCLs were washed twice in media at $600 \times g$

for 5 min at room temperature, counted, and approximately 25,000 cells added to relevant wells. Peptide pulsed LCLs were incubated with 2 µg/ml of peptide for 1 hour at 37°C and washed four times in media at $600 \times g$ for 5 min at room temperature. Plates were incubated at 37°C overnight. After approximately 18 hours, media was carefully removed and assayed for IFN-γ by ELISA.

2.4. Molecular Biology Techniques

Peptides from BcLF1 and BPLF1 were 20-mers that contained either an HLA-A*02 or HLA-B*07 predicted T cell epitope. Although predicted T cell epitopes may have some overlap with other HLA-restrictions, for future work, it would be desirable to screen donors independent of HLA-type. A more appropriate screening strategy is using a whole protein approach. Prior to the start of this project the BcLF1 had already been inserted into an appropriate vector. The aim of the molecular part of this project was to insert BPLF1 (and the invariant chain so that CD4+ T cell responses could be examined) into a vector.

2.4.1. Polymerase chain reaction (PCR)

For BPLF1 to be successfully inserted into a vector we had to first successfully amplify the BPLF1 gene. As BPLF1 is a relatively large gene with 9.5 kb (Whitehurst et al., 2012) we decided to amplify it in quarters. Polymerase chain reaction (PCR) was used to amplify BPLF1 and therefore, primers were designed using NCBI Primer Blast tool (Ye et al., 2012) (see table 4) obtaining four quarters of BPLF1. The annealing regions for amplifying the quarters of BPLF1 protein are shown in figure 5. Expand Long Template PCR System was used with different buffers and Phusion High-Fidelity PCR Kit. A PCR thermal cycler (Life technologies, Applied Biosystems GeneAmp PCR System 9700) was used and programmed with the following conditions: 35 cycles at 94°C for 2 min for initiation, at 94°C for 30 sec for denaturing, at 55°C for 30 sec for annealing, at 72°C for 1min/kbp for elongation, at 72°C for 7 min for final elongation. The obtained PCR amplicons were maintained at 4°C until electrophoresis.

Table 4: BPLF1 primer sequences.

Quarter	5' – 3' sequence	3' – 5' sequence
Quarter 1	ccgaagatgagtaacggcga	aaacaagggaagagcgggagag
Quarter 2	agtagggaccgatcgtctgtg	aaaagacgagcagccgaggct
Quarter 3	gacatgaaatcagcggtggtc	cggcccctaactctctttgtc
Quarter 4	cgggccctgagaaatcttatg	atcgcagacctcgagagactc

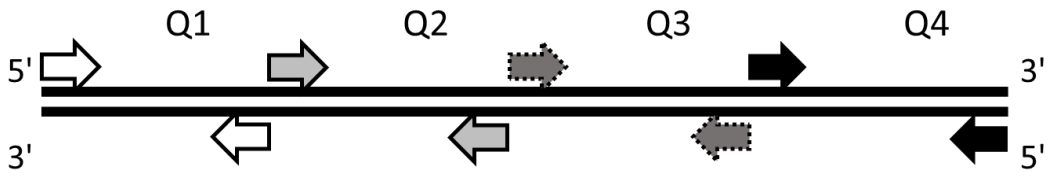

Figure 4: Schematic diagram of BPLF1 with primer positions.

2.4.2. Electrophoresis

The obtained PCR amplicons of BPLF1 were electrophoresed on a 1.5% low melting point agarose (LMPA) gel and visualized by ethidium bromide staining (EtBr). Gel for electrophoresis was a mixture of agarose powder at concentration of 1.5 g mixed with 98 ml of distilled water, 2 ml of 50x TAE and 5 µl of EtBr. Amplicons were mixed with loading dye before adding 5 µl onto agarose gel. Amplicons were electrophoresed for 30 - 45 min (120V). The DNA Molecular Weight Marker X (Roche) was used as the orientation marker of DNA separation. The DNA separation was visualized using a UV light.

2.4.3. Ligation of invariant chain into pENTR1A plasmid

In order to insert BPLF1 into virus vector the invariant chain had to be inserted into appropriate vector first and as a vector the pENTR1A plasmid was used. The pENTR1A vector, containing kanamycin resistance gene, was cut at restriction sites with the restriction enzymes Sal-I and Xho-I. The antarctic phosphatase was added to neutralize phosphate ends. Restriction enzymes were inactivated by heating to 65°C for 20 min. The invariant chain (synthesised by GeneArt) was cut with the restriction enzyme Xho-I and heated to 65°C for 20 min to neutralize restriction enzyme. The pENTR1A vector and the invariant chain were combined together in microcentrifuge tube in a ratio of 1:2 and incubated at 25°C for 5 min to obtain ligation constructs (see figure 5).

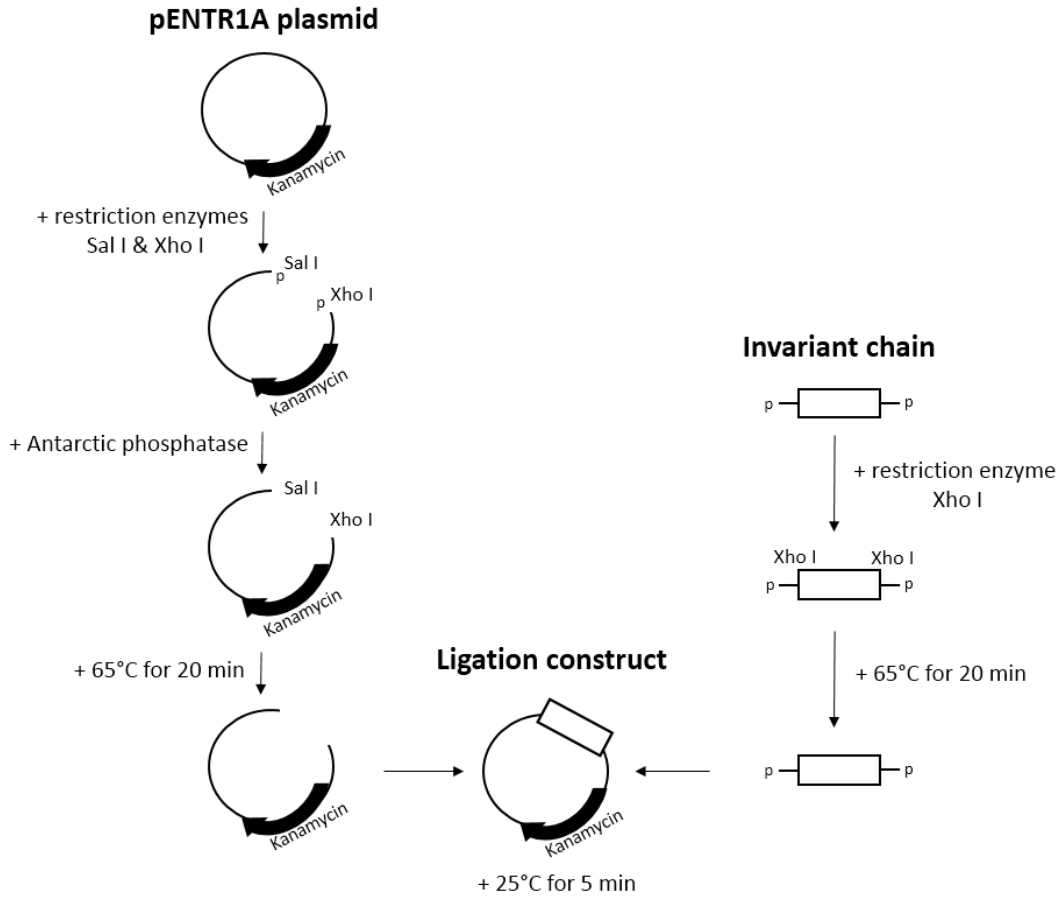

Figure 5: Schematic diagram of ligation of the Invariant chain into pENTR1A plasmid.

2.4.4. Transfection of modified pENTR1A plasmid into competent cells

The obtained ligation constructs, positive control containing kanamycin resistance gene (GFP-LC3 plasmid) and the negative control (pENTR1A plasmid) were used to transfect competent cells (*E. Coli*). The ligation products, GFP-LC3 plasmid and pENTR1A plasmid were added into separate microcentrifuge tubes. The competent cells were added into each microcentrifuge tube and the mixtures were incubated on ice for 30 min. Microcentrifuge tubes were transferred into the water bath and incubated at 42°C for 30 sec and transferred on ice for one minute (heat shock). The LB media was added into microcentrifuge tubes and competent cells were transferred into a rotary shaker for 1 hour at 37°C, 5% CO_2. The competent cells were plated onto agar plates, containing kanamaycin antibiotic at concentration of 100 µl/ml, and incubated overnight at 37°C, 5% CO_2.

2.4.5. Colony selection

The competent cells containing kanamaycin resistance gene expanded into colonies which were selected and transferred into tubes, single colony per tube. The LB media was added with kanamycin antibiotic at concentration of 100 µl/ml. The culture was incubated overnight in rotary shaker at 37°C, 5% CO_2.

2.4.6. Plasmid DNA purification and DNA digestion

After the overnight incubation the colonies expanded. In order to obtain plasmid DNA from competent cells the DNA was purified using QIAprep spin miniprep kit (QIAGEN, Sussex, UK). The cultured competent cells were transferred in microcentrifuge tubes and centrifuged at $17{,}900 \times g$ for 30 sec. Competent cells were re-suspended in buffer P1. The buffer P2 was added and cultures were thoroughly mixed. The buffer N3 was added lizing the competent cells. The mixtures were centrifuged at $17{,}900 \times g$ for 10 min. Supernatant from each microcentrifuge tube was transferred onto the QIAprep spin columns and centrifuged at $17{,}900 \times g$ for 30 sec. Onto the columns the

PE washing buffer was added and QIAprep spin columns were centrifuged at $17{,}900 \times g$ for 30 sec. QIAprep spin columns were placed in a clean microcentrifuge tube adding buffer EB and left for a minute and centrifuged at $5{,}500 \times g$ for a minute. Purified DNA was digested with the restriction enzymes Xba-I and Not-I to identify whether the invariant chain has been correctly ligated into the pENTR1A plasmid. Furthermore, the Nco I and Eco-RV were used to identify the orientation of the invariant chain. The digested DNA constructs were electrophoresed in a 2% agarose gel and visualized by ethidium bromide staining at 140V for 25 min. After the identification of potential constructs containing the invariant chain with sense orientation, constructs were sent for a DNA sequencing (School of Biosciences, University of Birmingham, UK) to obtain the DNA sequences.

2.4.7. Preparation of DNA constructs for electroporation

At standard "heat shock" method of transfection described in section 2.4.4 we obtained very low transfection efficiency. Therefore, we decided to use electroporation to increase the transformation.

The ligation constructs were modified as described in section 2.4.3. Constructs were electrophoresed in a 2% agarose gel and visualized by ethidium bromide staining. The constructs were visualized by the UV light and cut out of agarose gel. To extract obtained constructs the QIAquick Gel Extraction Kit (QIAGEN, Sussex, UK) was used. The constructs in agarose gel were transferred into microcentrifuge tube and buffer QG was added. Microcentrifuge tube with ligation constructs (DNA samples) was incubated at 50°C for 10 min. Isopropanol was added and the DNA samples were transferred to the QIAquick column and washed three times by centrifuging at $17{,}900 \times g$ for 1 minute using buffer QG and buffer PE. The flow-through was discarded and QIAquick column was centrifuged at $17{,}900 \times g$ for 1 minute. The QIAquick column was transferred onto new clean microcentrifuge tube and elution buffer was added. Microcentrifuge tube with DNA samples was centrifuged at $17{,}900 \times g$ for 1 minute. The purified DNA was quantified using nanodrop

spectrophotometer (Thermo Scientific, Wilmington, USA) and transferred into microcentrifuge tube with prepared NEB 5-alpha electrocompetent cells (*E. Coli*) (New England Biolabs).

2.4.8. Electroporation of *E. Coli* electrocompetent cells

Electrocompetent cells were cultured in LB media overnight in rotary shaker at 37°C, 5% CO_2 and transferred into fresh LB media and incubated in a rotary shaker until OD_{600nm} was approximately 0.4 measuring by spectrophotometer. The electrocompetent cells were centrifuged at $6000 \times g$ for 10 min at 4°C, re-suspended in ice-cold sterile distilled water and washed three times at $6000 \times g$ for 10 min at 4°C. Cells were aliquoted into ice-cold electroporation cuvets and pre-cold DNA was added. The electroporation cuvets containing electrocompetent cells and ligation constructs (DNA) were incubated on ice for 30 min and placed into electroporation apparatus (Bio-Rad Gene Pulser). Electroporation apparatus was set to 2.5 kV, 25µF and 200 Ω and DNA/cells mix was pulsed. After the electroporation the LB media was added into cuvets. The electrocompetent cells were grown on agar plates, containing kanamaycin antibiotic at concentration of 100µl/ml, and incubated overnight at 37°C, 5% CO_2. The colonies were selected and plasmid DNA was purified and digested as described in sections 2.4.5 and 2.4.6.

3. Results

3.1. Cellular Biology results

To study T cell responses to selected proteins MCP, encoded by BcLF1, and LTP, encoded by BPLF1, nine donors were screened from wide range of the HLA-class I types (see figure 6).

	Donor HLA-class I type					
Donor	**HLA-A**		**HLA-B**		**HLA-C**	
1	2	24	39		6	7
2	1		7	8	?	?
3	3	11	15	35	3	4
4	23	30	7	44	4	7
5	1	2	44	57	5	7
6	1	11	7	35	4	7
7	2		47	60	3	17
8	2	11	51	60	3	15
9	2	24	27	35	2	4

Figure 6: Donor HLA-class I type. In *ex-vivo* and *in-vitro* experiments nine donors from wide range of HLA-class I types were screened for T cell responses. Question mark (?) denotes that the HLA-class I type is not known.

3.1.1. Ex-vivo T cell responses to predicted T cell epitopes of EBV proteins MCP and LTP

The IFN-γ ELISPOT assay was used to examine whether T cell responses to predicted T cell epitopes of EBV proteins MCP and LTP were detectable *ex-vivo*. PBMCs from seven EBV-seropositive healthy donors were tested for five MCP peptide pools containing three to four T cell epitopes per pool, and six LTP peptide pools containing four to five epitopes per pool. The full list of peptide pools is presented in table 2. The quantification of IFN-γ producing T cells was conducted after an overnight incubation.

On average donors responded to 3/5 MCP peptide pools and 4/6 LTP peptide pools. The majority of *ex-vivo* T cell responses measured were small under 60 spots/million cells (figure 8). Donor 1 showed no detectable response *ex-vivo.* Donor 5 and 8 responded to all 11 pools when measured *ex-vivo*. Donor 5 T cell responses to pools 4 – 7 were low, below 60 spots/million cells and to pools 1 - 3 and 8 - 11 *ex-vivo* responses were of medium size (61 -120 spots/million cells) to very high (>181 spots/million cells). The largest *ex-vivo* T cell response was seen in donor 5 in pools 10 and 11 representing responses to predicted T cell epitopes of EBV protein LTP (see figure 7 and 8).

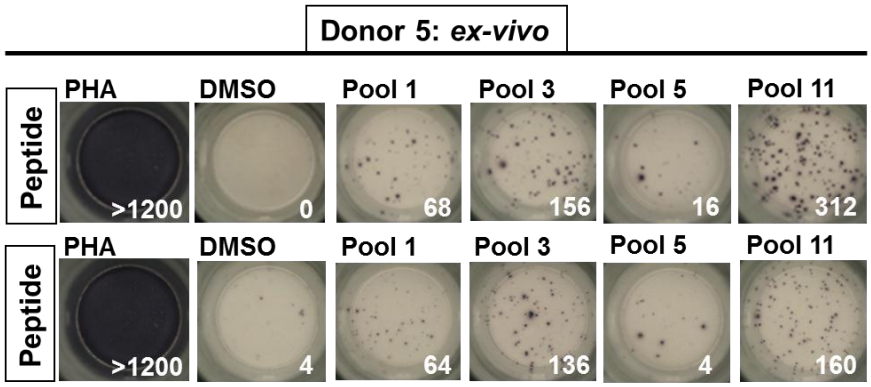

Figure 7: Donor 5 *ex-vivo* example. Figure presents *ex-vivo* T cell responses to predicted T cell epitopes. Donor 5 showed a large response to positive control - PHA (>1200 spots/million cells) and no response to negative control – DMSO suggesting there was no background. Donor 5 responses to pools 1 and 5 were low (below 70 spots/million cells) whereas responses to pools 3 and 11 were medium (156 spots/million cells) to high (312 spots/million cells).

	BcLF1 (MCP)					***BPLF1 (LTP)***					
	A2			**B7**		**A2**			**B7**		
Donor	Pool 1	Pool 2	Pool 3	Pool 4	Pool 5	Pool 6	Pool 7	Pool 8	Pool 9	Pool 10	Pool 11
1											
2											
4											
5											
6											
7											
8											

Spots/million cells	Colour
0	
1 - 60	
61 – 120	
121 – 180	
>181	

Legend: Figure represents *ex-vivo* responses to predicted T cell epitopes as spots/million cells (PBMCs). Donor 3 and 9 were not included when measuring *ex-vivo* T cell responses for technical reasons. The figure shows the number of stimulating pools with magnitude of response.

Figure 8: *Ex-vivo* donor responses to T cell peptide pools of EBV proteins MCP and LTP. The responses are presented as mean value of both duplicate wells after subtracting the values of negative control (DMSO). The DMSO values ranged between 0 to 16 spots/million cells.

Ex-vivo analysis of T cell responses to control peptides (see table 3) showed that donors exhibit an EBV-specific immune response, even in the absence of an MCP or LTP specific response. For each donor two control peptides were selected on the basis of past experiments (data not shown). As can be seen from figure 9, all donors with the exception of donor 1, exhibit EBV-specific immunity that is detectable ex-vivo.

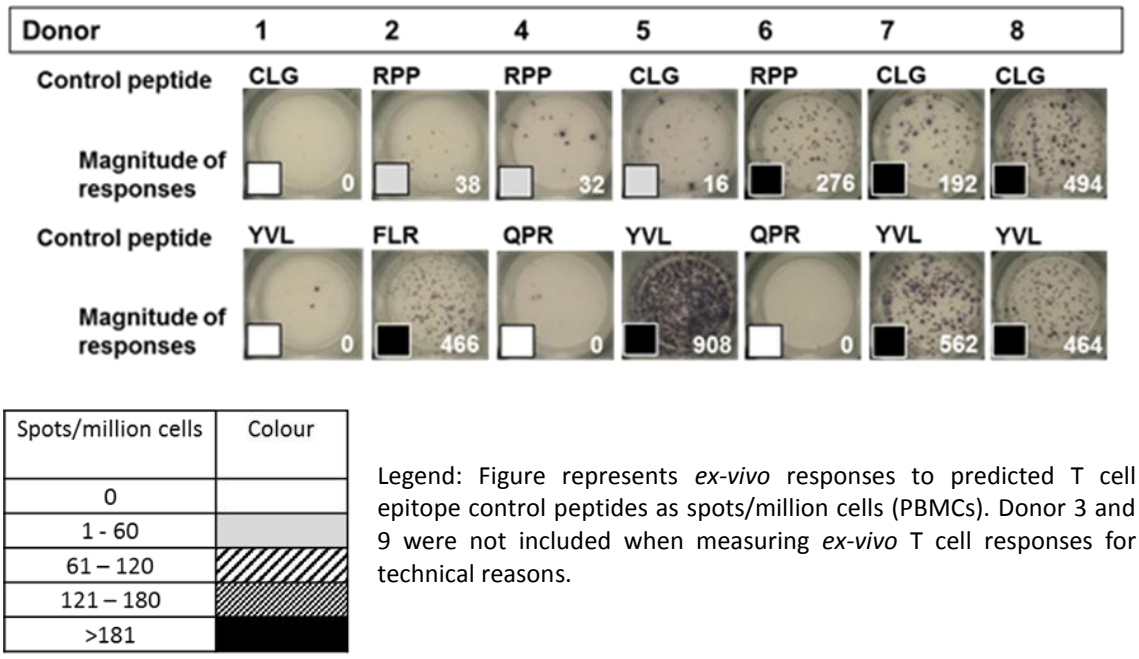

Spots/million cells	Colour
0	
1 - 60	
61 – 120	
121 – 180	
>181	

Legend: Figure represents *ex-vivo* responses to predicted T cell epitope control peptides as spots/million cells (PBMCs). Donor 3 and 9 were not included when measuring *ex-vivo* T cell responses for technical reasons.

Figure 9: *Ex*-vivo donor T cell responses to control peptides. For each donor there were two control peptides selected for determination of reliability of IFN-γ ELISPOT assay. Donor T cell responses to control peptides were low (responses to RPP and CLG control peptides in donors 2, 4 and 5) to large (responses to FLR, YVL, RPP and CLG in donors 2, 5, 6, 7 and 8). In donors 2, 4 and 6 there were no response to control peptides CLG, YVL and QPR. The quantified responses are presented as mean value of both duplicate wells after subtracting the values of negative control (DMSO).

3.1.2. In-vitro T cell responses to predicted T cell epitopes of EBV proteins MCP and LTP

As T cell responses to MCP and LTP were low and on the limit of detection ex-vivo, a 7-day cultured IFN-γ ELISPOT was used to confirm the initial results. It was anticipated that very low frequency responses would expand to a detectable level. PBMCs from nine EBV-seropositive healthy donors were cultured as described in section 2.3.10. The T cell responses to five MCP peptide pools containing three to four T cell epitopes per pool, and six LTP peptide pools containing four to five epitopes per pool were examined with IFN-γ ELISPOT. After 7 days, cells were washed, and transferred onto ELISPOT plates. One of the duplicate wells was re-challenged with peptide, the other well, which had seen peptide 7 days prior, served as a negative control. The quantification of IFN-γ producing T cells was conducted after an overnight incubation.

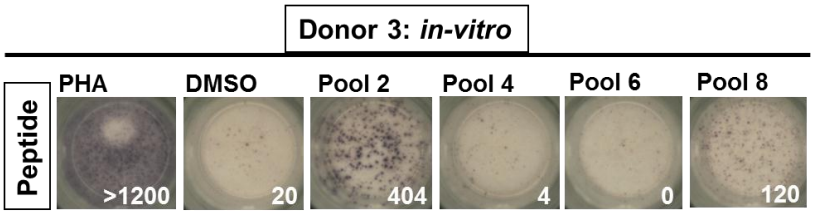

Figure 10: Donor 3 *in-vitro* example. Figure presents *in-vitro* T cell responses to predicted T cell epitopes from donor 3. Donor 3 showed a large response to positive control - PHA (>1200 spots/million cells) and low response to negative control. Donor 3 showed no response to pool 6 and a low response to pool 4 (below 100 spots/million cells) whereas responses to pools 8 and 2 were medium (120 spots/million cells) to high (404 spots/million cells). On the figure only one duplicate well is presented as the second duplicate well was a negative control and all values presented are subtracted from negative controls.

On average, *in vitro* data showed that donors responded to 3/5 MCP peptide pools and 4/6 LTP peptide pools. The *in-vitro* T cell responses ranged between 4 spots/million cells up to 404 spots/million cells and the majority of T cell responses were low under 100 spots/million cells. However, there was a clear increase in number of T cell responses defined as being of 'medium' intensity, ranging from 100 to 300 spots/million cells.

Interestingly, donor 1 showed T cell responses to four peptide pools of MCP and five peptide pools of LTP and in peptide pools 6 and 10 T cell responses were ranked as medium despite the fact that in *ex-vivo* there were no detectable T cell responses.

In donor 2 there was an increase in T cell response. For example, in peptide pool 3 where 8 spots/million cells were detected *ex-vivo*, there was 172 spots/million cells detected *in-vitro* experiment. In peptide pool 6, where there was, interestingly, no response detected in *ex-vivo* experiment, in *in-vitro* experiment there was a medium response. The low responses seen in peptide pools 5, 8 and 10 when measured *ex-vivo* were undetectable when measuring *in-vitro* T cell responses.

The T cell responses in donor 3 were low to high in peptide pool 2 with 404 spots/million cells (see figure 10).

In donor 4 there was an appearance of a low T cell response in peptide pool 1 which was not detected *ex-vivo* but T cell responses seen in peptide pools 2, 7 and 8

were undetectable when measuring *in-vitro* T cell responses. The remaining T cell responses detected *ex-vivo* have when measured *in-vitro* increased.

Donor 5 responded to all peptide pools *ex-vivo* however, *in-vitro* T cell responses to peptide pools 3, 7 and 8, were no longer detectable.

In donor 6 T cell responses seen *ex-vivo* expanded except in peptide pools 4 and 6 where the T cell responses measured *ex-vivo* were no longer detectable *in-vitro.* Furthermore, in donor 7 all T cell responses detected *ex-vivo* expanded however, the T cell response detected *in-vitro* in peptide pool 6 ranked as medium was *ex-vivo* not detected. In donor 8 the T cell responses in peptide pools 5 and 9 detected as low measured *ex-vivo* when measured *in-vitro* were no longer detected (see figure 11).

Interestingly, in 3/4 donors where T cell responses in peptide pool 6 were undetectable *ex-vivo* the T cell responses became detectable when measuring *in-vitro*.

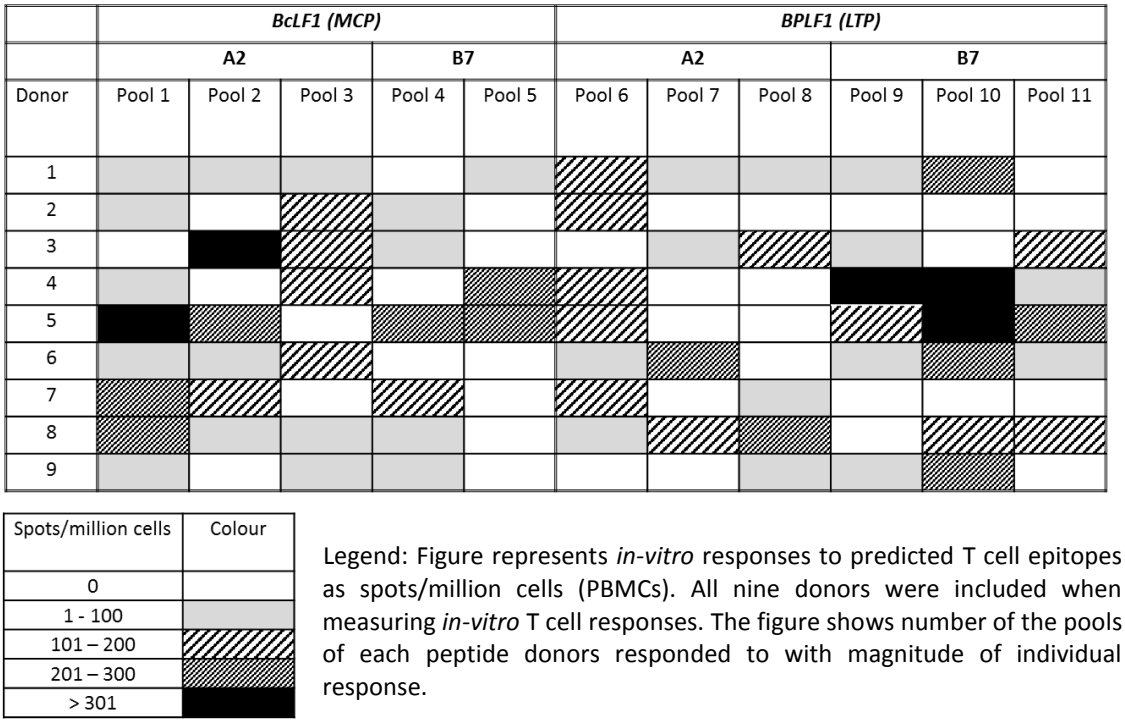

Legend: Figure represents *in-vitro* responses to predicted T cell epitopes as spots/million cells (PBMCs). All nine donors were included when measuring *in-vitro* T cell responses. The figure shows number of the pools of each peptide donors responded to with magnitude of individual response.

Figure 11: In-vitro donor responses to T cell pools of EBV proteins MCP and LTP.

In *in-vitro* ELISPOT assay control peptides were also used to assess EBV-specific immune response, even in the absence of an MCP or LTP specific response. The same control peptides were used as for the *ex-vivo* experiment.

In donor 1 when measured *ex-vivo* there were no T cell responses detected to control peptides CLG and YVL however, in *in-vitro* there were medium T cell responses. In donors 2 and 3 there was an increase in T cell response from measuring *ex-vivo* to *in-vitro* to control peptide RPP whereas, in donor 7 increase was seen in both control peptides. However, in donor 8 T cell responses to control peptides CLG and YVL decreased when measuring *in-vitro*.

The T cell responses to control peptide QPR when measured *ex-vivo* were undetectable but there were T cell responses detectable *in-vitro* in donors 3 and 6. However, in donor 5 T cell responses were changing in the opposite manner as there were a low T cell responses to control peptide CLG *ex-vivo* but *in-vitro* the T cell responses were no longer detected. In donor 9 medium T cell responses were observed (see figure 12).

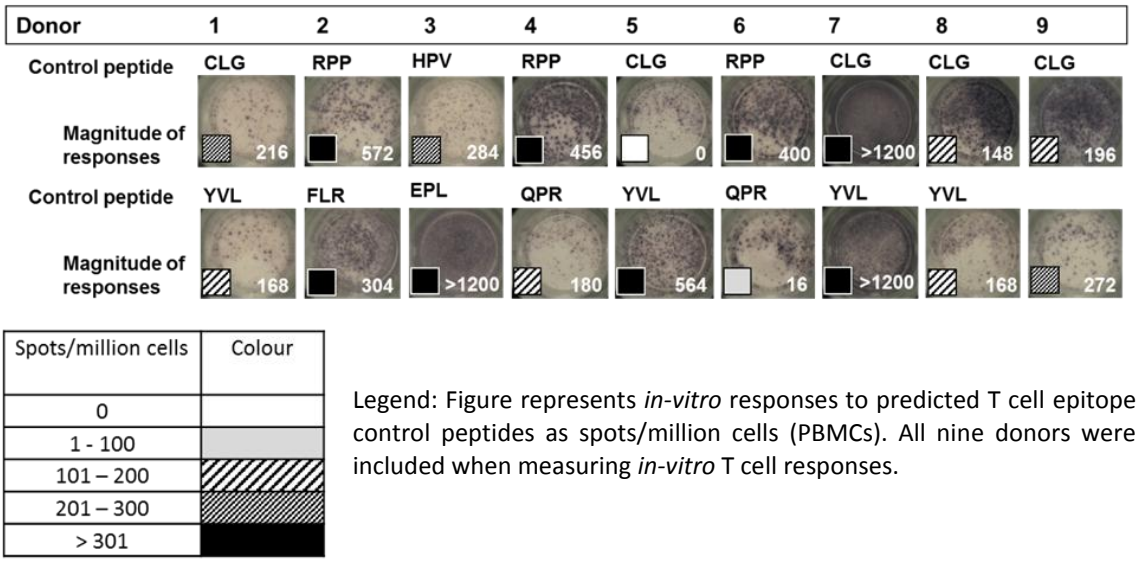

Legend: Figure represents *in-vitro* responses to predicted T cell epitope control peptides as spots/million cells (PBMCs). All nine donors were included when measuring *in-vitro* T cell responses.

Figure 12: *In-vitro* donor T cell responses to control peptides. For each donor there were two control peptides selected for determination of reliability of IFN-γ ELISPOT assay. There was no T cell responses detected for control peptide CLG in donor 5. Approximately the same number of donor T cell responses were characterised as medium or high. The highest T cell responses were observed for control peptides HPV (donor 3), YVL and CLG (donor 7). Only the T cell responses in re-challenged wells are presented on the figure. The magnitudes presented are obtained after subtracting from the negative control which was in this case the non re-challenged well.

Donor T cells responded to a different number of peptide pools when measured *ex-vivo* and *in-vitro*. The responding number of pools stayed roughly stable from *ex-vivo* to *in-vitro* experiment (see table 5).

Table 5: Number of peptide pools eliciting a response in donors. N/A denotes that data was not obtained as assay was not performed due to technical reasons.

	Ex-vivo		***In-vitro***	
Donor	BcLF1	BPLF1	BcLF1	BPLF1
1	0	0	4	5
2	4	2	3	1
3	N/A	N/A	3	4
4	3	6	3	4
5	5	6	4	4
6	4	5	3	5
7	3	1	3	2
8	5	6	4	5
9	N/A	N/A	3	3

The T cell responses measured *ex-vivo* and *in-vitro* were compared in seven donors as in donor 3 and 9 *ex-vivo* ELISPOT was not performed. Table 6 presents expansion in T cell responses which expanded from 11 to 97-fold. The highest expansion was observed in donor 1 and the lowest expansion in donor 6 (see table 6).

Table 6: Average fold expansion in T cell responses from *ex-vivo* to *in-vitro* experiment. T cell responses have increased over seven day of culture. Increase is presented as fold expansion.

Donor	***1***	***2***	***4***	***5***	***6***	***7***	***8***
Average fold expansion for all responding pools	97	77	21	13	11	35	12

3.1.3. CD4+ and CD8+ T cell responses to MCP and LTP peptides

To determine which subset of T cells (CD4+ T cells and/or CD8+ T cells) responded to predicted T cell epitopes from EBV proteins MCP and LTP, four representative donors were re-examined. Polyclonal T cell lines were established using peptide pools known to elicit an IFN-γ response. The CD4+ T cells were isolated and preparations were assayed using ELISPOT assay as described in section 2.3.12.

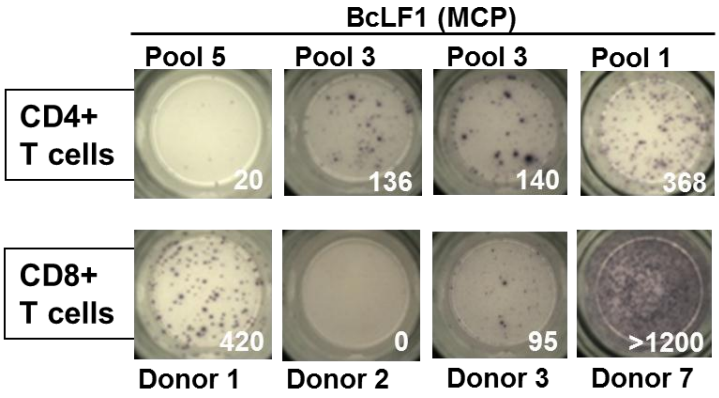

Figure 13: Examples of CD4+ and CD8+ T cell responses. The CD4+ and/or CD8+ T cell responses were measured with INF-γ ELISPOT assay with peptide pools known to elicit an IFN-γ response in donors 1, 2, 3 and 7. In donors 1 and 2 the separation in T cell subset responses is clear, as in donor 1 T cell responses are seen only in CD8+ T cells and in donor 2 only in CD4+ T cells. In donors 3 and 7 T cell responses are seen in both subsets of T cells.

In two donors (donor 1 and 2) the separation in responses of T cell subsets was clearly seen as in donor 1 there was a large predominant CD8+ T cell response to the peptide pool 5 and in donor 2 the T cell response to peptide pool 3 was predominant in CD4+ T cells. Whereas, in two donors (donor 3 and 7) responses to predicted T cell epitopes were seen in both subsets of T cells (see figure 15 and 16).

Donor 1		
	Spots/million cells	
Pool	CD4+ T-cells	CD8+ T-cells
5*	15	415
6#	0	10
8#	0	20
10#	25	5

Donor 2		
	Spots/million cells	
Pool	CD4+ T-cells	CD8+ T-cells
3*	100	5
6#	15	0

Donor 3		
	Spots/million cells	
Pool	CD4+ T-cells	CD8+ T-cells
2*	75	5
3*	70	105
8#	0	10

Donor 7		
	Spots/million cells	
Pool	CD4+ T-cells	CD8+ T-cells
1*	466	254
6#	108	140

Figure 14: Responses of T cell subsets to peptide pools. To identify which T cell subsets responded to peptide pools donor T cells (donor 1, 2, 3 and 7) were screened with peptide pools known to elicit an IFN-y response. In donors 1 and 3 experiment was repeated three times, in donor 2 two times and in donor 7 the experiment was repeated four times. Values are presented as mean values obtained in all four experiments. The asterisk (*) denotes that peptide pool belongs to MCP and hashtag (#) denotes that the peptide pool belongs to LTP.

3.1.4. Clones

Following limiting dilution assay, 145 potential clones were identified established from donor 1. Potential clones were examined for IFN-y responses to the stimulating peptide pool by IFN-Y ELISA. 11 clones showed IFN-y responses above background (data not shown). These clones were expanded using the Rapid Expansion Protocol (section 2.3.17.).

3.1.5. Characterisation of T cell clones

After two weeks, T cell clones were examined for CD4 or CD8 expression by fluorescence-activated cell sorting (FACS). Figure 15 shows representative dot plots from two clones. Five clones were CD4+ and six were CD8+.

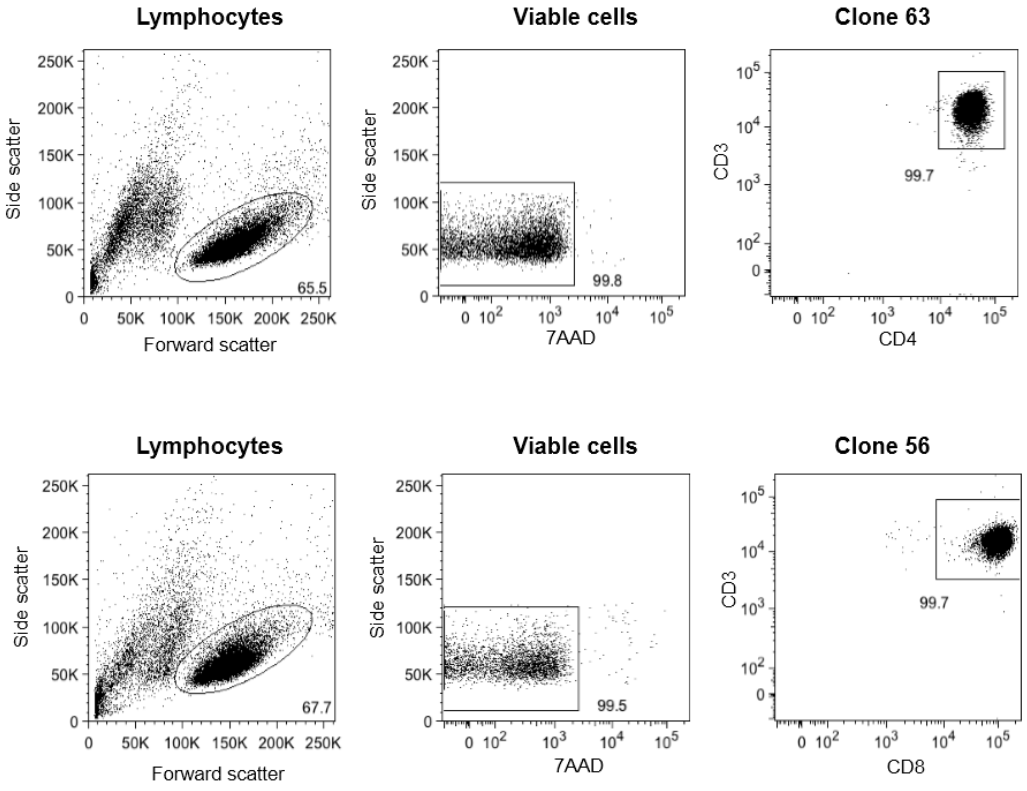

Figure 15: Flow cytometry analysis of T cell clones. Lymphocytes were gated on the forward *versus* side-scatter. Viable cells were identified on the basis of 7-aminoactinomycin D (7-AAD) exclusion (viable cells). T cell clones were examined for CD3 and CD4 or CD8 expression.

3.1.6. HLA restriction of T cell clones

The CD8+ T cell clones were assessed for IFN-γ production in response to peptide. Selected LCLs from seven donors and autologous LCLs were pulsed with peptide. Two CD8+ T cell clones (56 and 88) are presented in figure 16. LCLs were selected to share only one or two HLA-alleles with the representative donor from which CD8+ T cell clones were derived. The CD8+ T cell clones 56 and 88 showed a low responses when measuring released IFN-γ with 750 and 1300 pg/ml when combined with presenting autologous LCLs. But overall the responses from clones 56 and 88 when combined with LCLs 1-6 were low suggesting this CD8+ T cell clones were not HLA-A2, HLA-A*24, HLA-B*39 or HLA-C*07. When CD8+ T cell clones were combined with LCLs from LCL-donor 7 there was a large IFN-γ response with 742 pg/ml in CD8+ T cell clone 56 and 1222 pg/ml in CD8+ T cell clone 88. Data obtained from IFN-γ ELISA assay therefore showed that T cell clones 56 and 88 are HLA-C*06 restricted.

	HLA-A (i)	HLA-A (ii)	HLA-B (i)	HLA-B (ii)	HLA-C (i)	HLA-C (ii)
Autologous	2	24	39	/	6	7
LCL 1	1	2	44	55	3	5
LCL 2	1	11	7	35	4	7
LCL 3	2	24	27	35	2	4
LCL 4	2	/	44	/	5	16
LCL 5	2	29	7	44	7	16
LCL 6	2	/	39	44	1	5
LCL 7	11	30	13	35	6	/

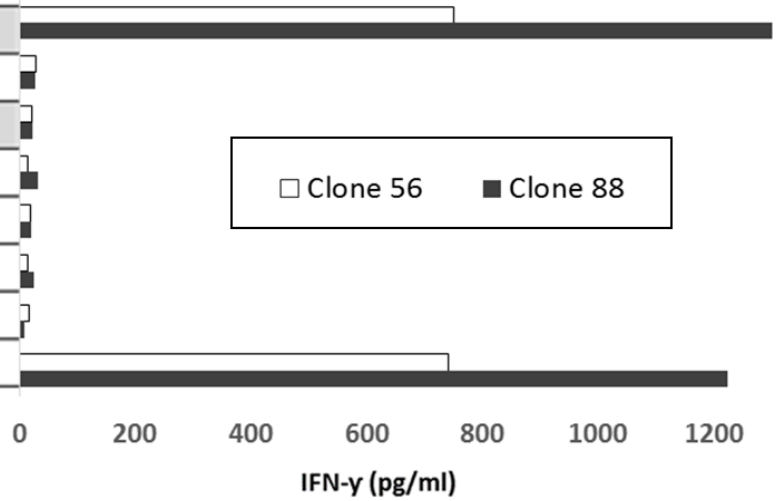

Figure 16: The CD8+ T cell clones HLA-restriction. The figure presents HLA types of presenting LCLs and the IFN-γ responses obtained from CD8+ T cell clones 56 and 88. Responses from autologous LCLs and LCLs from LCL-donors 1-6 were low. However, the response when combined with LCLs from LCL-donor 7 were large. Therefore, data showed that CD8+ T cell clones 56 and 88 are HLA-C*06 restricted. This experiment was conducted in duplicates and average values are presented.

3.1.7. Recognition of lytic LCLs

The CD4+ T cell clones were assessed to see whether clones recognised lytic LCLs. In the assay latent and lytic LCLs were used to assess whether CD4+ T cell clones recognise lytic LCLs. As marker of potential infection media was used. When CD4+ T cell clones were combined with latent LCLs there were no IFN-γ released. However, large responses were observed when CD4+ T cell clones were combined with latent LCLs and peptide pool 5 or only with peptide pool 5. When CD4+ T cell clones were combined with lytic LCLs there were an IFN-γ released. Data obtained from IFN-γ ELISA assay therefore showed that CD4+ T cell clones recognise lytic LCLs.

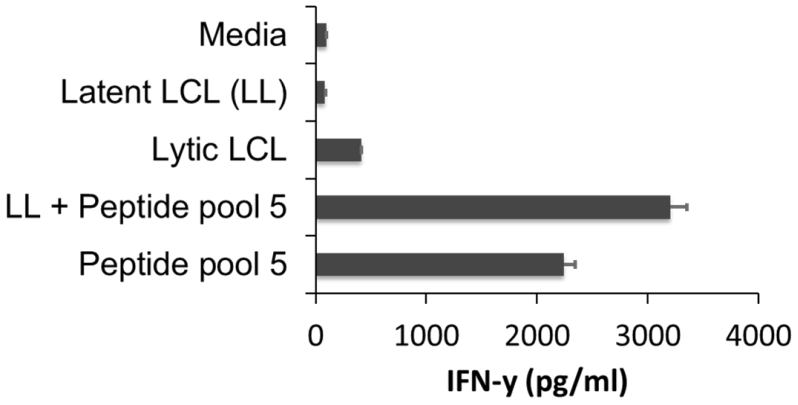

Figure 17: The CD4+ T cell clones recognition of lytic LCLs. To confirm that LCLs were in lytic cycle staining for BZLF1 was performed and LCLs were inspected by flow cytometry. Approximately 10% of LCLs in the culture were lytic (data not shown). Data obtained suggests that the CD4+ T cell clones recognised lytic LCLs. Latent LCL (LL) was a BZLF1 knock out LCL that was unable to go into lytic cycle.

3.2. Molecular biology results

3.2.1. Amplification of BPLF1 gene

The BPLF1 gene which is approximately 9.5 kb long was amplified in quarters to be inserted into an appropriate vector which would allow screening of the T cell responses with a whole protein regardless of the HLA-type. The BcLF1 gene encoding the MCP was successfully inserted into a vector before the start of this project. In order to optimise the reaction different kits and buffers were used. The Expand Long Template (ELT) PCR System with buffers 1 and 3, and Phusion High-Fidelity (HF) PCR Kit were used. The ELT buffer 1 is used for amplification of fragments from 0.5 to 12 kb whereas buffer 3 is used for amplification of fragments longer than 15 kb. We decided to optimise our reaction with this buffer even so our fragments were approximately 8 kb long. The Phusion High-Fidelity PCR Kit contains High-Fidelity DNA Polymerases which is used for long or difficult amplifications.

Quarters 1 and 4 were successfully amplified using the Expand Long Template (ELT) PCR System with buffers 1 and 3 with addition of dimethyl sulfoxide (DMSO) as presented on figure 18. The successfully obtained amplicons are seen as lines which can be visible between 3054 bp and 2036 bp mark. For further experiments quarters 1 and 4 amplified with ELT buffer 3 were meant to be used.

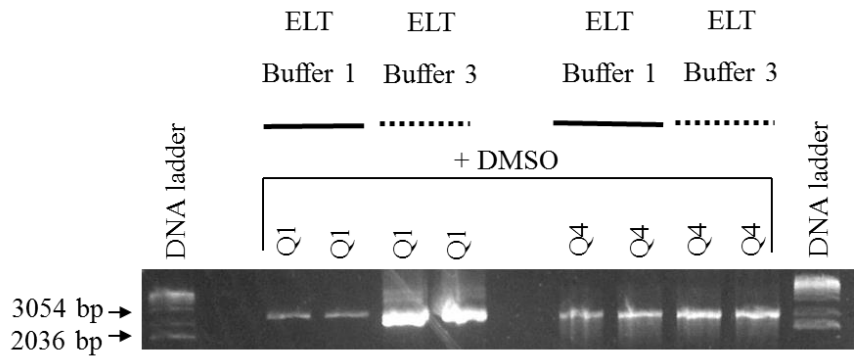

Figure 18: PCR amplicons of BPLF1 quarter 1 and 4. Quarter 1 and quarter 4 were amplified using Expand Long Template PCR System (ELT) with added dimethyl sulfoxide (DMSO) and buffer 1 or buffer 3 and electrophoresed on 1.5% LMPA gel. Quarters are visual between 3054 bp and 2036 bp mark. The Q1 and Q4 denotes quarter 1 and quarter 4.

Quarters 2 and 3 were successfully amplified using the Phusion High-Fidelity (HF) PCR Kit with addition of dimethyl sulfoxide (DMSO) as presented on figure 19. The successfully obtained amplicons are seen as lines which can be visible between 3054 bp and 2036 bp mark. For further experiments all four amplified quarters were meant to be used.

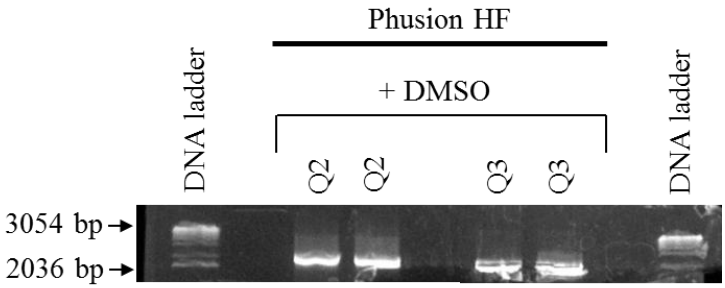

Figure 19: PCR amplicons of quarter 2 and 3 on 1.5% LMPA gel. Quarter 2 and 3 were amplified using Phusion High-Fidelity PCR Kit (Phusion HF) with added dimethyl sulfoxide (DMSO) and electrophoresed on 1.5% LMPA gel. Quarters are visual between 3054 bp and 2036 bp mark. The Q2 and Q3 denotes quarter 2 and quarter 3.

3.2.2. Insertion of invariant chain into a vector

The first step of molecular cloning involved insertion of invariant chain into appropriate vector allowing screening for CD4+ T cell responses. After successfully inserted invariant chain we would continue with second step which involved molecular cloning of amplified BPLF1 gene quarters into appropriate vector already containing invariant chain. The cloning process was repeated three times in order to increase transformation efficiency as presented on figure 20. In third experiment we used electroporation and transformation efficiency increased for approximately 3.7-fold in comparison to second experiment and 200-fold in comparison to the first experiment as in first and second experiment electroporation was not used.

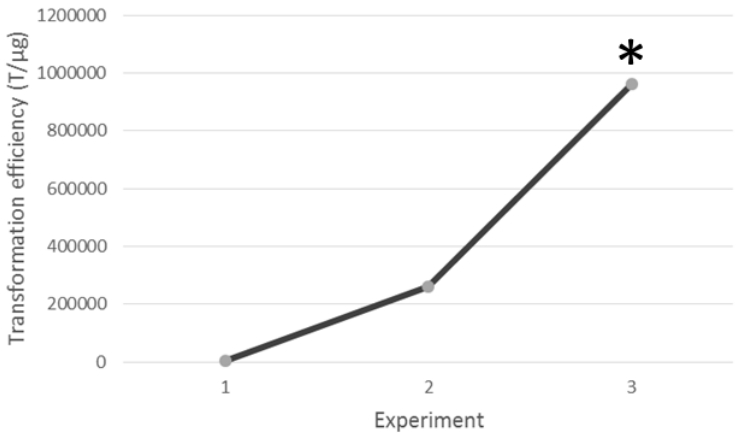

Figure 20: Transformation efficiency (T/µg). Figure presents transformation efficiency of all experiments. Data presented was obtained from three experiments. Asterisk (*) denotes transformation efficiency in experiment three where electroporation was used. With use of electroporation transformation efficiency increased dramatically as it was 3.7-fold higher in comparison to second experiment and as high as 200-fold in comparison to the first experiment.

After transformation DNA samples with potential constructs containing invariant chain were selected and digested as described in section 2.4.6 to identify DNA samples containing plasmid pENTR1A with invariant chain. Samples containing invariant chain were identified as the invariant chain in the DNA sample construct was seen as second line below 220 bp (figure 21).

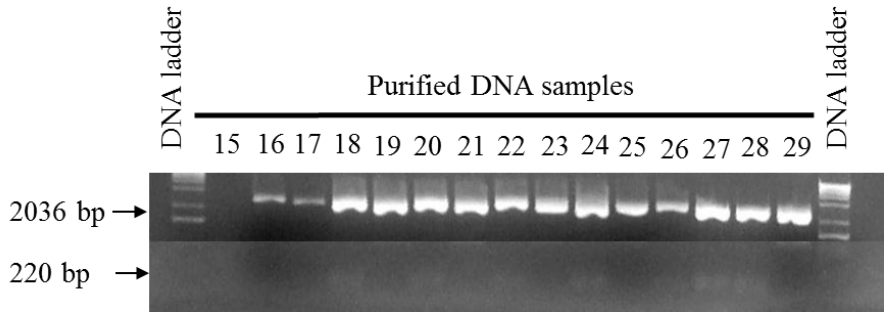

Figure 21: Identification of samples containing invariant chain. Example figure presents purified DNA samples on agarose gel. Samples containing potential successfully obtained plasmid pENTR1A with invariant chain are visualised as second line below 220 bp. Numbers (15 – 29) denote sample number.

Furthermore, DNA samples with potential constructs containing invariant chain were digested as described in section 2.4.6 to identify the orientation of inserted invariant chain. Invariant chain in sense orientation was on agarose gel visualised as a second line below 517 bp (figure 22).

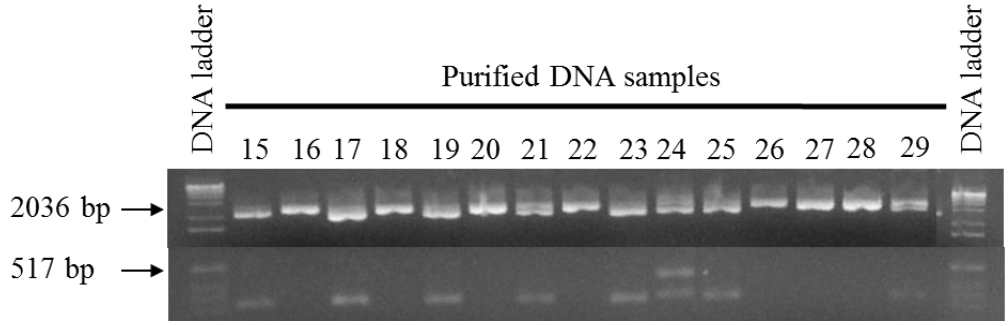

Figure 22: Identification of invariant chain orientation. Example figure presents purified DNA samples on agarose gel. Samples containing plasmid pENTR1A with invariant chain in sense orientation are visualised as a single line below 517 bp. Numbers (15 – 29) denote sample number.

The identified DNA samples containing invariant chain in sense orientation were sent for a DNA sequencing and DNA sequences were obtained (data not shown). However, despite positive identification of DNA samples on agarose gel non of the sequenced DNA samples contained the right DNA sequence. Therefore, we did not achieve the aim of successfully inserting the BPLF1 gene into the vector in the duration of this project, as we were not able to insert the invariant chain into the vector.

4. Discussion

EBV is one of the eight human herpesviruses that infects >90% of the world population. Most people are infected without knowing it as they become infected during infanthood presenting no symptoms. EBV is also classified as group 1 agent – carcinogenic to humans (Taylor and Blackbourn, 2011) and is one of the oncoviruses (Schiller and Lowy, 2010, Butt and Miggin, 2012). In 2008 there were approximately 200,000 new cases (10%) of EBV associated malignancies worldwide (Cohen et al., 2011, de Martel et al., 2012) therefore, prevention of primary infection is important and novel vaccines need to be developed as past EBV vaccine attempts have failed. However, two successful examples of vaccines consisting of surface antigens (i.e. hepatitis B surface antigen HBsAg in hepatitis B vaccine (Keating and Noble, 2003)) and capsid proteins (i.e. major capsid protein L1 of human papilloma virus types 6, 11, 16 and 18 in quadrivalent HPV vaccine (Bryan, 2007)) are very encouraging. The aim of this thesis was to investigate T cell responses in healthy EBV-seropositive donors to two EBV structural proteins MCP, encoded by BcLF1, and LTP, encoded by BPLF1. The MCP is the largest among EBV capsid proteins and the LTP is the largest among EBV tegument proteins (Johannsen et al., 2004). Despite of the fact that this two proteins are large and abundantly expressed their importance at primary infection is still poorly understood. Therefore, it was necessary to investigate MCP and LTP potency as possible targets of future prophylactic EBV vaccine which would prevent EBV-associated malignancies and infectious mononucleosis.

The results of the cellular part presented in this thesis have shown that T cells obtained from healthy EBV-seropositive donors do respond to MCP and LTP epitopes. Moreover, T cell responses expanded after 7 days of culture. Furthermore, after CD4+ T cell depletion from four representative donors we have observed predominant T cell responses from one subset of T cells (CD4+ or CD8+ T cells) in two donors. In other donors we have observed responses from both subsets of T cells. We successfully established T cell clones specific for MCP from one representative donor (donor 1) and determined whether clones were CD4+ or CD8. Subsequently, CD8+ T cell clones 56

and 88 were HLA-restricted showing that they were HLA-C*06 restricted. Additionally, the results showed that CD4+ T cell clones recognised lytic LCLs. Overall, the work suggests that the MCP and LTP do elicit immunogenic T cell responses in healthy EBV-seropositive people highlighting the potential of structural proteins as EBV vaccine targets. Based on the current work, the EBV structural protein BcLF1 might be a suitable candidate, if it can be established that T cells targeting this protein, recognise (and kill) cells infected with EBV early in the infective cycle (i.e. within 24 hours).

The first question we addressed in cellular biology part of this project was whether people have T cells that recognise the MCP and LTP. It has been suggested that MCP is not expressed on the surface of infected cells in healthy EBV-seropositive people (Prang et al., 1997). However, the results of this project imply that T cells obtained from healthy EBV-seropositive donors do indeed recognise predicted epitopes of the MCP and LTP. For example, donor 1 did not exhibit a detectable ex-vivo response, however, after seven days of culture, responses were readily observed. Further, both CD4+ and CD8+ T cell clones were obtained from donor 1. In donor 5 we observed very high T cell responses to peptide pools 10 and 11 showing recognition of epitopes derived from the LTP. It can be confirmed that the results reported are not laboratory error: all values were compared to negative controls (DMSO) to rule out non-specific responses as a result of infection. Further, to monitor the reliability of the assay, control peptides from EBV proteins known to elicit a response in donors were used.

The next question to address was whether the obtained *ex-vivo* T cell responses would expand over time, therefore T cells were cultured for 7 days. As expected, the responses from these *in-vitro* experiments were higher than *ex*-vivo responses. For example in donor 4, ex-vivo responses in peptide pool 10 were 8 spots/million cells. Following 7 days of culture, this donor exhibited a response of 324 spots/million cells. Therefore, results confirmed the expansion of T cell responses after 7 days of culture. Interestingly, T cell responses to some peptide pools were that were observed *ex-vivo* were undetectable in the *in-vitro* experiments. Considering that *ex-vivo* T cell responses were sometimes very low and close to the limit of detection, it is likely that

some responses were indeed spurious results. This highlights the utility of using the seven days of culture experiments to confirm responses. Indeed, some responses were not detected *ex-vivo* were detectable after expansion seven days later.

Following the confirmation that T cells recognise epitopes derived from the MCP and LTP and that the T cell responses expand over time, the next question to address was which subset of T cells (CD4+ and/or CD8+ T cells) exhibits this response. For some of the EBV structural proteins relative immune-dominance for CD4+ and CD8+ T cell responses have already been determined. For example, the largest and most frequent responses come from latent proteins and are directed towards proteins such as EBNAs 1, 2 and 3A (Hislop et al., 2007). However, CD4+ T cell responses have been so far less studied (Precopio et al., 2003). In only 4/11 peptide pools we observed clear dominance of T cell responses of only one subset of T cells. The responses derived from the CD8+ T cells. However, in other peptide pools the majority T cell responses derived from both subsets. This data was derived by separating CD4+ T cells using magnetic beads, and assaying the resulting CD4+ cells separately from the remainder (i.e., all other cells including CD8+). A possible reason for observing T cell responses in both pools of T cells might be due to impure separation of cells. Good practice would be to check the purity of isolated CD4+ T cells using flow cytometry, however this was not feasible in the current project. An alternative to separating CD4+ T cells using magnetic beads that might result in greater purity is sorting cells using a flow cytometric approach.

Once it was established that healthy donors exhibit frequent T cell responses to the MCP and LTP the next part of this thesis aimed to generate and characterise T cell clones. We successfully obtained T cell clones specific for MCP but were unable to obtain LTP-specific clones. Cloning was undertaken using IFN-γ capture. MCP-specific T cells were obtained after the first attempt at cloning, whereas LTP-specific clones were not generated despite several attempts. It might be that an alternative enrichment strategy would yield different results, such as CD137 capture (for CD8+ T cells) and CD154 capture (for CD4+ T cells).

After successfully generating MCP-specific clones and expanding the cells, the project next undertook an HLA class-I restriction experiment. T cell clones 56 and 88 were HLA-C*06 restricted. The current work is novel by showing that an HLA-C*06 restricted epitope exists within the MCP. Unfortunately, it was beyond the scope of this project to identify the stimulating peptide within the pool of predicted T cell epitopes, nor was it possible to restrict the 20mer peptides down to the minimal 9mer epitope.

The last question to address in cellular biology part of the project was whether CD4+ T cell clones specific for MCP recognise lytic LCLs. The results showed a very small response to the autologous latent (i.e., B95.8) LCLs, which likely represents the small number of LCLs in the lytic cycle. However, this response was barely above background. Importantly, there was a T cell response to lytic LCLs (of which 10% had been confirmed to be lytic). This response was clearly higher than the response to the latent LCLs, but much lower than the peptide-pulsed autologous LCLs. The relatively small response might suggest that there is a low natural expression of an epitope derived from the MCP on the surface of LCLs, or more likely reflects the small number (i.e., only 10% of cells). It should be considered that staining for the late antigen VCA might be a more accurate alternative to BZLF1 staining to establish how many LCLs are in lytic cycle. If it can be shown that the MCP is expressed to a high level on infected cells early in the infective cycle, and the frequent T cell response shown by the present study results in killing of infected cells, then structural proteins such as the MCP might warrant further investigation as vaccine candidates.

The aims of molecular biology part of this project were to amplify the BPLF1 gene that encodes the LTP and to insert the invariant chain into the pENTR1A vector alongside BPLF1. The relevance of this part of the project was to create a tool to assess T cell responses to the LTP using a whole antigen approach that is independent of HLA-type. In the current project, we were able to amplify the BPLF1 gene by PCR in four quarters. Previous attempts at amplifying BPLF1 as the entire gene, or the gene split into two had failed (data not shown in this thesis) – likely due to the size of the gene.

Unfortunately we were not able to insert the invariant chain into pENTR1A vector, shown by incorrect DNA sequences in the constructs. This might be due to contamination of samples in the molecular cloning process. Therefore, we were not able to proceed to the next step where we would insert the BPLF1 gene. Further work is required to generate tools to screen T cell responses to EBV structural proteins that are independent of HLA-type.

SUMMARY, CONSIDERATIONS AND FUTURE WORK:

In this project only nine donors were screened for T cell responses therefore, to validate these preliminary findings a larger number of healthy EBV-seropositive people should be screened for T cell responses to EBV structural proteins. Also to confirm that MCP and LTP can only be detected in EBV-seropositive people EBV-seronegative people should be screened for T cell responses to MCP and LTP even though, it is suggested that T cell responses to the LTP cannot be detected in EBV-seronegative people (Schmaus et al., 2004). Furthermore, people with IM and EBV malignant tumours should be screened for MCP and LTP to examine whether they exhibit impaired immunity. If this is the case, and the MCP and LTP are shown to be efficacious vaccine candidates, then a vaccine would be particularly warranted in these individuals.

The prediction of T cell epitopes method used in cellular biology part of this project is not the only strategy for screening T cell responses. Screening using a whole antigen approach is also desirable as it is not dependent on HLA-type. Unfortunately, this was not achieved in the current project. Using T cell epitopes that were predicted to be HLA-A*02 or HLA-B*07 restricted should in theory only elicit responses in HLA-A*02 or HLA-B*07 donors. Nevertheless, donor 3 included in our project was HLA-A*03 and 11 and HLA-B*15 and 35 and exhibited T cell responses to the predicted T cell epitopes from both MCP and LTP. Thus, despite using a combination of three online prediction algorithms, and only selecting peptides that concurred, predictions are clearly only an estimate, and generate T cell epitopes of other specificities. However, using a T cell

epitope prediction algorithm is a more informed way of dissecting a protein randomly, and is more cost effective than buying overlapping peptides.

In addition to circumventing the methodological limitations of this project (e.g., attempting different T cell cloning techniques, and persevering with the molecular biology), further experiments should be conducted to validate preliminary results presented in this thesis. The result would be to expand the knowledge of T cell responses to the MCP and LTP. The first experiment could include successful establishment of T cell clones specific for LTP. Furthermore, experiments to identify minimal T cell epitopes for both the MCP and LTP would have to be conducted. This could be achieved by systematically shortening the sequence of stimulating T cell epitopes from 20mers down to 9mers, screening T cell clones for IFN-γ production. It was shown in this thesis that CD4+ T cell clones specific for the MCP recognise lytic LCLs. It was shown in this thesis that CD4+ T cell clones specific for the MCP recognise lytic LCLs. A consideration is what the source of the antigen was and its route of presentation to the T cell. For example, it is currently unknown whether CD4+ T cells are directly recognising endogenously processed and presented antigen by the lytic LCL, or whether this antigen is derived from viral particles released from other lytic cells which have then bound to neighbouring LCLs with epitopes being processed and presented from the abundant virion protein to the T cells. This could be addressed by an experiment that would require a full HLA-restriction of the CD4+ T cell clones. In the experiment to explain the source of antigen, CD4+ T cell clones would be incubated with two different panels of LCLs at the same time. First, HLA-mismatched LCLs expressing a full panel of EBV proteins would be added to T cells, and, as with all LCLs, a number of these cells would be in lytic cycle, the proportion of which could be shown by BZLF1 or VCA staining and flow cytometry. Second, BZLF1 knock out LCLs with the HLA-type matched to the CD4+ T cell clones would also be added. IFN-γ produced by CD4+ T cell clones would indicate that antigens and/or virus are being released from the lytic LCLs (which would not be recognised by the clones) but would be taken up and processed by the latent BZLF1 knock out LCLs. In turn, antigen presented to clones by the BZLF1 LCLs would be recognised due to matched HLA-typing. As the BZLF1

knock out LCLs cannot enter lytic cycle, the presentation of BcLF1 epitopes could only be a result of virions/antigen being released from the mismatched LCLs. This experiment would clarify whether cell/cell contact would be needed or antigen could be recognised directly by the CD4+ T cell clones.

Irrespective of the source of antigen, the above result and discussion implies that CD4+ T cells may recognise newly infected B cells. Along with examining a similar effect in CD8+ T cells, it would be of importance to examine how quickly after infection, the MCP and LTP proteins are expressed, and how quickly a T cell response can be detected. If MCP or LTP-specific T cells recognise (and kill) B cells very early in the infective cycle (i.e., within 24 hours) then it might be that these EBV structural proteins are good vaccine targets. To further investigate MCP and LTP specific T cell responses, killing assays could be performed to inspect whether T cell clones destroy their targets. For a prophylactic vaccine to be successful, it would need to generate long lasting T cell immunity that both recognises and eliminates infected cells.

CONCLUSION:

The results of this thesis show that healthy people exhibit frequent CD4+ and CD8+ T cell responses to two EBV structural proteins, the MCP and LTP. The results of this thesis imply that the MCP and LTP are expressed in healthy EBV-seropositive people. The most important finding in this project is that CD4+ T cell clones specific for the MCP recognise lytic LCLs. The results presented are preliminary but promising.

References

ADAMS, M. J. & CARSTENS, E. B. 2012. Ratification vote on taxonomic proposals to the International Committee on Taxonomy of Viruses (2012). *Arch Virol,* 157**,** 1411-22.

ADHIKARY, D., BEHRENDS, U., BOERSCHMANN, H., PFÜNDER, A., BURDACH, S., MOOSMANN, A., WITTER, K., BORNKAMM, G. W. & MAUTNER, J. 2007. Immunodominance of lytic cycle antigens in Epstein-Barr virus-specific CD4+ T cell preparations for therapy. *PLoS One,* 2**,** e583.

ALBERTS, B., JOHNSON, A., LEWIS, J., RAFF, M., ROBERTS, K. & WALTER, P. 2007. *Molecular Biology of the Cell,* New York, Garland Science.

BANKS, T. A. & ROUSE, B. T. 1992. Herpesviruses--immune escape artists? *Clin Infect Dis,* 14**,** 933-41.

BIRK, T., KRISTENSEN, K., HARBOE, A., HANSEN, T. B., INGMER, H., DE JONGE, R., TAKUMI, K. & AABO, S. 2012. Dietary proteins extend the survival of Salmonella Dublin in a gastric acid environment. *J Food Prot,* 75**,** 353-8.

BRYAN, J. T. 2007. Developing an HPV vaccine to prevent cervical cancer and genital warts. *Vaccine,* 25**,** 3001-6.

BUTT, A. Q. & MIGGIN, S. M. 2012. Cancer and viruses: a double-edged sword. *Proteomics,* 12**,** 2127-38.

CHEN, K. & CERUTTI, A. 2011. The function and regulation of immunoglobulin D. *Curr Opin Immunol,* 23**,** 345-52.

COHEN, J. I. 2000. Epstein-Barr virus infection. *N Engl J Med,* 343**,** 481-92.

COHEN, J. I., FAUCI, A. S., VARMUS, H. & NABEL, G. J. 2011. Epstein-Barr virus: an important vaccine target for cancer prevention. *Sci Transl Med,* 3**,** 107fs7.

COHEN, J. I., MOCARSKI, E. S., RAAB-TRAUB, N., COREY, L. & NABEL, G. J. 2013. The need and challenges for development of an Epstein-Barr virus vaccine. *Vaccine,* 31 Suppl 2**,** B194-6.

COMBADIERE, B. & LIARD, C. 2011. Transcutaneous and intradermal vaccination. *Hum Vaccin,* 7**,** 811-27.

CROIA, C., SERAFINI, B., BOMBARDIERI, M., KELLY, S., HUMBY, F., SEVERA, M., RIZZO, F., COCCIA, E. M., MIGLIORINI, P., ALOISI, F. & PITZALIS, C. 2012. Epstein-Barr virus persistence and infection of autoreactive plasma cells in synovial lymphoid structures in rheumatoid arthritis. *Ann Rheum Dis*.

DAVISON, A. J. 2011. Evolution of sexually transmitted and sexually transmissible human herpesviruses. *Ann N Y Acad Sci,* 1230**,** E37-49.

DE MARTEL, C., FERLAY, J., FRANCESCHI, S., VIGNAT, J., BRAY, F., FORMAN, D. & PLUMMER, M. 2012. Global burden of cancers attributable to infections in 2008: a review and synthetic analysis. *Lancet Oncol,* 13**,** 607-15.

DOUGAN, M. & DRANOFF, G. 2012. Immunoterapy of cancer. *In:* WANG, R. (ed.) *Innate Immune Regulation and Cancer Immunotherapy.* New York: Springer New York.

DRABORG, A. H., DUUS, K. & HOUEN, G. 2012. Epstein-Barr virus and systemic lupus erythematosus. *Clin Dev Immunol,* 2012**,** 370516.

ELLIOTT, S. L., SUHRBIER, A., MILES, J. J., LAWRENCE, G., PYE, S. J., LE, T. T., ROSENSTENGEL, A., NGUYEN, T., ALLWORTH, A., BURROWS, S. R., COX, J., PYE, D., MOSS, D. J. & BHARADWAJ, M. 2008. Phase I trial of a CD8+ T-cell peptide epitope-based vaccine for infectious mononucleosis. *J Virol,* 82**,** 1448-57.

FLESCH, I. E., WONG, Y. C. & TSCHARKE, D. C. 2012. Analyzing CD8 T cells in mouse models of poxvirus infection. *Methods Mol Biol,* 890**,** 199-218.

GASTALDELLO, S., HILDEBRAND, S., FARIDANI, O., CALLEGARI, S., PALMKVIST, M., DI GUGLIELMO, C. & MASUCCI, M. G. 2010. A deneddylase encoded by Epstein-Barr virus promotes viral DNA replication by regulating the activity of cullin-RING ligases. *Nat Cell Biol,* 12**,** 351-61.

GILDEN, D. H., MAHALINGAM, R., COHRS, R. J. & TYLER, K. L. 2007. Herpesvirus infections of the nervous system. *Nat Clin Pract Neurol,* 3**,** 82-94.

GIUDICE, E. L. & CAMPBELL, J. D. 2006. Needle-free vaccine delivery. *Adv Drug Deliv Rev,* 58**,** 68-89.

GU, S. Y., HUANG, T. M., RUAN, L., MIAO, Y. H., LU, H., CHU, C. M., MOTZ, M. & WOLF, H. 1995. First EBV vaccine trial in humans using recombinant vaccinia virus expressing the major membrane antigen. *Dev Biol Stand,* 84**,** 171-7.

HENSON, B. W., PERKINS, E. M., COTHRAN, J. E. & DESAI, P. 2009. Self-assembly of Epstein-Barr virus capsids. *J Virol,* 83**,** 3877-90.

HISLOP, A. D., TAYLOR, G. S., SAUCE, D. & RICKINSON, A. B. 2007. Cellular responses to viral infection in humans: lessons from Epstein-Barr virus. *Annu Rev Immunol,* 25**,** 587-617.

HUI, E. P., TAYLOR, G. S., JIA, H., MA, B. B., CHAN, S. L., HO, R., WONG, W., WILSON, S., JOHNSON, B. F., EDWARDS, C., STOCKEN, D. D., RICKINSON, A. B., STEVEN, N. M. & CHAN, A. T. 2013. Phase 1 trial of recombinant Modified Vaccinia Ankara (MVA) encoding Epstein-Barr viral tumor antigens in nasopharyngeal carcinoma patients. *Cancer Res*.

JANEWAY, C. A. J., TRAVERS, P. & WALPORT, M. 1999. *Immunobiology: the immune system in health and disease*, Current Biology Publications.

JEMAL, A., BRAY, F., CENTER, M. M., FERLAY, J., WARD, E. & FORMAN, D. 2011. Global cancer statistics. *CA Cancer J Clin,* 61**,** 69-90.

JOHANNSEN, E., LUFTIG, M., CHASE, M. R., WEICKSEL, S., CAHIR-MCFARLAND, E., ILLANES, D., SARRACINO, D. & KIEFF, E. 2004. Proteins of purified Epstein-Barr virus. *Proc Natl Acad Sci U S A,* 101**,** 16286-91.

KEATING, G. M. & NOBLE, S. 2003. Recombinant hepatitis B vaccine (Engerix-B): a review of its immunogenicity and protective efficacy against hepatitis B. *Drugs,* 63**,** 1021-51.

KUTOK, J. L. & WANG, F. 2006. Spectrum of Epstein-Barr virus-associated diseases. *Annu Rev Pathol,* 1**,** 375-404.

LONG, H. M., TAYLOR, G. S. & RICKINSON, A. B. 2011. Immune defence against EBV and EBV-associated disease. *Curr Opin Immunol,* 23**,** 258-64.

LOSSIUS, A., JOHANSEN, J. N., TORKILDSEN, Ø., VARTDAL, F. & HOLMØY, T. 2012. Epstein-Barr virus in systemic lupus erythematosus, rheumatoid arthritis and multiple sclerosis—association and causation. *Viruses,* 4**,** 3701-30.

LOUIS, C. U., STRAATHOF, K., BOLLARD, C. M., ENNAMURI, S., GERKEN, C., LOPEZ, T. T., HULS, M. H., SHEEHAN, A., WU, M. F., LIU, H., GEE, A., BRENNER, M. K., ROONEY, C. M., HESLOP, H. E. & GOTTSCHALK, S. 2010. Adoptive transfer of EBV-specific T cells results in sustained clinical responses in patients with locoregional nasopharyngeal carcinoma. *J Immunother,* 33**,** 983-90.

LUZURIAGA, K. & SULLIVAN, J. L. 2010. Infectious mononucleosis. *N Engl J Med,* 362**,** 1993-2000.

MEYDING-LAMADÉ, U. & STRANK, C. 2012. Herpesvirus infections of the central nervous system in immunocompromised patients. *Ther Adv Neurol Disord,* 5**,** 279-96.

MICHELOW, P., WRIGHT, C. & PANTANOWITZ, L. 2012. A review of the cytomorphology of Epstein-Barr virus-associated malignancies. *Acta Cytol,* 56**,** 1-14.

MOSER, M. & LEO, O. 2010. Key concepts in immunology. *Vaccine,* 28 Suppl 3**,** C2-13.

MÜNZ, C. & MOORMANN, A. 2008. Immune escape by Epstein-Barr virus associated malignancies. *Semin Cancer Biol,* 18**,** 381-7.

NEUTRA, M. R. & KOZLOWSKI, P. A. 2006. Mucosal vaccines: the promise and the challenge. *Nat Rev Immunol,* 6**,** 148-58.

OGEMBO, J. G., KANNAN, L., GHIRAN, I., NICHOLSON-WELLER, A., FINBERG, R. W., TSOKOS, G. C. & FINGEROTH, J. D. 2013. Human Complement Receptor Type 1/CD35 Is an Epstein-Barr Virus Receptor. *Cell Rep*.

PARKER, K. C., BEDNAREK, M. A. & COLIGAN, J. E. 1994. Scheme for ranking potential HLA-A2 binding peptides based on independent binding of individual peptide side-chains. *J Immunol,* 152**,** 163-75.

PATRONOV, A. & DOYTCHINOVA, I. 2013. T-cell epitope vaccine design by immunoinformatics. *Open Biol,* 3**,** 120139.

PERCIVAL, S. L., EMANUEL, C., CUTTING, K. F. & WILLIAMS, D. W. 2012. Microbiology of the skin and the role of biofilms in infection. *Int Wound J,* 9**,** 14-32.

PRANG, N. S., HORNEF, M. W., JÄGER, M., WAGNER, H. J., WOLF, H. & SCHWARZMANN, F. M. 1997. Lytic replication of Epstein-Barr virus in the peripheral blood: analysis of viral gene expression in B lymphocytes during infectious mononucleosis and in the normal carrier state. *Blood,* 89**,** 1665-77.

PRECOPIO, M. L., SULLIVAN, J. L., WILLARD, C., SOMASUNDARAN, M. & LUZURIAGA, K. 2003. Differential kinetics and specificity of EBV-specific CD4+ and CD8+ T cells during primary infection. *J Immunol,* 170**,** 2590-8.

RAMMENSEE, H.-G., BACHMANN, J., EMMERICH, N. N., BACHOR, O. A. & STEVANOVIC, S. 1999. SYFPEITHI: database for MHC ligands and peptide motifs. *Immunogenetics.*

RAPPUOLI, R., MANDL, C. W., BLACK, S. & DE GREGORIO, E. 2011. Vaccines for the twenty-first century society. *Nat Rev Immunol,* 11**,** 865-72.

ROSE, M. A., ZIELEN, S. & BAUMANN, U. 2012. Mucosal immunity and nasal influenza vaccination. *Expert Rev Vaccines,* 11**,** 595-607.

SALIMI, N., FLERI, W., PETERS, B. & SETTE, A. 2012. The immune epitope database: a historical retrospective of the first decade. *Immunology,* 137**,** 117-23.

SCHIFFER, J. T. & COREY, L. 2013. Rapid host immune response and viral dynamics in herpes simplex virus-2 infection. *Nat Med,* 19**,** 280-90.

SCHILLER, J. T. & LOWY, D. R. 2010. Vaccines to prevent infections by oncoviruses. *Annu Rev Microbiol,* 64**,** 23-41.

SCHMAUS, S., WOLF, H. & SCHWARZMANN, F. 2004. The reading frame BPLF1 of Epstein-Barr virus: a homologue of herpes simplex virus protein VP16. *Virus Genes,* 29**,** 267-77.

SHAW, P. L., KIRSCHNER, A. N., JARDETZKY, T. S. & LONGNECKER, R. 2010. Characteristics of Epstein-Barr virus envelope protein gp42. *Virus Genes,* 40**,** 307-19.

SHOUVAL, D. 2003. Hepatitis B vaccines. *J Hepatol,* 39 Suppl 1**,** S70-6.

SITKI-GREEN, D., COVINGTON, M. & RAAB-TRAUB, N. 2003. Compartmentalization and transmission of multiple epstein-barr virus strains in asymptomatic carriers. *J Virol,* 77**,** 1840-7.

SMITH, P. K., KROHN, R. I., HERMANSON, G. T., MALLIA, A. K., GARTNER, F. H., PROVENZANO, M. D., FUJIMOTO, E. K., GOEKE, N. M., OLSON, B. J. & KLENK, D. C. 1985. Measurement of protein using bicinchoninic acid. *Anal Biochem,* 150**,** 76-85.

SOKAL, E. M., HOPPENBROUWERS, K., VANDERMEULEN, C., MOUTSCHEN, M., LÉONARD, P., MOREELS, A., HAUMONT, M., BOLLEN, A., SMETS, F. & DENIS, M. 2007. Recombinant gp350 vaccine for infectious mononucleosis: a phase 2, randomized, double-blind, placebo-controlled trial to evaluate the safety, immunogenicity, and efficacy of an Epstein-Barr virus vaccine in healthy young adults. *J Infect Dis,* 196**,** 1749-53.

STRAUS, S. E., COHEN, J. I., TOSATO, G. & MEIER, J. 1993. NIH conference. Epstein-Barr virus infections: biology, pathogenesis, and management. *Ann Intern Med,* 118**,** 45-58.

TAYLOR, G. S. & BLACKBOURN, D. J. 2011. Infectious agents in human cancers: lessons in immunity and immunomodulation from gammaherpesviruses EBV and KSHV. *Cancer Lett,* 305**,** 263-78.

TIERNEY, R. J., EDWARDS, R. H., SITKI-GREEN, D., CROOM-CARTER, D., ROY, S., YAO, Q. Y., RAAB-TRAUB, N. & RICKINSON, A. B. 2006. Multiple Epstein-Barr virus strains in patients with infectious mononucleosis: comparison of ex vivo samples with in vitro isolates by use of heteroduplex tracking assays. *J Infect Dis,* 193**,** 287-97.

TSELIS, A. 2012. Epstein-Barr virus cause of multiple sclerosis. *Curr Opin Rheumatol,* 24**,** 424-8.

VAN LIER, R. A., TEN BERGE, I. J. & GAMADIA, L. E. 2003. Human CD8(+) T-cell differentiation in response to viruses. *Nat Rev Immunol,* 3**,** 931-9.

VINER, K., PERELLA, D., LOPEZ, A., BIALEK, S., NEWBERN, C., PIERRE, R., SPELLS, N. & WATSON, B. 2012. Transmission of varicella zoster virus from individuals with herpes zoster or varicella in school and day care settings. *J Infect Dis,* 205**,** 1336-41.

WANG, M., HE, H. J., TURKO, I. V., PHINNEY, K. W. & WANG, L. 2013a. Quantifying the cluster of differentiation 4 receptor density on human T lymphocytes using multiple reaction monitoring mass spectrometry. *Anal Chem,* 85**,** 1773-7.

WANG, M., YIN, B., MATSUEDA, S., DENG, L., LI, Y., ZHAO, W., ZOU, J., LI, Q., LOO, C., WANG, R. F. & WANG, H. Y. 2013b. Identification of Special AT-Rich Sequence Binding Protein 1 as a Novel Tumor Antigen Recognized by CD8(+) T Cells: Implication for Cancer Immunotherapy. *PLoS One,* 8**,** e56730.

WHITEHURST, C. B., VAZIRI, C., SHACKELFORD, J. & PAGANO, J. S. 2012. Epstein-Barr virus BPLF1 deubiquitinates PCNA and attenuates polymerase η recruitment to DNA damage sites. *J Virol,* 86**,** 8097-106.

WU, T. T., BLACKMAN, M. A. & SUN, R. 2010. Prospects of a novel vaccination strategy for human gamma-herpesviruses. *Immunol Res,* 48**,** 122-46.

YE, J., COULOURIS, G., ZARETSKAYA, I., CUTCUTACHE, I., ROZEN, S. & MADDEN, T. L. 2012. Primer-BLAST: a tool to design target-specific primers for polymerase chain reaction. *BMC Bioinformatics,* 13**,** 134.

YU, M. & VAJDY, M. 2010. Mucosal HIV transmission and vaccination strategies through oral compared with vaginal and rectal routes. *Expert Opin Biol Ther,* 10**,** 1181-95.

ZAVALA-RUIZ, Z., STRUG, I., WALKER, B. D., NORRIS, P. J. & STERN, L. J. 2004. A hairpin turn in a class II MHC-bound peptide orients residues outside the binding groove for T cell recognition. *Proc Natl Acad Sci U S A,* 101**,** 13279-84.

ZEPP, F. 2010. Principles of vaccine design-Lessons from nature. *Vaccine,* 28 Suppl 3**,** C14-24.

UNIVERSITY OF BIRMINGHAM

PROJECT 2: ANALYSING THE TRANSCRIPTIONAL RESPONSE TO HISTONE DEACETYLASE INHIBITORS TREATMENT IN NORMAL AND CANCER CELL LINES

BY

TEJA BAJT

This project is submitted in partial fulfilment of the requirements for the award of the MRes in Molecular and Cellular Biology.

Supervisor: Prof Bryan M Turner

Institute of Biomedical Research
University of Birmingham
July 2013

Abstract

The leading cause of death in developed countries is attributed to cancer thus, cancer is becoming a major health problem worldwide as in 2008 there were 12.7 million new cases and 7.6 million people died of cancer worldwide. Therefore, the progress in treatment options is of crucial importance as even in the 21st century cancer treatment is still challenging.

The overall progress of medicine has opened new possibilities of potential advanced therapies and one of them is the epigenetic therapy involving the treatment with HDAC inhibitors such as valproic acid (VPA). In order to any new chemotherapeutic agent becomes available for treatment the effects have to be characterized and responses of normal and cancer cells have to be assessed.

In our project we have utilized microarray analysis to examine transcriptional response in lymphoblastoid cell line (LCLs) and Burkitt lymphoma cells (BLs). Our results showed an increased histone acetylation levels in treated cells and changes in cell cycle with cell cycle arrest in LCLs and BLs. Additionally, in some BLs substantial apoptosis was observed. In LCLs we also observed morphological changes in treated groups. When performing gene ontology (GO) analysis we saw enrichment in GO terms cell cycle in LCLs whereas, in BLs GO terms related to small cell lung cancer, prostate cancer and p53 signalling pathway were enriched. This results suggest that VPA may be affecting tumour signalling pathways in cancer cells but do not affect normal cells.

Acknowledgements

I would firstly like to thank my supervisor Prof Bryan M Turner for giving me the opportunity to work within his research group and for his guidance and advices in the thesis writing. I would also like to thank to my tutor Dr John A Halsall for all his support and guidance in laboratory and in the thesis writing. In addition, I would also like to thank Dr Karl P Nightingale who gave me advices on thesis writing. All their help and advices have been highly valued all through the project.

I would also like to thank Charlotte Rutledge, Maaike Wiersma, Edith Terrenoire and Hannah Goss who also provided much help in the lab. Thank you for welcoming me to your group.

Last but not least, I would like to thank my family and Danijel for their unconditional support. Without them being always there for me I would not achieve this.

Abbreviations

APS	Ammonium persulfate
BL	Burkitt's lymphoma
BSA	Bovine Serum Albumin
dH_20	Distilled water
DMSO	Dimethyl sulfoxide
DNA	Deoxyribonucleic acid
EDTA	Ethylene-diamine-tetra-acetic acid
FBS	Fetal Bovine Serum
HCl	Hydrochloric acid
LCL	Lymphoblastoid cell line
PBS	Phosphate-Buffered Saline
PCR	Polymerase Chain Reaction
PMSF	Phenylmethanesulfonyl Fluoride
RNA	Ribonucleic acid
RPMI	Roswell Park Memorial Institute media
SDS	Sodium dodecyl sulfate
TAE	Tris-acetate-EDTA buffer
TBS-T	Tris-Buffered Saline
TEB	Triton Extraction Buffer
TEMED	N'-tetramethylethylenediamine
$u.p.H_2O$	Ultra pure water
VPA	Sodium valproate

List of Contents

List of Figures and Tables

1. Introduction

1.1. Overview

Cancer has become a leading cause of death in developed countries whereas, in developing countries it is the second leading cause of death (Jemal et al., 2011). Even in the 21st century, with remarkable progress in molecular and cellular biology, cancer treatment is still challenging. In general the treatment consists of chemotherapy, immunotherapy, hormonal therapy, radiation therapy and surgery (Baskar et al., 2012). However, in pursuance for a new strategies for cancer treatment epigenetic therapy emerged (Mai and Altucci, 2009), as epigenetic defects were found in many diseases and the majority of them were cancers (Nakao, 2001). Epigenetic defects, such as redistribution of histone modifications (Ghai et al., 2013), can occur due to changes in the epigenome promoting transcriptional repression of tumour suppressor genes causing tumourigenesis and cancer progression (Carew et al., 2008). Therefore, epigenetic therapy which corrects epigenetic defects shows a promising potential towards advanced cancer treatment (Peedicayil, 2006). Acetylation is one of many histone modifications and is regulated by histone acetyltransferases (HATs) and histone deacetylases (HDACs). HDACs are transcriptional repressors and can repress tumour suppressor genes promoting tumour initiation. However, histone deacetylases inhibitors (HDACi) can restore normal expression levels of tumour suppression genes suppressed by HDACs (Bannister and Kouzarides, 2011). This project examined transcriptional response to HDACi treatment with valproic acid (VPA) in normal and cancer cell lines. The results of this project provide new insight in potential new chemotherapeutic agent.

1.2. Epigenetics

Epigenetics is a specific field of genetics and the word itself actually means “outside conventional genetics” (Jaenisch and Bird, 2003). In the middle of the 20th century genetic code was discovered and it was thought that genetic information is passed

from one cell to another with no changes except if mutations occur. It was elucidated decades later that there is another code termed the epigenetic code which can be altered depending on epigenetic marks but is heritable through cell proliferation (Huidobro et al., 2013). Epigenetics refers to the control of gene expression and cell phenotype without altering genomic DNA sequence (Bachmann and Bergmann, 2012, Tang et al., 2013, Ngalamika et al., 2012, Weitzman, 2012, Huidobro et al., 2013) by chromatin remodelling such as DNA methylation, histone modifications (e.g. methylation and acetylation of the histones) and non-coding RNAs (Bachmann and Bergmann, 2012).

1.3. Chromatin

In every cell of the human body there is 2 meters of DNA encoding approximately 23,000 protein-coding genes (Roopra et al., 2012) which are the template of our heredity (Jenuwein and Allis, 2001). $3x10^9$ bases of DNA needs to be packed into the nucleus in such a way as to be accessible for gene transcription replication and repair processes when necessary. Therefore, DNA is wrapped around basic proteins termed histones in a highly organised manner. The DNA -histones complex is called chromatin (Jenuwein and Allis, 2001, Roopra et al., 2012). Chromatin was first described 130 years ago (Hübner et al., 2013) and abnormal chromatin in cancer cell in 1914 by Theodor Boveri (Boveri, 1914). However, the true modern description of chromatin appeared in 1920 by Heitz (Heitz, 1929).

Chromatin plays a crucial role in regulation of gene expression as packaging of DNA regulates the genes accessibility (euchromatin) or inaccessibility (heterochromatin) to transcription (Hübner et al., 2013). The basic unit of chromatin is the nucleosome (Jiang and Pugh, 2009, Zentner and Henikoff, 2013), consisting of DNA wrapped around histones with linker DNA (Jenuwein and Allis, 2001, Hübner et al., 2013, Roopra et al., 2012, Inche and La Thangue, 2006, Tóth et al., 2013), which are 10 - 80 bp apart forming a 10 nm fibre termed “beads on a string”. When compacted even tighter the 10 nm fibre forms a higher order helical fibre 30nm in diameter with 6 - 11

nucleosomes per turn. 30 nm fibres have been so far only identified *in-vitro* but there is no clear evidence of 30 nm fibres *in-vivo*. These fibres are further condensed by addition of scaffold proteins into even higher order fibres in interphase and into 200 - 300 nm chromonema structure in mitotic chromosomes. Depending on the position in nucleus, the differentiation stage of the cell, the cell cycle etc. chromatin changes in structure (figure 1) (Hübner et al., 2013).

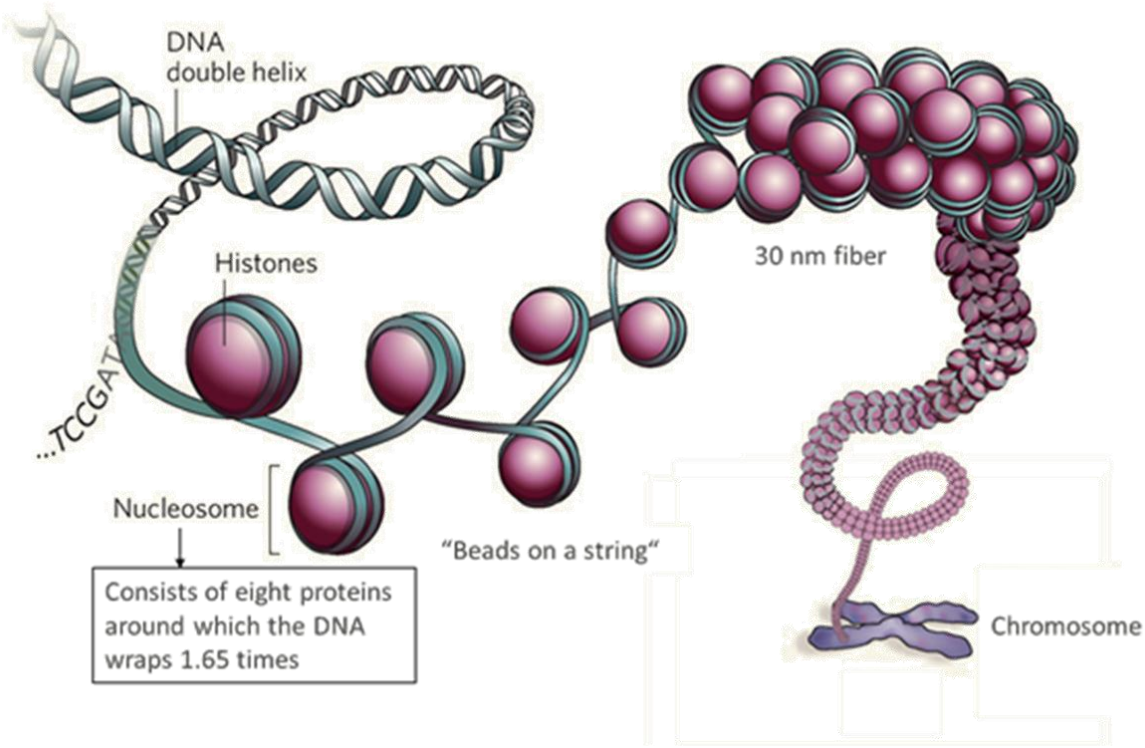

Figure 1: Chromatin structure and packaging. DNA double helix wraps around histones forming histone – DNA complex termed nucleosome which forms a higher order complex termed chromatosome with histone H1. This structure is termed "beads on a string" and is 10 nm in diameter. With further compaction 30 nm fibre is formed and with increased levels of compaction fibre is compacted into chromosomes. Adapted from (Baylin and Schuebel, 2007).

1.4. Nucleosomes

Position of nucleosomes on the genome is not random (Bai and Morozov, 2010) as proven with new advanced technologies which allowed nucleosome maps of some species, including human (Jiang and Pugh, 2009). Nucleosomes consist of 146 bp DNA

wrapped around an octamer of core histone proteins (an H3-H4 tetramer and two copies of H2A-H2B dimer) with linker histone protein H1 in 1.65 negatively supercoiled turns (Luger et al., 1997) (figure 2).

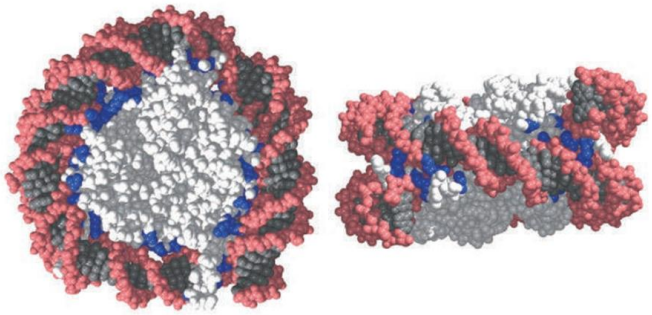

Figure 2: Nucleosome structure. Structure of the nucleosome obtained by x-ray crystallography showing histones (light grey) with DNA (dark grey with dark pink) and lysine residues between DNA and the histones (blue) (front and side view) (Jiang and Pugh, 2009).

Nucleosomes regulate accessibility of genes to transcriptional machinery (Roopra et al., 2012) and nucleosome maps revealed that 90% of promoters have a low number of nucleosomes. Those regions are termed nucleosome-depleted regions (NDR) (Bai and Morozov, 2010) or nucleosome-free regions (NFR) (Jiang and Pugh, 2009). Regulation is accomplished in several distinct ways, through replacement of core histones and repositioning or eviction of histones from DNA (Zentner and Henikoff, 2013).

1.4.1. Nucleosome positioning and transcription regulation

There are a few mechanisms by which nucleosome positioning regulates transcription of protein-coding genes in genome. Firstly, promoters are usually located in NDR which allows free binding of transcription factors to the promoter and consequently nucleosomes on both sides of the promoter are evicted, exposing all functional sites, thus allowing gene transcription. Secondly, nucleosomes can occupy activator binding sites. After the attachment of nucleosome remodelling enzymes, binding of transcription activators on the activator is enabled. The nucleosomes get evicted and

transcription can begin. Genes can nevertheless still be repressed suggesting there are other repressor mechanisms in place. Thirdly, when a promoter is in the NDR bound to the activator, neighbouring nucleosomes are evicted to allow transcription but return to their position to repress transcription. This is a cyclic process. Fourthly, in the case of two promoters regulating one gene, the first promoter, located in the NDR, is activated causing eviction of neighbouring nucleosomes where the second promoter is located. Activation of the second promoter promotes further depletion of nucleosomes and activation of protein-coding gene (Bai and Morozov, 2010).

1.4.2. Nucleosomes and DNA access

Another way of controlling gene transcription is by controlling the accessibility of transcription machinery to the DNA being wrapped on nucleosomes. There are three mechanisms; the first mechanism involves nucleosome sliding exposing the target gene to transcription machinery. The second mechanism requires ATP-dependent chromatin remodelling complexes (e.g. SWI/SNF) which exploit ATP from hydrolysis and binds to DNA forming DNA loops. The third mechanism involves nucleosome eviction for successful transcription by anti-silencing function 1 (Asf1) and specific chaperone (Chz1) (Jiang and Pugh, 2009) (figure 3).

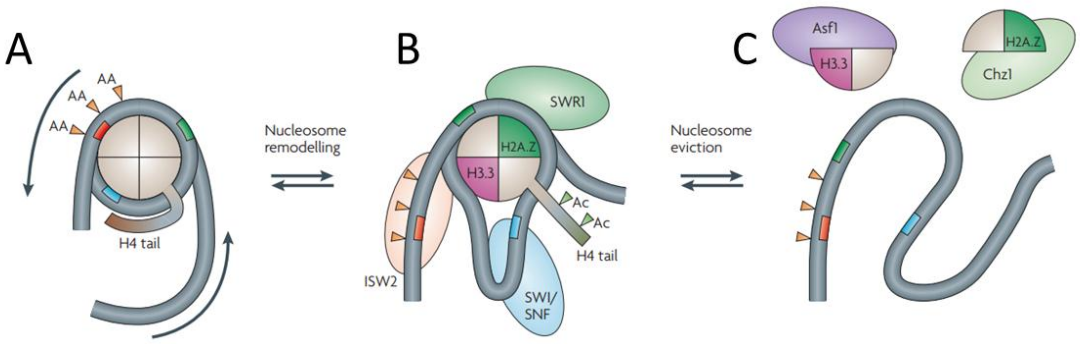

Figure 3: Mechanisms for transcriptional regulation. A) A non-modified, stable nucleosome where gene in red can be only accessible by nucleosome sliding indicated with arrows. B) Nucleosome with remodelling enzymes creating DNA loops, gene in blue can become accessible. C) Nucleosome eviction is sometimes necessary for transcriptional machinery to be able to bind to the DNA (Jiang and Pugh, 2009).

1.5. Histone modifications

There is another mechanism by which nucleosome properties can be altered – histone modifications (Zentner and Henikoff, 2013). The histones as part of the nucleosomes have N-terminal tails sticking out from the nucleosomes which are prone to posttranslational modifications. Methylation and acetylation (Roopra et al., 2012) are the most frequent histone modifications (Nightingale et al., 2006).

Genetic code describes information in the genome whereas the histone code extends the information of the genetic (DNA) code with additional information of existing protein interactions within the epigenome (Jenuwein and Allis, 2001). The hypothesis that histone tails with modification marks provide binding sites for effector proteins was first suggested by Turner *et al.* in 1992 (Turner et al., 1992, Turner, 1993). The bromodomain, for example, recognises modification marks for acetylation activating transcription and chromodomains recognise modification marks for methylation repressing transcription (Inche and La Thangue, 2006).

There are over 100 distinct modifications described and the list is still increasing. The most studied histone modifications are methylation and acetylation (Zentner and Henikoff, 2013).

1.5.1. Methylation

Histone methylation was discovered 40 years ago by Murray (Murray, 1964). It can occurs as methylation of H3 and H4 histones with mono-, di-, and trimethyl groups per residue when methylation occurs on lysine residues (Kumar et al., 2012). However, it occurs as mono- and dimethyl groups per residue when methylation occurs on arginine residues (Zentner and Henikoff, 2013). The SET domain starts methylation on lysine residues; however, methylation on arginine residues starts by co-activator arginine methyltransferase (CARM1) and protein arginine methyl transferase (PRMT1) (Kumar et al., 2012).

1.5.2. Acetylation

Acetylation was the first described histone modification, discovered in 1961 (Phillips, 1963). Acetylation of lysine residues is regulated by histone acetyltransferases (HATs) and histone deacetylases (HDACs) (Bannister and Kouzarides, 2011, Zentner and Henikoff, 2013).

HATs neutralize positive charge between DNA and lysine residues by addition of acetyl group from acetyl CoA to the side chain of the lysine residue (Bannister and Kouzarides, 2011) on the N-terminal tail of the histone (Sterner and Berger, 2000). The histone – DNA connection or nucleosome - nucleosome interactions weaken due to neutralization of the lysine residue causing chromatin to become loose around the nucleosome. Transcription is therefore increased due to higher accessibility of the transcription machinery to the DNA (Inche and La Thangue, 2006, Sterner and Berger, 2000). There are two types of HATs. Type A HATs acetylate N-terminal tails of histones with three families GNAT, MYST and CBP/p300. Type B HATs acetylate only free histones in the cytoplasm (Bannister and Kouzarides, 2011).

HDACs have the opposite effect on transcription as HATs, as they have deacetylation effects, restoring the positive charge of lysine residues on histones (Bannister and Kouzarides, 2011) by removing the acetyl groups from the histones (Kumar et al., 2012). Therefore, they are predominantly transcriptional repressors. There are several classes of HDACs; class I, II a/b, III and IV (Bannister and Kouzarides, 2011). Class I (HDAC 1, 2, 3 and 8), class II a/b (HDAC 4, 5, 6, 7, 9 and 10) and class IV (HDAC 11) are zinc dependent HDACs whereas, class III (SIRT 1, 2, 3, 4, 5, 6 and 7) are NAD^+ dependent HDACs (Carew et al., 2008, Glaser, 2007, Cortez and Jones, 2008). Observations have shown overexpression and/or misregulation of HDACs in cancer cells without HDAC genes being mutated (Inche and La Thangue, 2006). Changes in the genome are not reversible however, changes in the epigenome are, and can be achieved by use of “epigenetic drugs” such as HDAC inhibitors (Bannister and Kouzarides, 2011, Tang et al., 2013).

1.6. HDAC inhibitors

One of the important hallmarks of cancer are the changes in the epigenome which promote transcriptional repression of tumour suppressor genes causing increased tumorigenesis and cancer progression. Repression of tumour suppressor genes is evident in many types of cancer such as colon cancer, prostate cancer, breast cancer etc. (Carew et al., 2008). Therefore, HDAC inhibitors (HDACi) are important anti-cancer targets (Inche and La Thangue, 2006) as they induce inhibition of cancer cells, promote apoptosis and induce differentiation (Bannister and Kouzarides, 2011), thus, offering a promising target for pharmacological inhibition of cancer (Carew et al., 2008).

HDACi were developed to alter epigenetic changes and restore normal expression levels of tumour suppression genes. These HDACi are *short-chain fatty acids* (valproic acid (VPA) and butyrate), *hydroxamic acids* (suberoylanilide hydroxamine acid (SAHA), Trichostatin-A (TSA), LBH589, PXD101 and tubacin), *benzamides* (MS-278) and *cyclic tetrapeptides* (depsipeptide) which are not target specific but do inhibit only specific classes of HDACs (figure 4). HDACi increase distance between the nucleosome and the DNA allowing higher accessibility to DNA, resulting in increased transcription (Tang et al., 2013). Furthermore, HDACi induce apoptosis through the extrinsic pathway of apoptosis by increased expression of death ligand TRAIL which starts apoptosis only in transformed cells but not in normal cells (Carew et al., 2008). For example, the HDACi SAHA can be almost 1000-fold more toxic for malignant T-cells in comparison to non-malignant T-cells (Zhang et al., 2005). Additionally, HDACi affect apoptosis also through the intrinsic pathway of apoptosis by down-regulating pro-apoptotic genes and up-regulating anti-apoptotic genes. Therefore, cancer cells undergo apoptosis. Furthermore, HDACi inhibit angiogenesis, which is of a high importance for tumour formation and metastases development, by decreasing pro-angiogenic factors (e.g. vascular endothelial growth factor (VEGF) and hypoxia-inducible factor-1α (HIF1α). Moreover, HDACi not only affect histone modifications and restore normal expression levels in tumour suppressor genes but also affect non-histone proteins (e.g. p53, Rb, tubulin, E2F1) (Carew et al., 2008, Marks and Xu, 2009).

1.7. HDACi as chemotherapeutics

Anti-cancer properties of the HDACi are already used in clinical trials to potentially obtain new HDACi chemotherapeutics. SAHA has already been approved by Food and Drug Administration (FDA) for treatment of cutaneous T-cell lymphoma (Carew et al., 2008, Cortez and Jones, 2008), following approval of Depsipeptide (Romidepsin) (Marks and Xu, 2009). Also in phase I is LBH589 and in phase II are PXD101, butyrate, depsipeptide and MS-275 (Carew et al., 2008). Whereas, VPA is in phase III (Marks and Xu, 2009) (figure 5).

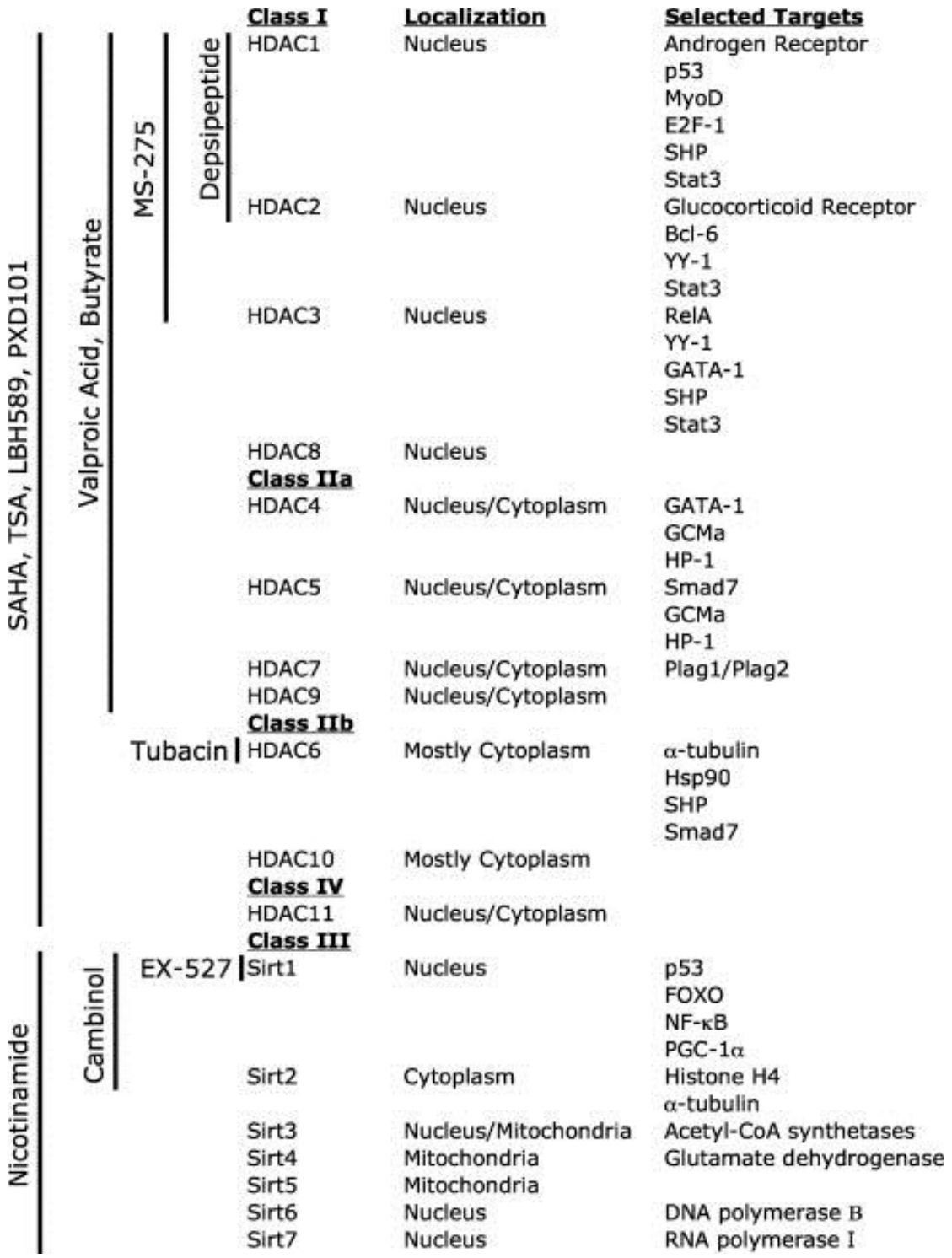

Figure 4: HDACi with target HDACs. Different HDAC inhibitors target different classes of HDACs (Carew et al., 2008).

Class	Compound	Potency	Clinical trials
Hydroxamates	Vorinostat, Zolinza (SAHA)	µM	FDA approved
	Panobinostat (LBH589)	nM	Phase II
	Belinostat (PDX101)	µM	Phase II
Short-chain fatty acids	Valproic acid (VPA)	mM	Phase III
	Butyrate	mM	Phase II
Cyclic tetrapeptide	Depsipeptide (Romidepsin, FK228)	nM	FDA approved
Benzamides	Entinostat (MS-275)	µM	Phase II

Figure 5: Clinical status of HDACi (Carew et al., 2008, Marks and Xu, 2009).

HDACi as chemotherapeutics can be administrated in many combinations such as two epigenetic drugs together, epigenetic drug and conventional chemotherapeutic (Cortez and Jones, 2008), epigenetic drug and new targeted agents or epigenetic drug in combination with radiation treatment. Data suggest a good correlation between epigenetic drugs and gemcitabine, paclitaxel, cisplatin, etoposide and doxorubicin as HDACi promote apoptosis, enabling higher potency of conventional chemotherapeutics (Carew et al., 2008). HDACi also increase sensitivity of cancer cells to conventional chemotherapeutics when chemotherapy resistance occurs (e.g. cisplatin resistance) as HDACi allow better interactions between chemotherapeutic and DNA by chromatin loosening. Furthermore, HDACi can be used in treatment of solid tumour as in hematologic malignancies (Cortez and Jones, 2008). According to the service of the U.S. National Institutes of Health termed Clinical Trials there are 355 clinical trials worldwide investigating HDACi as chemotherapeutics. The majority of clinical trials are in the USA (251 clinical trials) (figure 6) and Europe is second (49 clinical trials) (figure 7). The most studies focuses on acute myelocytic leukemia (AML) (44 studies) following by research on B-cell lymphomas (BCL) (36 studies) (ClinicalTrials.gov, 2013).

Figure 6: HDACi clinical trials worldwide in 2013. There are 355 clinical trials investigating HDACi as future chemotherapeutics. The most studies focuses on AML and BCL (ClinicalTrials.gov, 2013).

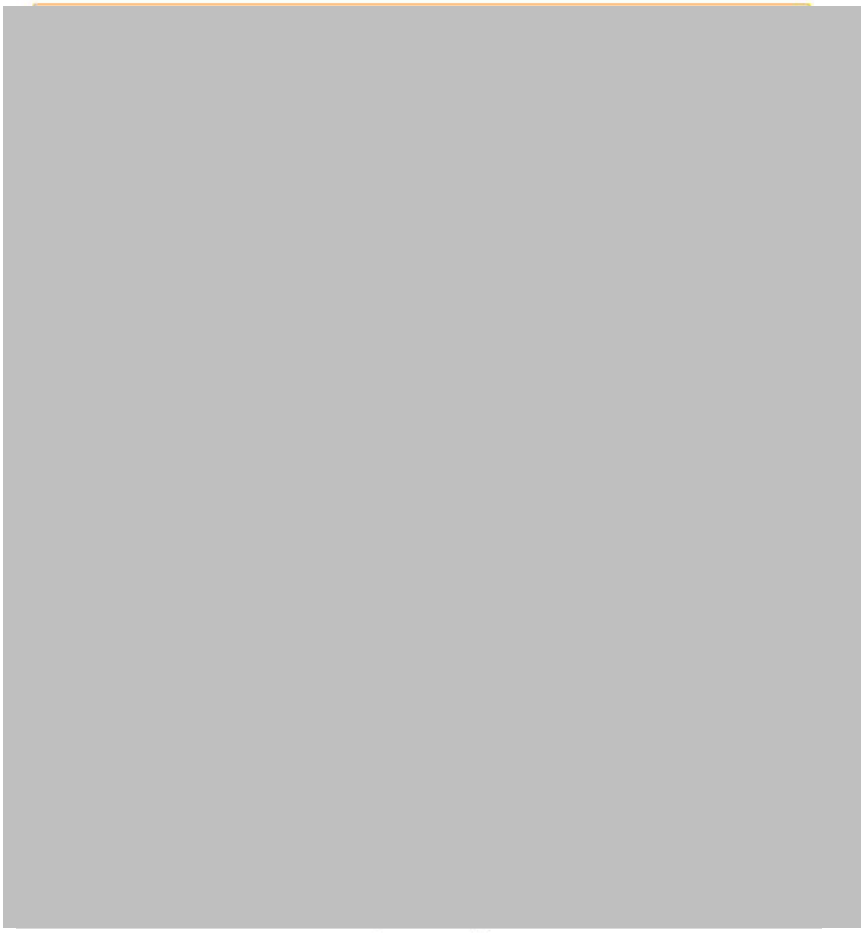

Figure 7: HDACi clinical trials in Europe in 2013. There are 49 clinical trials in Europe investigating HDACi as chemotherapeutics (ClinicalTrials.gov, 2013).

1.7.1. SAHA

SAHA is the first HDACi being approved by FDA for treatment of CTCL and is in phase II of clinical trials for solid tumours (Cortez and Jones, 2008) and in phase I-III clinical trials in combination with other chemotherapeutic drugs such as tamoxifen, bortezomib, oxaliplatin, carboplatin/paclitaxel etc. (Glaser, 2007). It is also known by the names Vorinostat and Zolinza™. It reacts as zinc chelator and binds in catalytic domain and inhibits HDACs class I and II (figure 5) (Mann et al., 2007, Cortez and Jones, 2008). SAHA is a small molecule with IUPAC formula $C_{14}H_{20}N_2O_3$ and molecular weight 264.32g/mol (Duvic and Vu, 2007). The drug is available as oral drug in 100 mg capsules. It has been proven when administrated in combination with other chemotherapeutic drugs SAHA has additive or synergetic effect. It has low toxicity but if occur it is expressed as fatigue, diarrhoea, dehydration etc. (Glaser, 2007).

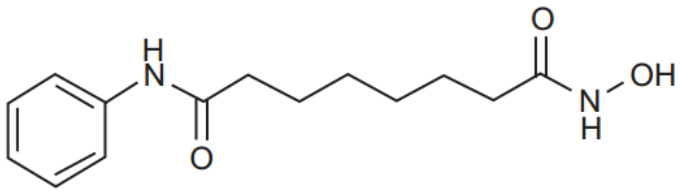

Figure 8: Suberoylanilide hydroxamic acid structure (Duvic and Vu, 2007).

1.7.2. VPA

VPA is an antiepileptic drug and mood stabilizer (Bialer, 2012, Blaheta et al., 2005) synthesised by Burton in 1882 (Chateauvieux et al., 2010). The anti-cancer effects such as inhibited proliferation, induced differentiation and decreased apoptosis (Cortez and Jones, 2008) were first observed in 1997 (Blaheta et al., 2005). VPA is well tolerated in adults and stable (Cortez and Jones, 2008) with half life time of 9 to 16 hours. However, it can provoke side effects presenting as prolonged sleep duration in young patients, dermatological side effects, decreased fertility, neurological side effects etc. It inhibits HDACs classes I and II (figure 5) by increased acetylation (Nightingale et al., 2007), increasing transcriptional responses and increased DNA repair (Marks and Xu,

2009). As an antiepileptic drug it is available in many forms such as tablets, syrup and local injections (Chateauvieux et al., 2010). At the moment there are 22 studies worldwide studying effects of VPA as a chemotherapeutic agent (ClinicalTrials.gov, 2013).

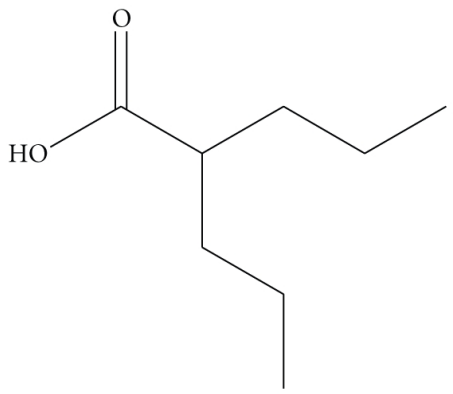

Figure 9: Valproic acid structure (Chateauvieux et al., 2010).

1.8. Summary, overview and aims of this thesis.

The aim of this project was to analyse the transcriptional response to histone deacetylase inhibitors treatment in normal and cancer cell lines. Whereas the properties of VPA as antiepileptic drug and mood stabilizer (Bialer, 2012, Blaheta et al., 2005) are well studied the anti-cancer effects and means of action are less understood despite that the increased acetylation (Nightingale et al., 2007), increasing transcriptional responses and increased DNA repair (Marks and Xu, 2009) have been observed. Our group has previously shown that lymphoblastoid cells show a limited short-term transcriptional response to VPA treatment that appears to protect them from aberrant histone modification and apoptotic effects. Therefore, the questions to address were:

1. How do non-malignant lymphoblastoid cells adapt to long-term exposure to VPA?
2. How do malignant Burkitts lymphoma cells respond to VPA treatment?
3. How do short-term transcriptional changes in Burkitts cells relate to their VPA response?

2. Materials and Methods

2.1. Reagents

Reagent in text	Formulation
10 x SDS loading buffer	1 M Tris pH 8, 10 mM EDTA, 10% SDS, 1.432 M β-mercaptoethanol, 0.1 g bromphenol blue
LCLs media	RPMI 1600 (Sigma Life sciences, USA), 10% main batch FBS (Sigma Life sciences, USA), 1% streptomycin and penicillin (Invitrogen), 1% L-glutamine
BL media	RPMI 1600, 10% main batch FBS, 1% streptomycin and penicillin, 1% L-glutamine, 1mM Hepes Buffer, Pyrovate 1:100, magic mix 1:100
Blocking solution	5% non-fat dry milk (Chivers, Ireland), TBS-T
Magic mix	BCS 10 mM, 10 x PBS, α-thioglycerol, u.p.H_2O
Propidium Iodide (PI) Staining Buffer	FACS buffer (PBS, 5% FBS, 0.02% NaN_3), 1mg/ml Propidium Iodide, 10mg/ml RNase A, 10% NP40 and 1mg/ml tri-sodium citrate
TEB	10% Triton x 100 (Sigma Life sciences, USA), 0.1M PMSF, 2% Sodium Azide, 10xPBS, ultra pure water
LCLs freezing mix	78% RPMI 1600, 10% main batch FBS, 1% streptomycin and penicillin, 1% L-glutamine, 10% DMSO
BL freezing mix	70% RPMI 1600, 20% main batch FBS, 10% DMSO

Other reagents	Source
QIAquick PCR Purification Kit	QIAGEN, Sussex, UK
QIAquick RNeasy Mini Kit	QIAGEN, Sussex, UK
cDNA Synthesis System Kit	Roche, UK
Coomassie reagent	Thermo Scientific, USA
Gene expression array analysis kit	NimbleGen, UK
SuperScript™ III Reverse Transcriptase Kit	Invitrogen, UK

2.2. Methods

2.2.1. 7 day exposure of LCLs to sodium valproate (VPA)

LCL responses to exposure to sodium valproate (VPA) were measured at four time points (day 1, 3, 5 and 7) and at three experimental conditions (untreated control group, 0.5 mM VPA and 1 mM VPA) to establish appropriate time points and concentration of VPA for further experiments. Every second day half of the culture media with VPA was removed and replaced by fresh media or fresh media with 0.5 or 1 mM VPA to ensure stable concentration of VPA for the duration of the experiment. At each time point photos were taken to observe potential morphological changes. All together there were twelve groups with different experimental conditions. At each time point cells were collected for Fluorescence-activated cell sorting (FACS) analysis and Western Blotting analysis. Cells were collected from *in-vitro* culture and centrifuged at 350 x g for 5 min at 4°C. Pellets were re-suspended in PBS with sodium butyrate and cells were counted. Cells were collected ($1x10^6$) for FACS analysis and centrifuged at 1500 min x g for 5 min at 4°C. Pellets were re-suspended in 70% ethanol and stored at -20°C. The remaining cells were centrifuged at 350 x g for 5 min at 4°C. Pellets were loosened and stored at -80°C for acid extraction of the histones.

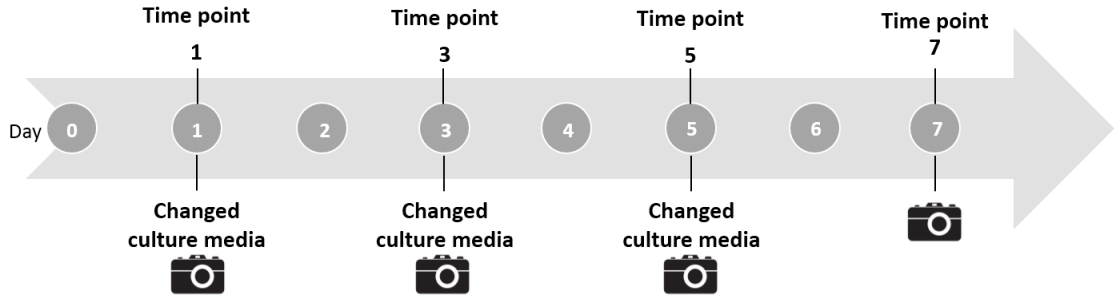

Figure 10: Timeline of experiment with 7 day long exposure of LCLs to VPA. LCLs in culture were exposed to VPA for 7 days. Fresh media or fresh media with VPA at different concentrations (0.5 and 1 mM VPA) was replaced every second day and photos were taken to observe potential morphological changes. At each time point (day 1, 3, 5 and 7) cells were collected for FACS analysis and Western Blotting analysis.

2.2.2. 14 day exposure of LCLs to 0.5 mM sodium valproate (VPA)

To evaluate long-term effects of VPA on global gene expression an experiment was conducted treating LCLs with 0.5 mM VPA for 14 days. Cells were collected at four time points (day 1, 4, 7 and 14). Every second day half of the culture media was removed and replaced by fresh media or fresh media with 0.5 mM VPA to ensure stable concentration of VPA for the duration of the experiment. Photos were taken before adding the fresh media every second day to observe potential morphological changes. There were three biological replicates (groups A, B and C) for RNA analysis alongside a fourth group for Western Blotting analysis (group W). At each time point cells were collected for Western Blotting analysis from group W. Cells from groups A, B and C were collected for FACS analysis and Microarray analysis. Cells for Western Blotting and FACS were collected as described in section 2.2.1. Cells for Microarray analysis were collected from *in-vitro* culture and centrifuged at 350 x g for 5 min at 4°C. Pellets were loosened and stored at -80°C for further RNA purification.

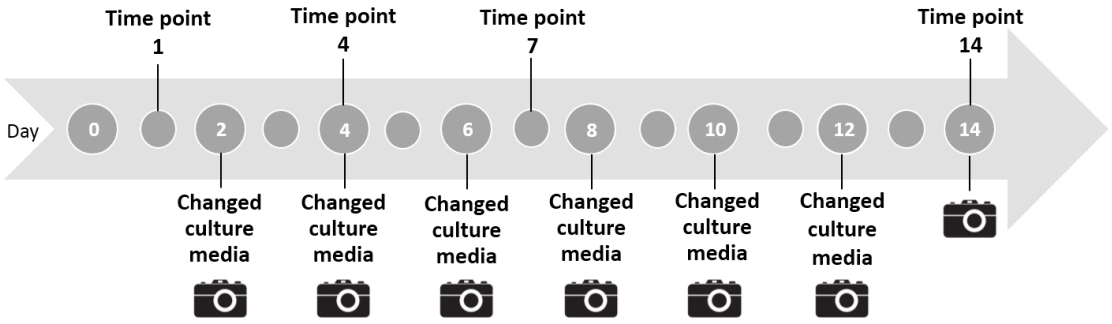

Figure 11: Timeline of experiment with 14 day long exposure of LCLs to 0.5 mM VPA. LCLs in culture were exposed to VPA for 14 days. Fresh media or fresh media with 0.5 mM VPA was replaced every second day and photos were taken to observe potential morphological changes. At each time point (day 1, 4, 7 and 14) cells were collected for FACS analysis, Western Blotting analysis and Microarray analysis.

2.2.3. 24 hour exposure of BLs to VPA

Three Burkitt lymphoma cell lines (BLs) 30, 31 and 41 were exposed to different VPA concentrations (5mM, 1mM, 0.5mM and 0.2mM) to observe cell cycle responses of cells 24 h post-treatment. BLs were seeded into 6 well plates and treated with VPA. After 24 h cells were collected for further FACS analysis and prepared as described in section 2.2.1.

2.2.4. Cell density of BLs in culture versus VPA treatment

BLs 30, 31 and 41 were seeded into 6 well plates at $1x10^6$, $3x10^6$ and $5x10^6$ and treated with VPA at concentrations of 0.5 mM and 5 mM with untreated control group. After 24 hour exposure to VPA BLs were collected for further FACS analysis and prepared as described in section 2.2.1.

2.2.5. BLs exposure to 1mM VPA

To evaluate effects of VPA on global gene expression in BL cell lines, an experiment was conducted treating BL cell lines 30, 31 and 41 for 30 min, 60 min and 120 min with 1 mM VPA alongside untreated control group. BLs were seeded at $1x10^6$ cells/ml. There were three biological replicates for each BL cell line (groups A, B and C) for RNA analysis alongside fourth group for Western Blotting analysis (group W). At each time point cells were collected for Western Blotting analysis from groups W. Cells from groups A, B and C were collected for Microarray analysis. Cells for Western Blotting were collected as described in section 2.2.1. Cells for Microarray analysis were collected from *in-vitro* culture and centrifuged at 350 x g for 5 min at 4°C. Pellets were loosened and stored at -80°C for further RNA purification.

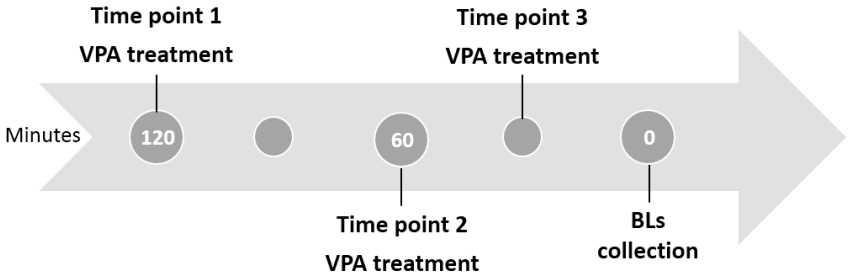

Figure 12: Timeline of the experiment treating BLs with 1mM VPA for 30 min, 60 min and 120 min. BLs were treated and collected for Western Blotting and Micro array analysis 30, 60 and 120 min after treatment. BLs were collected for Western Blotting analysis and Microarray analysis.

2.2.6. Fluorescence-activated cell sorting (FACS) analysis

Collected cells re-suspended in 70% ethanol for FACS analysis were centrifuged at 350 x g for 5 min and washed twice in ice-cold PBS. Samples were re-suspended in *Propidium Iodide (PI) Staining Buffer* and incubated for 30 min at room temperature covered with tinfoil to exclude light. Samples were filtered through cell filters into polypropylene FACS tubes and analysed on the flow cytometer gated on the forward *versus* side-scatter. Data was analysed using Summit V.3.

2.2.7. Acid extraction of histones

Cell pellets were re-suspended in *TEB* buffer at concentration of $1x10^7$ cells/ml and incubated on ice for 10 min. Cells were washed by centrifuging at 900 x g for 10 min at 4°C. Supernatant was removed and cell pellets were re-suspended in half of the volume of *TEB* buffer and centrifuged at 900 x g for 10 min at 4°C. The supernatant was removed and cell pellets were re-suspended in 0.4N HCl at concentration of $4x10^7$ cells/ml. Cells were incubated overnight at 4°C. Cells were washed by centrifuging at 900 x g for 10 min at 4°C. Supernatant containing histones was removed to perform the Coomassie Protein Assay.

2.2.8. Coomassie Protein Assay

By dissolving bovine serum albumin (BSA) in u.p.H_2O, standards were prepared at concentration of 5.0, 1.0, 0.5, 0.25, 0.125, 0.0625mg/ml. Coomassie reagent was added (1 ml) to each cuvette following by 10 µl of each standard and samples containing histone extractions. Blank was produced by adding 10 µl u.p.H_2O to cuvette. Cuvettes were incubated for 5 min at room temperature and read at 595nm (GeneFlow Implen P300 Reader) blanking against the u.p.H_2O to obtain absorbance values for determination of histone concentrations.

2.2.9. Western Blotting assay

After each time course global acetylation levels in treated cells relative to controls was assayed by Western Blotting. Lower gel (15% acrylamide, 0.5% bisacrylamide, 0.375M TRIS, pH 8.8, 0.1% SDS, 0.03% APS, 0.1% TEMED) was poured into gel cassette and left to set. Isopropanol was layed on top for easier inspection of gel setting and was poured off before upper gel was poured into the gel cassette. Upper gel (3% acrylamide, 0.16% bisacrylamide, 0.125M TRIS, pH 6.8, 0.03 SDS, 0.03 APS, 0.1% TEMED). Samples containing histones were mixed in eppendorf tubes with 50% glycerol, *10xSDS loading buffer* and u.p.H_2O and incubated for 10 min at 99°C and then placed on ice for 5 min. Meanwhile, reservoir buffer was prepared which consisted of 0.1% SDS, 50mM TRIS and 380mM glycine. Gel cassettes were transferred into tank and reservoir buffer was poured into the tank. Prepared samples were loaded onto the gels. Gels were run for 3h at 20W, 60-80mA. SDS transfer buffer consisting of 25mM TRIS, 192mM glycine, 20% methanol and u.p.H_2O was prepared. For protein transfer, transfer cassettes were assembled placing gels onto the membrane, sponges and filter papers. Transfer cassettes were placed into transfer tank and top up with buffer. Blotting process was run for 3h at 160V, 300 mA. Transfer cassettes were disassembled and membranes were incubated for 5 min in Ponceau S dye (Sigma, UK) to check for effective transfer and equal loading of the proteins (histones) and rinsed with dH_2O. Membranes were blocked in *blocking solution* at room temperature for 1h and placed onto a rocking platform (Stuart rocker, SSL4). Membranes were probed with H3/H4

primary antibody pairs (first pair: H4K5ac (R41) & H3K9ac (R607); second pair: H4K16ac (R252) & H3K4me3 (R612)) and membranes were incubated at room temperature for 1h placed on the rocking platform. Membranes were washed in TBS-T for 10 min three times placed on the rocking platform. Secondary antibody Licor was added and membranes were incubated at room temperature for 1h placed on the rocking platform. Membranes were washed in TBS-T for 10 min three times placed on the rocking platform and scanned using LI-COR Odyssey Infrared Imaging System scanner and incubated overnight at 4°C in TBS-T placed on the rocking platform.

After overnight washing in TBS-T membranes were incubated in primary antibody H3 C-terminus (AB-1791) at room temperature for 1h placed on the rocking platform and washed in TBS-T for 10 min three times placed on the rocking platform. Second Rabbit IgG antibody (Rockland 611-131-122) was added and membranes were incubated at room temperature for 1h placed on the rocking platform and washed in TBS-T for 10 min three times placed on the rocking platform. Membranes were scanned using LI-COR Odyssey Infrared Imaging System scanner.

2.2.10. Thawing cells

Cells were thawed in a 37°C water bath and slowly re-suspended in RPMI media (LCLs media or BL media) using the drip-by-drip method. Cells were washed in RPMI media at 350 x g for 5 min. Cells were re-suspended in RPMI media and transferred into culturing flasks.

2.2.11. Freezing cells

Cells in RPMI media were centrifuged at 350 x g for 5 min, re-suspended in *LCLs* or *BL freezing mix* and transferred to a cryovials. Vials were frozen at −1°C/min to −80°C using a freezing container (Mr Frosty, Nalgene). Cells were moved to −196°C within 24 hours.

2.2.12. RNA extraction

RNA purification for Microarray analysis was performed using *RNeasy Mini Kit* (Qiagen, UK). Collected cells in pellet were thawed at room temperature and Buffer RLT was added. Homogenization of the samples was performed using needle and syringe. One volume of 70% ethanol was added and mixed by pipetting. Samples were transferred onto RNeasy Mini spin columns placed onto 2 ml collection tubes and centrifuged at 8000 x g for 15 sec. Flow-through was discarded and Buffer RW1 was added onto the columns. The columns were centrifuged at 8000 x g for 15 sec and flow-through was discarded. DNase I incubation mix containing DNase I solution and Buffer RDD was added onto the RNeasy columns membrane and left at room temperature for 15 min. Buffer RW1 was added onto the columns and columns were centrifuged at 8000 x g for 15 sec. Flow-through was discarded. Samples were washed twice with buffer RPE by centrifuging for 15 sec at 8000 x g and 2 min at 8000 x g. Flow-through was discarded. RNeasy spin columns were placed in centrifuge for 1 min to dry the membranes. RNeasy spin columns were placed into new collection tubes and RNase-free water was added. To elute RNA, columns were centrifuged for 1 min at 8000 x g twice. Eluted RNA samples were quantitated using nanodrop spectrophotometer (GeneFlow Implen P300 Reader) and analysed on 2% agarose gel.

2.2.13. Eletrophoresis of samples

Samples were electrophoresed in a 2% agarose gel in TAE for 30 - 40 min (70 - 75V) and visualized by GelRed dye (BioTium). Samples were mixed with loading buffer for visualisation before adding 10 µl onto agarose gel. 100 bp DNA Ladder marker (Invitrogen) was used as orientation marker of DNA separation. RNA or DNA separation was visualized using UV reader *(*BIO-RAD, Molecular Imager Gel Doc XR System).

2.2.14. Double stranded cDNA synthesis

Double stranded cDNA from RNA samples was synthesized using *cDNA Synthesis System Kit* (Roche, UK). RNA samples were thawed on ice and transferred into thin-walled PCR tubes adding oligo dT_{15} primer. Tubes were incubated for 10 min at 70°C and then immediately placed onto ice. RT-buffer, DTT, AMV, Protector RNase Inhibitor and dNTP-Mix were added and tubes were incubated for 60 min at 42°C. For terminating the reaction tubes were placed onto ice. The second strand of cDNA was synthesised adding 2^{nd} strand synthesis buffer, dNTP-mix, 2^{nd} strand enzyme blend and PCR water into the tubes with the samples. Samples were incubated for 2h at 16°C. T4 DNA Polymerase was added and samples were incubated for 5 min at 16°C. Reaction was terminated by adding EDTA. RNA was digested by adding RNase I and digested at 37°C for 30 min. Proteinase K was added and samples were incubated for 30 min at 37°C. Double stranded cDNA was cleaned using *QIAquick PCR Purification Kit* (Qiagen, UK). Buffer PB was added to the samples and samples were transferred onto QIAquick columns and centrifuged for 60 sec. Flow-through was discarded. Buffer PE was added and QIAquick columns were centrifuged for 60 sec. Flow-through was discarded and columns were centrifuged for another 1 min. QIAquick columns were transferred into new 1.5 ml microcentrifuge tubes. DNA was eluted by adding Buffer EB and centrifuged for 1 min following by elution buffer placed directly to QIAquick columns membrane. Columns were incubated for 1 min at room temperature and then centrifuged at 8000 x g for 1 min. Double stranded cDNA samples were quantitated using nanodrop spectrophotometer (GeneFlow Implen P300 Reader) and stored at -20°C.

2.2.15. Microarray analysis

To identify global gene expression changes *Gene expression array analysis kit* (NimbleGen, UK) was used.

Double-stranded cDNA samples were transferred into thin-walled tubes and labelled by adding diluted Cy3 Random Nonamers (Cy3 Random Nonamers with Random Primer Buffer and β-Mercaptoethanol) and PCR Grade Water. Samples were incubated

for 10 min at 98°C followed by quick-chill in ice-water bath for 2 min. The dNTP/Klenow master mix which contained dNTP Mix (10 mM each dNTP), PCR Grade Water, Klenow Fragment (3'-> 5' exo-) 50 U/µl was added to the reaction. Samples were incubated for 2 hours at 37°C protected from light. Reaction was stopped by adding the Stop Solution. Samples were transferred into new 1.5 ml microcentrifuge tubes containing isopropanol, mixed vigorously, incubated for 10 min at room temperature and centrifuged at 12,000 x g for 10 min. Supernatant was removed and pellets were rinsed and dislodged from tube walls by ice-cold 80% ethanol. Samples were centrifuged at 12,000 x g for 2 min and supernatant was removed. Samples were dried in a DNA vacuum concentrator (Thermo Scientific, SAVANT DNA 120 SpeedVac Concentrator) on low heat until dry protected from light. Samples were stored protected from light at -20°C overnight. Samples were spun down and pellets were rehydrated in PCR Grade Water and mixed vigorously for 30 sec, spun down to collect samples at the bottom of the microcentrifuge tubes and left on the bench to completely rehydrate. Samples were quantitated using nanodrop spectrophotometer (GeneFlow Implen P300 Reader). The 4ug labelled samples weredried in a DNA vacuum concentrator on low heat protected from light.

Dried pellet samples were re-suspended in Sample Tracking Control, mixed vigorously and spun down to collect contents at the bottom of the microcentrifuge tubes. Hybridization solution was added into the tubes which consisted of 2X Hybridization Buffer, Hybridization Component A and Alignment Oligo. Samples were mixed vigorously and spun down to collect the contents and incubated for 5 min at 95°C protected from light. Samples were transferred and incubated at 42°C until ready for sample loading. The HX12 Mixer-Slides were assembled using the Precision Mixer Alignment Tool (PMAT). The assembled HX12 Mixer-Slides were taken out of the PMAT and placed onto the heat block at 42°C for 5 min and transferred into the slide bay of the Hybridization System (NimbleGen,UK). Samples were loaded using a Gilson Microman pipette and hybridized for 20 hours at 42°C. After hybridization washing solutions I, II and III were prepared containing ultra-pure water, 10X Wash Buffer I, II or III and 1M DTT solution. Wash I was heated to 42°C as Washes II and III were kept at room temperature. The HX12 Mixer-Slides were disassembled using Mixer Disassembly

Tool submerged in Wash I. Slides were rinsed for 10 – 15 sec in Wash I at 42°C and placed into slide rack in Wash I at room temperature and rinsed for additional 2 min. Slides were transferred into Wash II and washed for 1 min. Slides were transferred to Wash III and washed for 15 sec. Slides were removed from the slide rack and dried using a microarray dryer. Slides were removed from the microarray dryer and scanned using a NimbleGen MS 200 Microarray Scanner, UK. Data was analysed using DEVA software and the free online accessible programme Database for Annotation, Visualization and Integrated Discovery (DAVID) v6.7 (Huang et al., 2009a, Huang et al., 2009b).

2.2.16. Single stranded cDNA for PCR validation

Single stranded cDNA for PCR validation was synthesized using *SuperScript™ III Reverse Transcriptase Kit* (Invitrogen, UK). The RNA samples were transferred into thin-walled tubes and were incubated for 5 min at 65°C with added oligo $(dT)_{12\text{-}18}$ and dNTP Mix and placed on ice for 1 min. The 5X First-Strand Buffer, 0.1 M DTT, RNaseOUT™ Recombinant RNase Inhibitor and SuperScript™ III RT were added. Samples were gently mixed by pipetting and incubated for 60 min at 50°C. Reaction was inactivated by incubating for 15 min at 70°C.

2.2.17. Polymerase chain reaction (PCR)

Polymerase chain reaction (PCR) was used to validate designed gene primers for Microarray analysis results. Primers were designed using the free online programmes Primer 3 (Rozen and Skaletsky, 2000) or NCBI Primer Blast tool (Ye et al., 2012). Basic Local Alignment Search Tool (BLAST) (Altschul et al., 1990) was used to validate selected primers for selected genes. A PCR thermal cycler (MJ Research PTC 200 Peltier Thermal Cycler) was used and programmed with the following conditions: 95°C for 5 min for initiation, 35 cycles of 95°C for 30 sec for denaturing, 50°C/60°C for 30 sec for annealing, 72°C for 30 sec/kbp for elongation. PCR products were maintained at 4°C and analysed on a 2% agarose gel as described in section 2.2.10.

3. Results

3.1. LCL responses to long-term (7 days) VPA treatment

To elucidate long-term effects of VPA treatment on normal cells we selected a lymphoblastoid cell line (LCLs) as a model for normal human cells as LCLs, though immortal in culture, are chromosomally stable and are widely used in genetic and functional studies (Tabish and Mulherkar, 2012). The experiment was conducted treating LCLs in culture for 7 days with 0.5 mM and 1 mM VPA. To address the question how VPA effects cell cycle and levels of global histone acetylation in LCLs, FACS and Western Blotting analysis were performed alongside observing the potential morphological changes by microscopy.

According to cell counts at each time point (day 1, 3, 5 and 7) growth curves were obtained. Control cells increased in numbers and similarly, the cells growing in 0.5 mM VPA showed some growth. The number of cells treated with 1 mM VPA were relatively stable in comparison to the number of seeded cells (figure 13). FACS analysis showed a minimal increase in apoptosis but a significant reduction in S phase, increasing with time and concentration of VPA (figure 14).

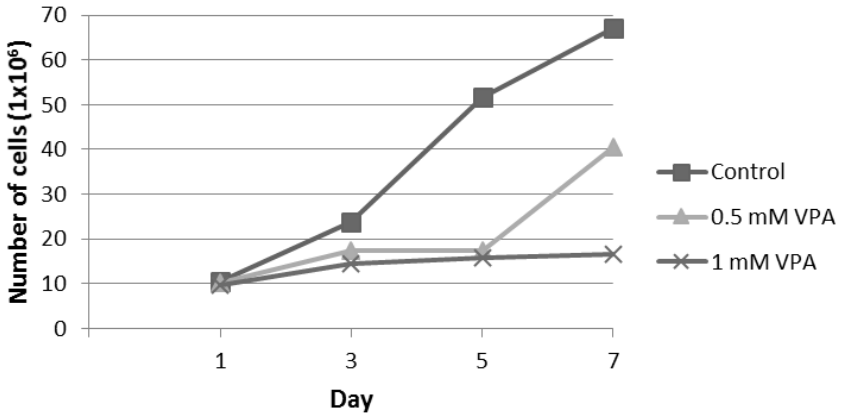

Figure 13: LCLs growth curves in 7 days long experiment. LCLs were counted at every time point (day 1, 3, 5 and 7) and growth curves were obtained. Control cells increased in numbers, whereas number of cells treated with 0.5 mM VPA has increased by 0.5-fold by day 7 in comparison to control cells. Number of cells treated with 1 mM VPA stayed relatively stable throughout the duration of the experiment.

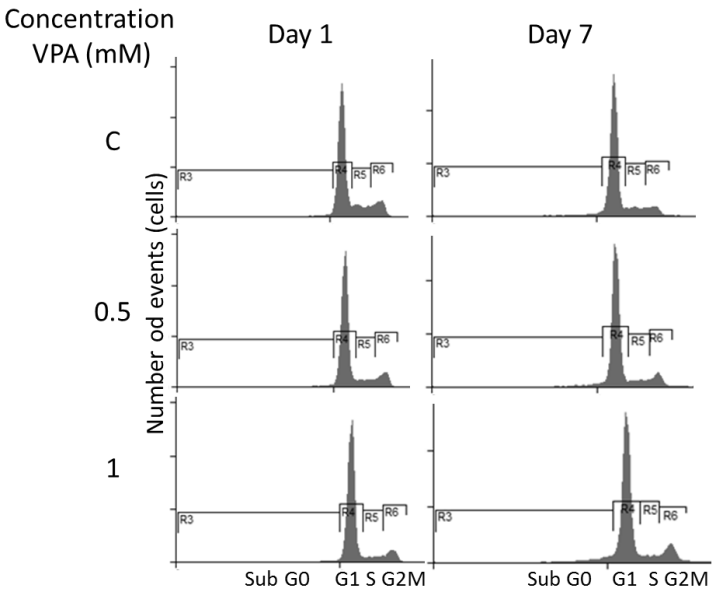

Figure 14: VPA impact on LCLs cell cycle in 7 day continuous VPA treatment. LCLs FACS analysis example pictures presenting LCLs cell cycle of control (C) cells and after treatment with 0.5 and 1 mM VPA. Proportion of cells versus VPA concentration are presented. Cells labelled as Sub G0 are either dead or apoptotic.

Western Blotting analysis was performed showing pronounced increase in acetylation of histones H3 and H4 after VPA treatment at day 1. The acetylation remained high thereafter. In untreated control cells parallel increase in acetylation was observed, for reasons that are not clear (figure 15).

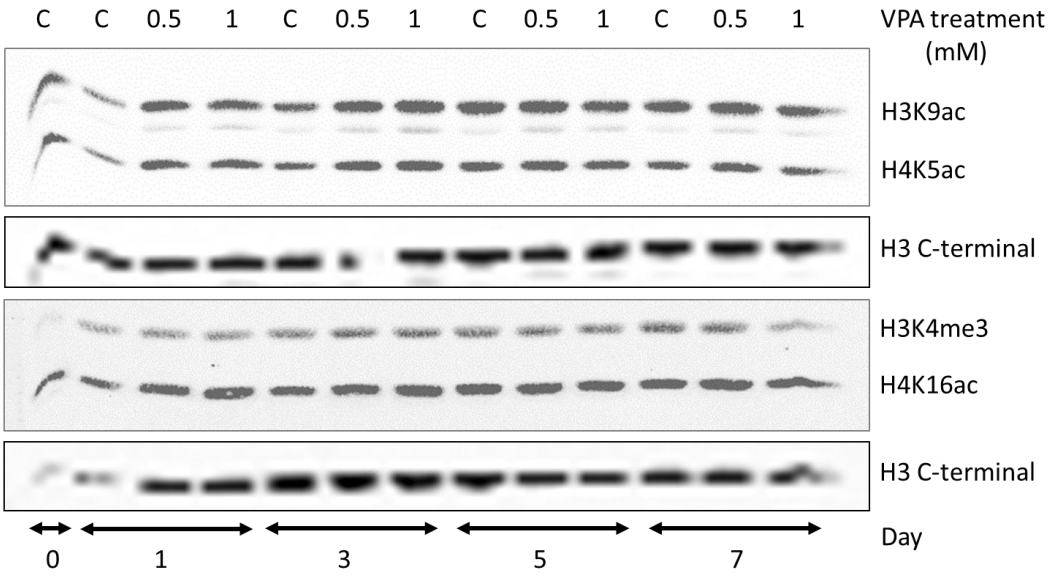

Figure 15: Western blotting analysis of LCLs treated for 1, 3, 5 and 7 days with 0.5 and 1 mM VPA. Blots present changes in histone acetylation levels of control (C) and treated cells (0.5 and 1) in histones H4K5ac, H3K9ac, H4K16ac, H3K4me3 and H3 C-terminal upon VPA treatment.

Alongside other analysis, potential morphological changes were observed by taking photos. Untreated control LCLs were growing in clumps and single cells were also observed through all 7 days of treatment. In treated LCLs there were fewer clumps and more single cells in culture. As treatment progressed, at both concentrations 0.5 and 1 mM the disappearance of clumps became clear. Five days after continuous treatment we started to observe morphological changes as cells in the control group were round in shape, whereas cells in treated groups became spiky, most dramatically at 1 mM VPA as presented in figure 16 below.

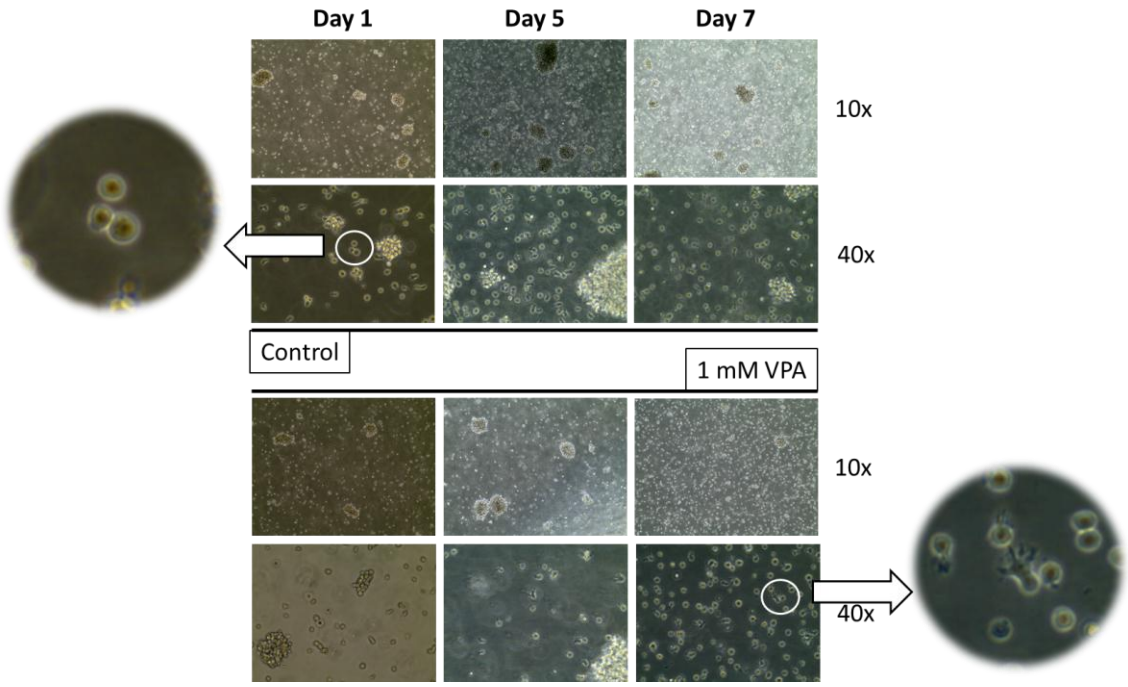

Figure 16: Example photos of LCLs in 7 days culture taken by light microscope. LCLs were treated for 1, 3, 5 and 7 days with 0.5 and 1 mM VPA. Photos were taken at 10x and 40x magnification and photos presented were taken from control groups and 1 mM VPA groups at day 1, 5 and 7. LCLs in control groups were growing in clumps with single cells however, treated LCLs were growing as single cells and clumps started to disappear with prolonged treatment. After 5 days of continuous treatment LCLs started to change shape from round to spiky.

3.2. LCL responses to long-term (14 days) 0.5 mM VPA treatment

After the 7 day experiment presented in section 2.1 we established the appropriate VPA concentration for our next experiment in which we treated LCLs for 14 days with 0.5 mM VPA. The aim of the experiment was to observe cell cycle changes and levels of global histone acetylation in LCLs by FACS analysis, Western Blotting analysis and identify gene expression changes by Microarray analysis. We also observed the potential morphological changes by microscopy.

According to cell counts at each time point (day 1, 4, 7 and 14) growth curves were obtained. Control cells proliferated by approximately 8-fold in 14 days of the experiment, whereas the number of cells treated with 0.5 mM VPA has increased slightly in the first four days and remained stable for the duration of the experiment (figure 17).

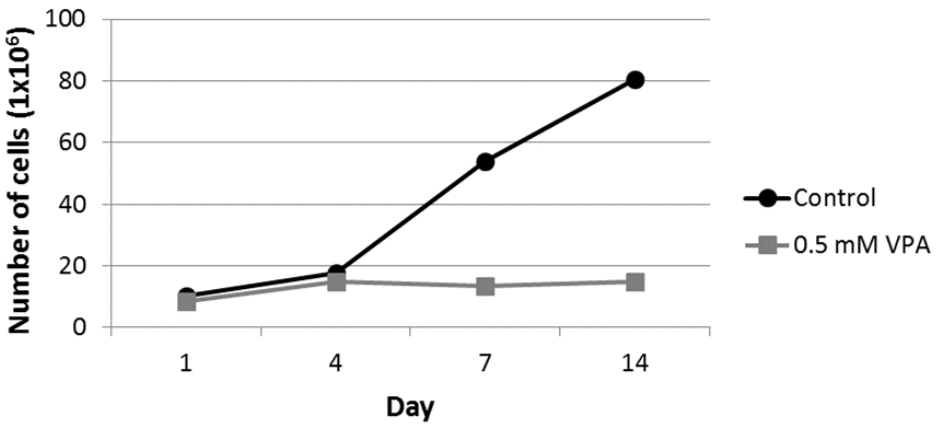

Figure 17: LCLs growth curves in 14 days long experiment. LCLs were counted at every time point (day 1, 4, 7 and 14) and growth curves were obtained. Control cells increased in numbers, whereas number of cells treated with 0.5 mM VPA has increased slightly in the first four days but remained relatively stable through the duration of the experiment.

Furthermore, Western blotting analysis showed pronounced increase in acetylation of histones H3 and H4 after 0.5 mM VPA treatment at day 1. The acetylation remained high thereafter. In untreated control cells parallel increase in acetylation was observed, for reasons that are not clear (figure 18).

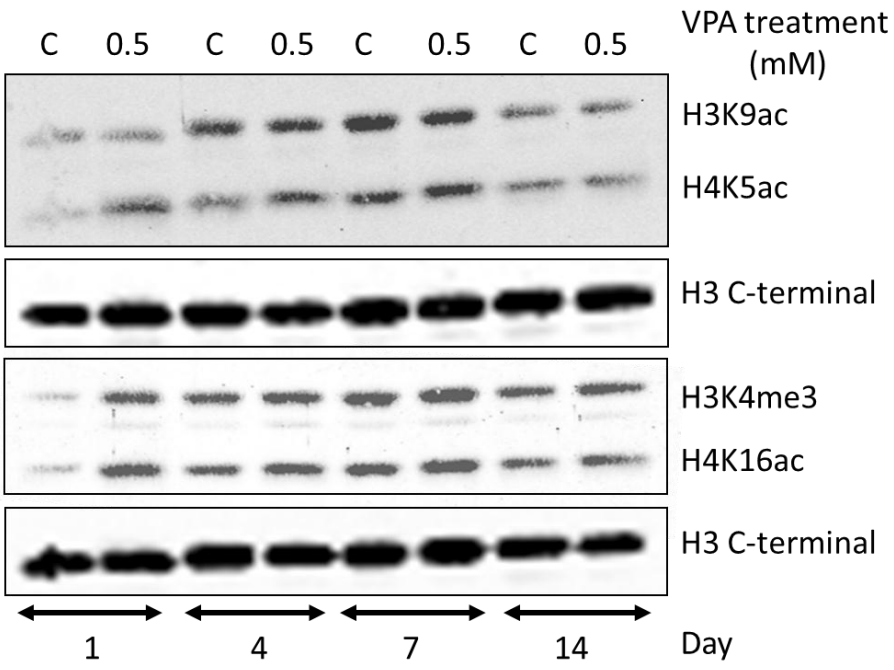

Figure 18: Western blotting analysis of LCLs treated for 1, 4, 7 and 14 days with 0.5 mM VPA. Blots present changes in histone acetylation levels of control (C) and treated cells (0.5) in histones H4K5ac, H3K9ac, H4K16ac, H3K4me3 and H3 C-terminal upon 0.5 mM VPA treatment.

Every second day photos were taken to observe potential morphological changes. In control groups, LCLs were growing in clumps and single cells were also observed. The treated cells in culture media with 0.5 mM VPA were growing as single cells with only a few clumps. After day 5 treated cells started to change morphologically from round shaped cells to spiky cells as presented in figure 19 below.

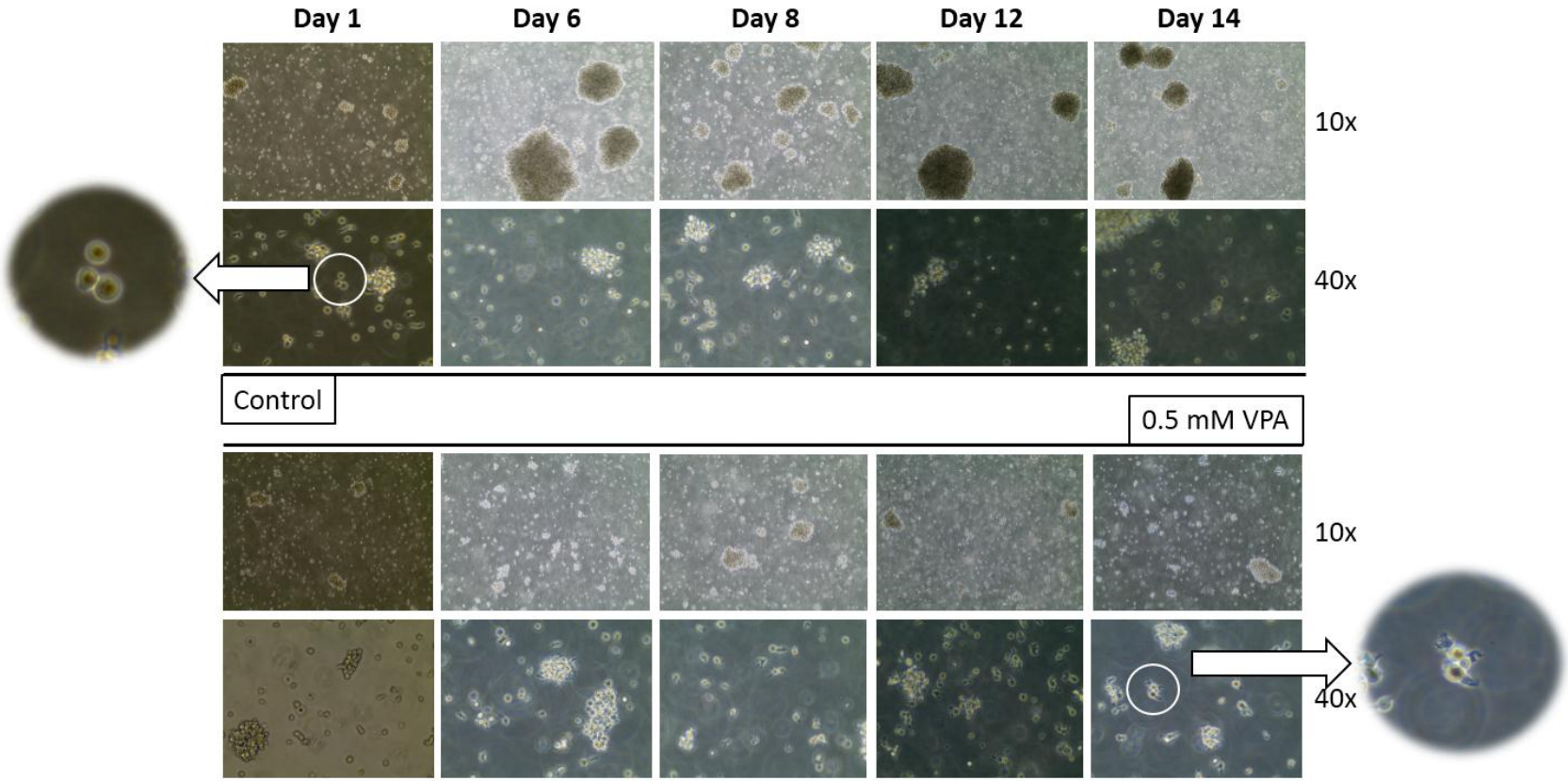

Figure 19: Example photos of LCLs in 14 days culture taken by light microscope. LCLs were treated for 1, 4, 7 and 14 days with 0.5 mM VPA. Photos were taken at 10x and 40x magnification and photos presented were taken from control groups and 0.5 mM VPA groups at days 1, 6, 8, 12 and 14. LCLs in control groups were growing in clumps with single cells however, treated LCLs were growing as single cells and clumps started to disappear with prolonged treatment. After 5 days of continuous treatment LCLs started to change shape from round to spiky.

To identify which genes change in LCLs upon VPA treatment we performed Microarray analysis and LCLs were collected as described in section 2.2.2. The cDNA from control and treated cells were hybridized to HX12 cDNA arrays. The intensities of probes hybridized with samples cDNA from control untreated and treated cells were compared (t-test). On the slide there were 44,049 human target gene sequences.

We identified differentially regulated genes by T-Test and a fold-change cut-off of 2-fold up or down in each time point. After one day of treatment only a small proportion of genes showed transcriptional change (202 genes, 169 up, 33 down), whereas after 4 days of treatment the transcriptional change was more abundant (1224 genes, 452 up, 772 down) with more genes being down regulated. After 7 days of treatment the number of genes with transcriptional change declined slightly (777 genes, 428 up, 348 down). The maximal transcriptional gene change in up regulated genes was seen at day 14 (1013 genes, 922 up, 91 down). Data suggests that the number of up regulated gene increased through the duration of the treatment while the number of down regulated gene peaked at day 4 and then declined (figure 20).

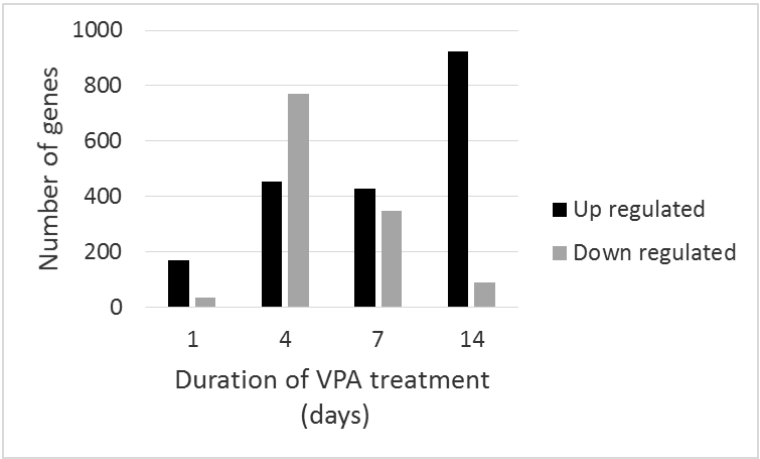

Figure 20: Changes in transcriptional levels in LCLs. Cells were treated for 1, 4, 7 and 14 days with 0.5 mM VPA and transcriptional responses were analysed with HX12 arrays. The number of genes that were more than 2-fold up regulated or down regulated at each time point are presented.

Interestingly, only 44 genes were significantly changed in all four time points (figure 21). Genes from all four time points were analysed using DAVID bioinformatics software to perform gene ontology (GO). Enrichment analysis was performed for genes that exhibited above 2-fold change. The four most significantly enriched gene classes from each time point are presented in table 1 below. The highest fold enrichment was observed at day 7 with GO terms cell cycle, organell lumen, chromosome and cytoskeleton.

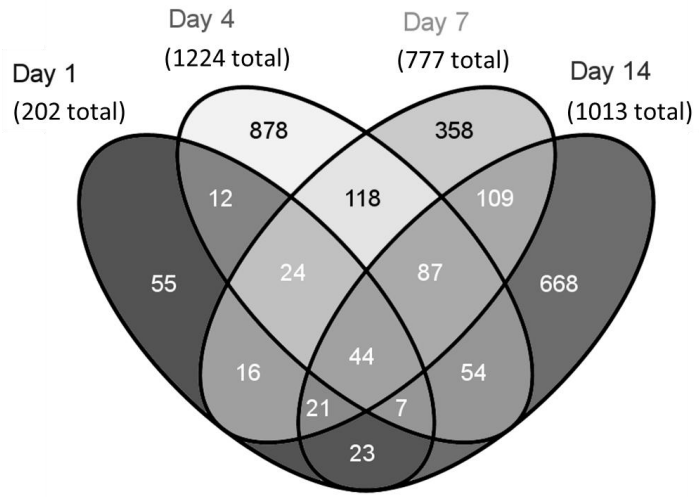

Figure 21: Venn diagram showing changed genes in 14 day long experiment. LCLs were treated for 1, 4, 7 and 14 days with 0.5 mM VPA. Genes transcription levels have changed significantly ($P<0.01$) upon VPA treatment detected by HX12 arrays (12 x 135,000 gene probes).

Table 1: LCLs gene ontology. DAVID bioinformatics software was used to perform gene ontology (GO) analysing genes from all four time points. Enrichment analysis was performed for genes that exhibited above 2-fold change. The four most significantly enriched gene classes from each time point are presented.

	Gene ontology term	Fold enrichment	P value
Day 1	Disulfid bond	3.09	3.02E-06
	Response to wounding	2.88	6.61E-05
	Transmembrane proteins	2.57	3.32E-05
	Regulation of phosphate metabolic process	2.11	0.003
Day 4	Cell adhesion	4.57	9.73E-06
	Disulfid bond	4.03	2.20E-06
	Cell cycle	3.09	0.005
	Immunoglobulins	2.77	4.06E-05
Day 7	Cell cycle	20.85	3.35E-23
	Organell lumen	16.41	1.58E-20
	Chromosome	13.97	3.69E-18
	Cytoskeleton	9.94	0.11
Day 14	Cell cycle	5.32	3.35E-06
	Plasma membrane	5.18	0.002
	Enzyme binding	4.77	5.69E-06
	Regulation of cell cycle	3.40	9.02E-05

3.3. 24 hours exposure of BLs to different concentration of VPA

To evaluate the effects of HDAC inhibitor VPA on malignant cells we as a cancer model used Burkitt lymphoma cell lines which are a B cell derived malignancy (Molyneux et al., 2012) and offer a valid comparison with our selected LCLs. In our experiments we used three BL cell lines (BL 30, 31 and 41) derived from primary BL tumours. These specific BLs were selected as being phenotypically very similar to each other and all negative for Epstein Barr Virus (EBV) thus removing any complications due to viral gene expression. BLs were treated with 0.2, 0.5, 1 and 5mM VPA for 24 hours to identify changes in cell cycle using FACS analysis.

When BL30 cells were treated with VPA there was a cell cycle arrest observed in G1 and G2M phase of cell cycle without a significant increase in apoptosis. The trend was even more evident at 5mM VPA. In BL 31 and 41 cell lines substantial apoptosis was observed without significant cell cycle arrest (figure 22).

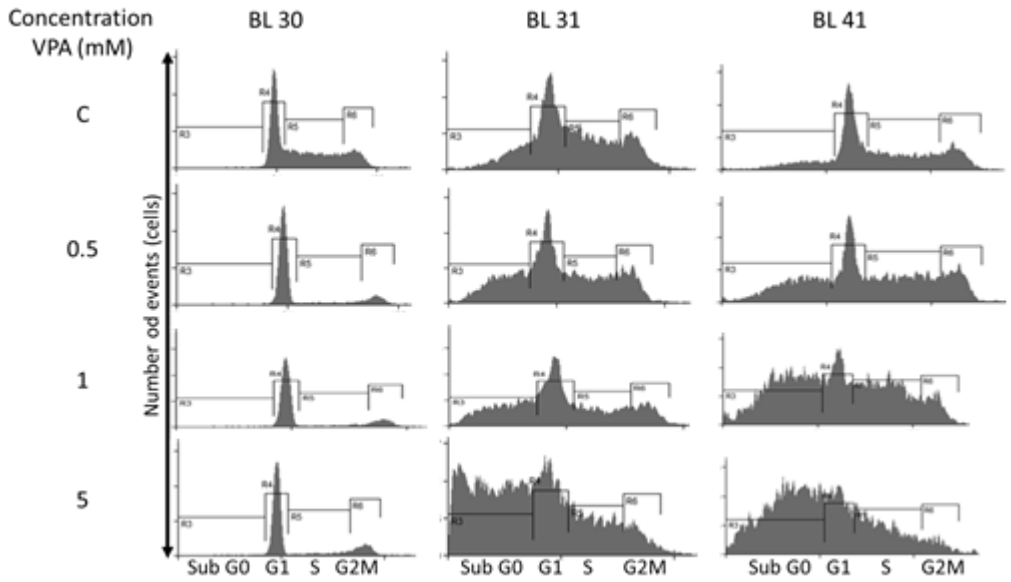

Figure 22: Cell cycle changes in BLs after 24 hours treatment with VPA. BLs FACS analysis pictures present BLs cell cycle of control cells (C) and cells after treatment with 0.5, 1 and 5 mM VPA. In BL 30 there was a cell cycle arrest in phases G1 and G2M without apoptosis. In BL 31 and 41 substantial apoptosis was observed without significant cell cycle arrest suggesting cells undergo apoptosis in all phases of cell cycle.

3.4. BLs cell density vs. VPA treatment

BLs 31 and 41 had a faster proliferation rate according to the observation of growth in culture in comparison to BL 30 cell line and this therefore raised the question whether BL 31 and 41 cell lines undergo apoptosis so significantly due to their faster proliferation rate and resultant overcrowding in culture resulting in higher apoptosis. Therefore, we designed an experiment to address the question, seeding all three BLs at different counts ($1x10^6$, $3x10^6$ and $5x10^6$ cells) and treating them with 0.5 and 5 mM VPA for 24 hours. The results were comparable to the results of the first BL experiment where BLs were treated with VPA described in section 3.3.

In BL 30 cell line cell cycle arrest was seen in G1 and G2M phase as loss of S phase of cell cycle but without significant apoptosis. In BL 31 and 41 cell lines there were no obvious cell cycle arrest but cells undergo apoptosis from all phases of cell cycle. Significant apoptosis was again seen when cells were treated with 5 mM VPA (figure 23).

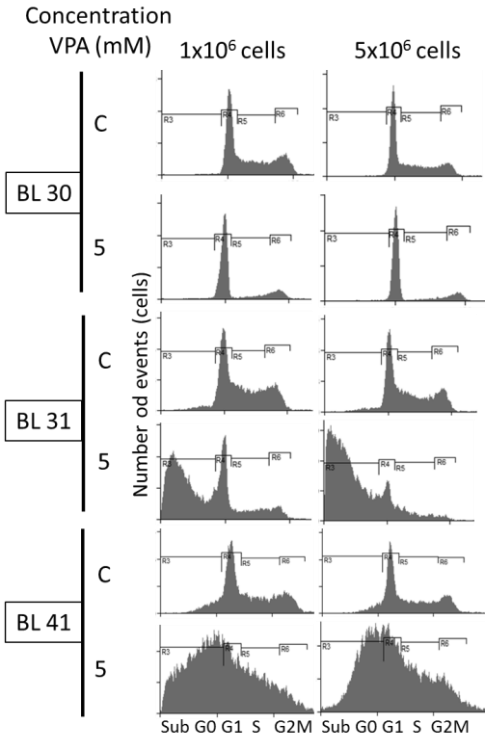

Figure 23: Cell cycle changes in BLs at different numbers of seeded cells. BLs were seeded at $1x10^6$, $3x10^6$ and $5x10^6$ cells and treated with 0.5 and 5 mM VPA for 24 hours. Example FACS pictures represent cell cycle profiles in control cells (C) and treated cells (5). Obtained profiles are comparable between different densities of seeded cells with the same concentration of VPA.

3.5. BLs early responses to VPA treatment

To elucidate early transcriptional responses of BLs to VPA treatment, a short-term experiment was conducted treating BLs in culture for 30, 60 and 120 min with 1 mM VPA. To address the question of how VPA affect levels of global histone acetylation in BLs Western Blotting analysis was performed. Furthermore, gene changes were identified by Microarray analysis.

Western Blotting analysis showed pronounced increase in acetylation levels of histones H3 and H4 in treated BL cell lines (BL 30, 31 and 41) with prolonged time. In untreated control BL cell lines (BL 30, 31 and 41) parallel increase in acetylation was observed, for reasons that are not clear (figure 24).

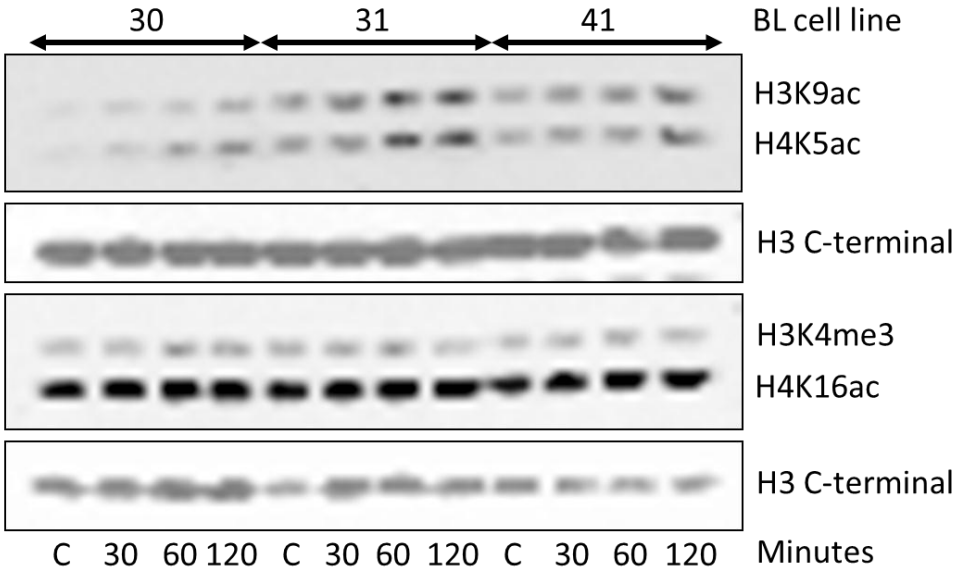

Figure 24: Western Blotting analysis of BLs. BLs (BL 30, 31 and 41) were treated for 30, 60 and 120 min with 1 mM VPA. Blots present acetylation levels of histones H3, H4 and H3 C-terminal tails in comparison to control untreated cells (C). With prolonged time acetylation levels are increasing seen as increased bulk in histones H3 and H4.

To identify which genes change in BLs upon VPA treatment we performed Microarray analysis and BLs were collected as described in section 2.2.2. The cDNA from control untreated and treated cells were hybridized to HX12 cDNA arrays. The intensities of probes hybridized with samples cDNA from control untreated and treated cells were compared (t-test).

On the slide there were 44,049 human target gene sequences and only 4091 (9.3%) in BL 30, 2044 (4.6%) in BL 31 and 1674 (3.8%) in BL 41 showed significant ($P<0.01$, 1.25-fold) changes, in total from all time points, in response to VPA. From all significant genes there were comparable numbers of up- and down- regulated genes, as there

were 2321 up regulated and 1779 down regulated genes in BL 30, 1163 up regulated and 884 down regulated genes in BL 31 and 539 up regulated and 1135 down regulated genes in BL 41 at all three time points (30, 60 and 120 min). Interestingly, only a very small number of genes were significantly changed in all three time points within the same cell line. In BL 30 only 35 genes (4091 total) were significantly changed in all three time points, in BL 31 only 7 (2044 total) and in BL 41 only 3 (1674 total) (figure 25).

Genes from all three BLs from each time point were independently analysed using DAVID bioinformatics software to perform gene ontology (GO). Enrichment analysis was performed for genes that exhibited above 1.25-fold change. The four most enriched gene classes are presented in table 2 below. GO analysis revealed no significant enrichment in ontology terms in BL 31 at 60 min. Interestingly anti-apoptosis, negative regulation of apoptosis and regulation of cell death were enriched in BL 30. In BL 31 the most interesting enriched GO terms were regulation of apoptosis and regulation of transcription and in BL 41 positive regulation of cell proliferation, negative regulation of protein kinase cascade and signal transduction.

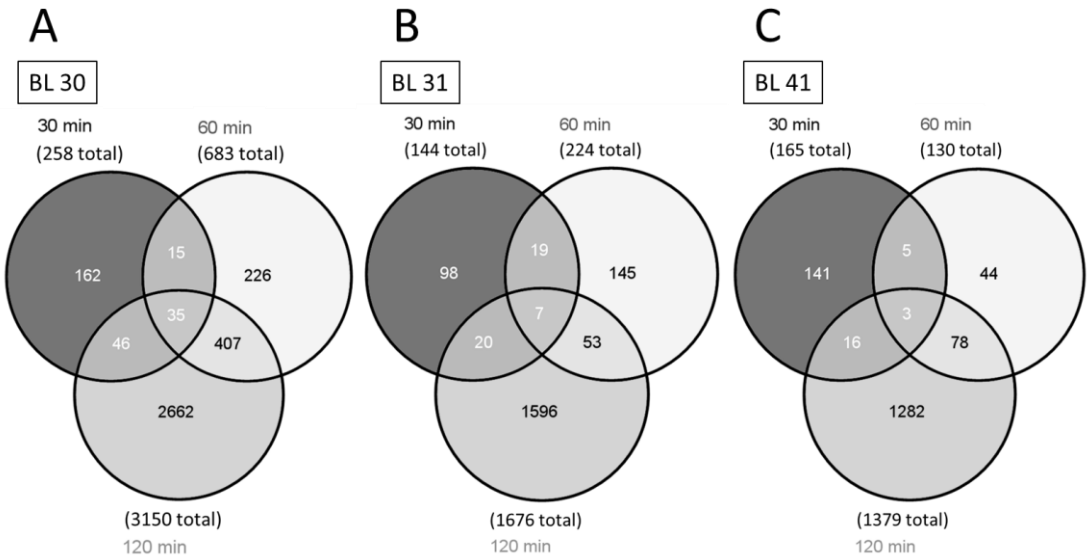

Figure 25: Venn diagram presenting numbers of significantly changed genes in BLs. Three cell lines of BLs were treated for 30, 60 and 120 min with 1 mM VPA. Genes transcription levels have changed significantly (P<0.01, 1.25-fold) upon VPA treatment detected by HX12 arrays (12 x 135,000 gene probes).

Table 2: Gene ontology for BL 30, 31 and 41. DAVID bioinformatics software was used to perform gene ontology (GO) analysing genes from all BLs. Enrichment analysis was performed for genes that exhibited above 1.25-fold change. The four most significantly enriched gene classes are presented each cell line. GO results revealed no significant enrichment in genes for BL 31 at 60 min (fold enrichment below 2) (denoted N/A). t30, t60 and t120 denote time points at 30, 60 and 120 min.

		Gene ontology term	Fold enrichment	P value
BL 30	t30	Immune response	2.41	3.30E-04
		Glicoprotein	1.14	0.20
		Disulfid bond	1.50	0.006
		Extracellular region path	2.41	3.30E-04
	t60	Anti-apoptosis	3.28	3.54E-05
		Negative regulation of apoptosis	2.55	7.26E-05
		Regulation of transcription	1.20	0.05
		Nucleus	1.16	0.04
	t120	Ion binding	1.17	2.22E-07
		Regulation of transcription	1.33	4.62E-08
		Anti-apoptosis	1.69	5.78E-04
		Regulation of cell death	1.25	0.004
BL 31	t30	Glycoprotein	1.70	6.50E-04
		Regulation of transcription	1.76	0.007
		Cell fate commitment	11.98	3.96E-06
		DNA binding	1.48	0.09
	t60	N/A	N/A	N/A
	t120	Regulation of apoptosis	1.54	1.28E-04
		DNA binding	1.37	3.04E-05
		Transcription	1.25	0.002
		Ion binding	1.08	0.06
BL 41	t30	Glycoprotein	1.90	9.85E-07
		Disulfid bond	2.13	5.63E-06
		Positive regulation of cell proliferation	3.70	6.98E-04
		Membrane	1.51	1.45E-04
	t60	Negative regulation of cell communication	6.81	4.48E-05
		Negative regulation of protein kinase cascade	15.66	0.01
		Negative regulation of signal transduction	6.80	1.55E-04
		Regulation of protein kinase cascade	3.01	0.14
	t120	Regulation of transcription	1.47	4.69E-10
		Negative regulation of gene expression	1.80	4.68E-05
		Transcription repressor activity	1.93	3.64E-04
		Zinc finger	1.56	3.70E-08

Additionally, we identified genes which showed changes in up regulation or down regulation by 1.25-fold in each time point. After 30 min of treatment only a small proportion of genes showed transcriptional changes (BL 30 - 258 genes, BL 31 - 144 genes and BL 41 - 165 genes). After 120 min of treatment the transcriptional change was more abundant (BL 30 - 3150 genes, BL 31 - 1676 genes and BL 41 - 1379 genes). In BL 30 and 31 there were more genes up regulated, whereas in BL 41 there were more genes down regulated. The maximal transcriptional changes were observed at the last time point (120 min) (figure 26).

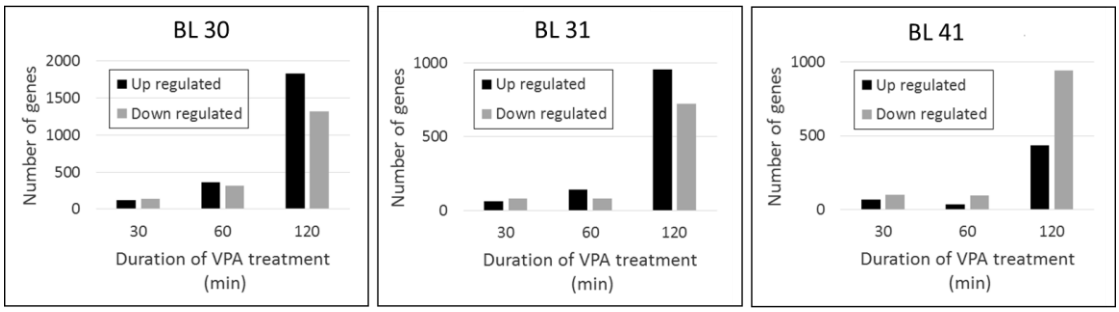

Figure 26: Changes in transcriptional levels in BLs. BLs were treated for 30, 60 and 120 min 1 mM VPA and transcriptional responses were analysed with HX12 arrays. The number of genes that were more than 1.25-fold up regulated or down regulated at each time point are presented.

Moreover, we combined data obtained from each time point from all three BL cell lines and analysed the results. Between all three cell lines (BL 30, 31 and 41) there were no genes significantly changed in all three cell lines at 30 min and only 4 genes at 60 min. Interestingly, there were 424 genes significantly changed at 120 min in all three BL cell lines (figure 27). These common genes at 120 min were significantly enriched for the ontology terms domain BTB (P=6.6E-4), zinc finger (P=2.3E-3), nucleus (P=6.8E-5) and regulation of transcription (P=2.6E-4).

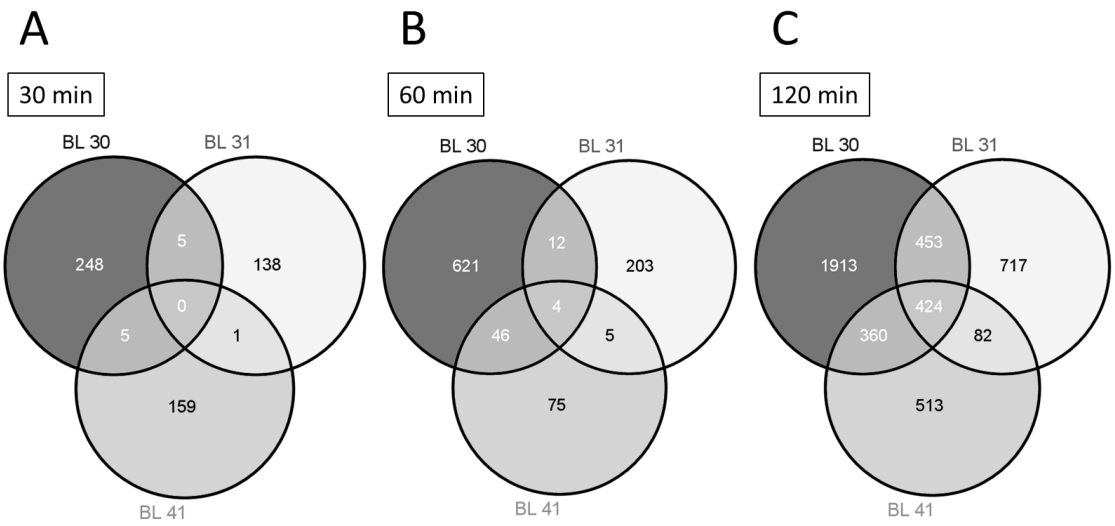

Figure 27: Venn diagram presenting numbers of significantly changed genes at each time point. BL 30, 31 and 41 data was combined and compared within time points. There were no significantly genes changed at 30 min and only 4 genes were significantly changed at 60 min. However, there were 424 genes significantly changes at 120 min.

Further analysis showed broadly similar number of significantly changed genes at 30 min between BL 30, 31 and 41. However, at 60 min there were increased number of significantly changed genes in BL 30 in comparison to BL 31 and 41 and similar at 120 min after treatment with VPA.

Furthermore, we combined all data obtained from all three cell lines BL 30, 31 and 41 and identified 444 genes (7809 total) being significantly changed in all three cell lines at 30, 60 and 120 min combined (figure 29). The common genes across all three BL cell lines were analysed using DAVID bioinformatics software to perform gene ontology (GO). Enrichment analysis was performed for genes that exhibited above 1.25-fold change. When comparing all 444 BLs common genes gene ontology terms appeared: Kelch (P=0.001), transcription (P=0.003), immune response (P=0.04), prostate cancer (P=0.02), small cell lung cancer (P=0.18), p53 signalling pathway (P=0.03) and apoptosis (P=0.01) (table 3).

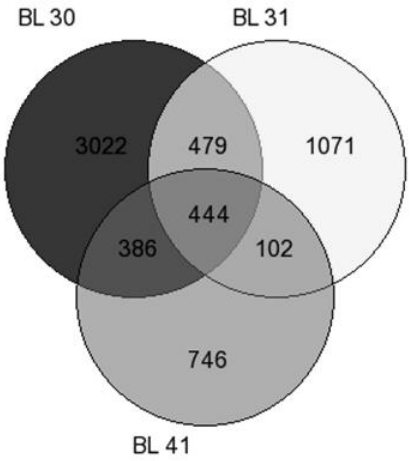

Figure 28: Significantly changed genes in all BL cell lines in all time points. There were 444 genes (7809 total) significantly changed in all three BL cell lines at 30, 60 and 120 min.

Table 3: BLs gene ontology. DAVID bioinformatics software was used to perform gene ontology (GO) analysing genes from 444 BLs common genes across all three BLs. Enrichment analysis was performed for genes that exhibited above 1.25-fold change. The seven most significantly enriched gene classes are presented.

Gene ontology term	Fold enrichement	P value
Kelch	2.69	0.001
Transcription	2.55	0.003
Immune response	2.40	0.04
Apoptosis	2.12	0.01
Prostate cancer	6.59	0.02
Small cell lung cancer	4.65	0.18
P53 signaling pathway	7.19	0.03

3.6. Gene comparison of LCLs to BL 30, 31 and 41

To evaluate gene changes in response to VPA treatment in normal and cancer cells, short-term gene expression changes in LCLs, determined previously in our lab using the same expression array set up (Halsall, unpublished data) were compared to BLs. There were 942 common genes between LCLs and BL 30, 471 common genes between LCLs and BL 31 and 532 common genes between LCLs and BL 41. All common genes between all four cell types were 243 (figure 29).

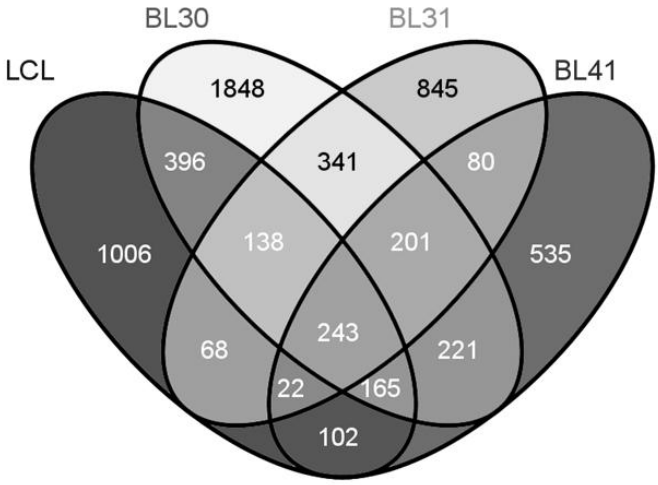

Figure 29: LCLs vs. BLs gene comparison. LCLs were compared to BLs to evaluate gene changes. There were 243 common genes between all four cell types.

4. Discussion

The aim of this thesis was to evaluate the effects of the HDAC inhibitor VPA on normal and cancer cells by identifying changes in cell cycles, global histone acetylation and changes in gene expression.

Even with the increased knowledge of cancer hallmarks and advances in therapy regimes treatment of cancer is still challenging (Baskar et al., 2012). Conventional chemotherapeutics are usually toxic to normal cells which is hazardous to the patients, causing mild to severe side effects (Peedicayil, 2006). Therefore, even more advanced therapies need to be discovered and one of the promising therapies is the epigenetic therapy with HDACi (Mai and Altucci, 2009). HDACi have been used as anti-epileptics since anti-convulsant effects were observed in 1963 (Chateauvieux et al., 2010) and more recently are also used as anti-cancer therapy (Cortez and Jones, 2008). Before specific HDACi become available as chemotherapeutic agent benefits and side effects have to be studied and the effects on cancer and normal cells must be identified and compared.

Results presented in this thesis showed that LCLs as well as BLs cell cycles were affected by VPA treatment. In LCLs there was no significant apoptosis observed whereas in two BL cell lines substantial apoptosis was observed. Furthermore, LCLs changed morphologically after day 5 of treatment, confirmed in two experiments where the onset was observed at the same day. Histone acetylation levels were increased in treatment groups of both cell types and GO showed enrichment of transcripts of genes involved in cell cycle and cell adhesion possible explaining regulation of cell cycle and changes in cell morphology in treated LCLs whereas, enrichment in apoptosis and regulation of transcription possible explaining substantial death and increase in acetylation levels in the treated BLs. Moreover, results showed that VPA selectively causes cell death of *some* BLs independent to cell density. These results showed a great potential of VPA to be used as chemotherapeutic agent as it induces cell death in cancer cells but not in normal cells and it works independent to

cell density suggesting that it could be used in treatment of solid tumours and hematopoietic cancers.

The first two questions we addressed in this project was whether VPA treatment affects LCLs cell cycle, histone acetylation levels and cell morphology in 7 and 14 days of treatment alongside analysing gene expression of cells treated for 14 days. Our results obtained by flow cytometry from both experiments showed cell cycle arrest at the G1/S and G2M boundaries, which confirms observations of cell cycle arrest by Carew (Carew et al., 2008). Minimal apoptosis was observed when LCLs were treated with VPA (figure 14) which confirms Quintás-Cardama findings that HDACi do not induce apoptosis in normal cells (Quintás-Cardama et al., 2011). This suggests that VPA might be a cell cycle specific chemotherapeutic agent as it induces cell cycle blocks at two boundaries. The minimal apoptosis might suggest that cells undergo senescence due to the treatment but do not undergo apoptosis. From the LCLs growth curve it was clear that treated LCLs grow slower in comparison to the control untreated group (figure 17) what may be due to cell cycle blocks and therefore, fewer cells were cycling. In addition to these findings LCLs changed morphologically from round shape to spiky with prolonged treatment suggesting that this might be due to differentiation or hyperacetylation of actin fibres. It has been previously shown that VPA increases acetylation levels (Nightingale et al., 2007). Our results confirmed increase in histone acetylation levels in treated LCLs due to inhibition of HDACs. However, the increased in acetylation levels was observed in untreated control cells as well, for reasons that are not clear. Gene ontology (GO) results suggest that amongst genes whose expression changed after VPA treatment, the most enriched GO terms were related to cell cycle as this GO term appeared at day 4, 7 and 14. Also at day 4 we observed enrichment in GO terms for cell adhesion and cytoskeleton which may explain morphological changes and is consistent with the observed morphological changes after day 5. These changes may also be a consequence of hyper-acetylation of non-histone proteins by HDACi influencing on cytoskeletal molecules altering cell morphology.

LCLs survived in long-term experiment treated with 1 mM VPA. However, 24 hour experiment with BLs with different concentrations of VPA revealed BLs undergo apoptosis much faster than LCLs and therefore a long-term experiment was not conducted. Instead, a short term experiment was conducted.

The next question to address was whether VPA treatment affects BLs cell cycle when treated for 24 hours. The obtained results presented this thesis showed clear evidence of cell cycle arrest at G1/S and G2M boundaries in BL 30 cell line with substantial apoptosis in BL 31 and 41 cell lines without clear cell cycle arrest suggesting that cells undergo apoptosis from all phases of cell cycle (figure 22). The results confirm findings from other research groups which show that HDACi induce cell cycle arrest (Carew et al., 2008, Shan et al., 2012). This might suggest that VPA is a cell cycle specific chemotherapeutic agent and that due to restoring of normal expression levels of tumour suppressor genes and potential activation of pro-apoptotic genes cells undergo substantial apoptosis. Both of these findings have been observed before when cancer cells were treated with HDACi (Bannister and Kouzarides, 2011, Quintás-Cardama et al., 2011).

Furthermore, to confirm that substantial apoptosis in BLs is not due to high cell density of cells in culture. The experiment was conducted showing that cell density does not affects the VPA effects again observing cell cycle arrest at G1/S and G2M boundaries in BL 30 cell line and substantial apoptosis in BL 31 and 41 cell lines without clear cell cycle arrest independent of cell density (figure 23). This suggests that VPA would potentially still be cytotoxic to cancer cells in tumours with high density of cancer cells, at initial formation of tumours and in hematopoietic cancers.

The last question to address in this project was whether VPA treatment affects BLs histone acetylation levels and gene expression levels when treated for 30, 60 and 120 min. In BLs the increased hyperacetylation was even more evident than in LCLs as it has increased significantly with prolonged time (figure 24) confirming the results obtained from Halsall et al. and Yi et al. (Halsall et al., 2012, Yi et al., 2013). However,

in untreated control BL cell lines (BL 30, 31 and 41) parallel increase in acetylation was observed, for reasons that are not clear.

GO results revealed differences when comparing enriched GO terms of LCLs and BLs in short-term experiments. In LCLs short-term experiment the earliest response was seen as enrichment in GO terms of LCLs at 30 min where terms related to regulation of apoptosis following by transcription and positive regulation of gene expression at 60 min and transcription, zinc finger and Kelch genes at 120 min were enriched (data not shown) (Halsall, unpublished data). However, in BL 30, in which cell cycle response strongly resembled LCLs, enrichment in GO terms related to regulation of apoptosis and anti-apoptosis, suggesting that BL 30 cell line might be more resilient to VPA treatment. Moreover, BL 30 strongly relates to LCLs in transcriptional response as when comparing the responding genes results of BL 30 cell line and LCLs, BL 30 had the biggest proportion of common genes with LCLs compared to BL 31 and 41. Also, the increased number of changed genes in BL 30, in comparison to BL 31 and 41, suggests that BL 30 had stronger transcriptional response to VPA. In BL 31 and BL 41 cell lines GO terms including genes for transcription and regulation of transcription were enriched suggesting that transcription was increased which was already suggested by Marks and Xu (Marks and Xu, 2009). When GO analysis was performed for all three BL cell lines combined GO terms apoptosis, transcription and immune response were increased again confirming findings by other research groups. Furthermore, GO terms prostate cancer, small cell lung cancer and p53 signalling pathway were enriched suggesting that VPA might be affecting tumour signalling pathways what was already observed in treatment with HDACi (Quintás-Cardama et al., 2011). The combined GO results for all three BLs suggests that VPA affects malignant cells by tumour signalling pathways as this was not observed in LCLs.

The limitations of this project could be the use of only one LCL cell line and a comparison to LCL cell lines from different donors would be welcome. Furthermore, this work was conducted as *in-vitro* experiments but experiments could be also conducted *in-vivo*.

However, the results presented in this thesis are very strong and convincing as results were obtained from data including three biological replicates which correlated well for each sample. Besides, all data was highly comparable between cell lines as all cell lines were B cell derived. Moreover, all our microarray slides were checked to have complete coverage.

Additionally to circumventing the limitations of this project, results have to be confirmed. Therefore, gene primers should be designed and real-time PCR should be performed to confirm the expression changes seen by microarray. Furthermore, experiments to investigate whether LCLs are really differentiating due to the VPA treatment could be conducted. This may be done by examining differentiating cell marker expression changes etc. which should be investigated. Moreover, as cell cycle arrest was observed at two boundaries it would be interesting to investigate whether LCLs would enter a cell cycle again once VPA treatment would finish. As some studies suggested that HDACi effects on correcting epigenetic defects could be reversible after the end of treatment (Peedicayil, 2006) this could be further investigated in BLs experiment with longer treatment period with subsequent withdrawal of VPA to assess acetylation levels and changes in gene expression levels. As cell cycle specific chemotherapeutic agents usually only work on cycling cells it would be interesting to investigate what would happen if cancer cells would achieve a plateau phase prior to VPA treatment as this is sometimes seen in solid tumours when discovered in a late stages. Would VPA still induce as high apoptosis as seen in this project? To obtain gene networks affected by VPA further data analysis is of high importance to obtain targets affected by VPA. Also, further experiments could be conducted using other types of cancers, e.g. T cell derived cancers which could be compared to T cell clones as a model for normal human cells. Furthermore, these results could be compared to results from SAHA treatment to assess the mean of action of different HDACi as SAHA is already used for treatment of T cell malignancies.

Results of this thesis showed that both LCLs and BLs experience a cell cycle arrest with cell death observed in BLs which was independent of cell density. LCLs also showed changes in cell morphology in response to VPA treatment. In all VPA treated cells histone acetylation levels were increased. One of the most important findings of this project was that normal cells do not undergo apoptosis when treated with VPA and are therefore more resilient to VPA, whereas some cancer cells do. This suggests that VPA is not as toxic to normal cells as other chemotherapeutic agents and this may lead to the conclusion that VPA is a promising candidate for advanced epigenetic chemotherapy.

References

ALTSCHUL, S. F., GISH, W., MILLER, W., MYERS, E. W. & LIPMAN, D. J. 1990. Basic local alignment search tool. *J Mol Biol,* 215**,** 403-10.

BACHMANN, N. & BERGMANN, C. 2012. Epigenetics and imprinting. *Arch Pediatr,* 19**,** 1145-7.

BAI, L. & MOROZOV, A. V. 2010. Gene regulation by nucleosome positioning. *Trends Genet,* 26**,** 476-83.

BANNISTER, A. J. & KOUZARIDES, T. 2011. Regulation of chromatin by histone modifications. *Cell Res,* 21**,** 381-95.

BASKAR, R., LEE, K. A., YEO, R. & YEOH, K. W. 2012. Cancer and radiation therapy: current advances and future directions. *Int J Med Sci,* 9**,** 193-9.

BAYLIN, S. B. & SCHUEBEL, K. E. 2007. Genomic biology: the epigenomic era opens. *Nature,* 448**,** 548-9.

BIALER, M. 2012. Why are antiepileptic drugs used for nonepileptic conditions? *Epilepsia,* 53 Suppl 7**,** 26-33.

BLAHETA, R. A., MICHAELIS, M., DRIEVER, P. H. & CINATL, J. 2005. Evolving anticancer drug valproic acid: insights into the mechanism and clinical studies. *Med Res Rev,* 25**,** 383-97.

BOVERI, T. 1914. Zur Frage der Entstehung maligner Tumoren. *G. Fischer*.

CAREW, J. S., GILES, F. J. & NAWROCKI, S. T. 2008. Histone deacetylase inhibitors: mechanisms of cell death and promise in combination cancer therapy. *Cancer Lett,* 269**,** 7-17.

CHATEAUVIEUX, S., MORCEAU, F., DICATO, M. & DIEDERICH, M. 2010. Molecular and therapeutic potential and toxicity of valproic acid. *J Biomed Biotechnol,* 2010.

CLINICALTRIALS.GOV. 2013. *Histone deacetylase inhibitors and cancer* [Online]. U.S. National Institutes of Health. Available: http://clinicaltrials.gov/ct2/results/map?term=histone+deacetylase+inhibitors+and+cancer [Accessed 18.07. 2013].

CORTEZ, C. C. & JONES, P. A. 2008. Chromatin, cancer and drug therapies. *Mutat Res,* 647**,** 44-51.

DUVIC, M. & VU, J. 2007. Update on the treatment of cutaneous T-cell lymphoma (CTCL): Focus on vorinostat. *Biologics,* 1**,** 377-92.

GHAI, V., SHARMA, K., ABBI, K. K., SHIMKO, S. & EPNER, E. M. 2013. Current approaches to epigenetic therapy for the treatment of mantle cell lymphoma. *Adv Exp Med Biol,* 779**,** 257-66.

GLASER, K. B. 2007. HDAC inhibitors: clinical update and mechanism-based potential. *Biochem Pharmacol,* 74**,** 659-71.

HALSALL, J., GUPTA, V., O'NEILL, L. P., TURNER, B. M. & NIGHTINGALE, K. P. 2012. Genes are often sheltered from the global histone hyperacetylation induced by HDAC inhibitors. *PLoS One,* 7**,** e33453.

HEITZ, E. 1929. Heterochromatin, chromocentren, chromomeren. *Berichte der Deutschen Botanischen Gesellschaft***,** 274-284.

HUANG, D. W., SHERMAN, B. T. & LEMPICKI, R. A. 2009a. Bioinformatics enrichment tools: paths toward the comprehensive functional analysis of large gene lists. *Nucleic Acids Res,* 37**,** 1-13.

HUANG, D. W., SHERMAN, B. T. & LEMPICKI, R. A. 2009b. Systematic and integrative analysis of large gene lists using DAVID bioinformatics resources. *Nat Protoc,* 4**,** 44-57.

HUIDOBRO, C., FERNANDEZ, A. F. & FRAGA, M. F. 2013. The role of genetics in the establishment and maintenance of the epigenome. *Cell Mol Life Sci,* 70**,** 1543-73.

HÜBNER, M. R., ECKERSLEY-MASLIN, M. A. & SPECTOR, D. L. 2013. Chromatin organization and transcriptional regulation. *Curr Opin Genet Dev,* 23**,** 89-95.

INCHE, A. G. & LA THANGUE, N. B. 2006. Chromatin control and cancer-drug discovery: realizing the promise. *Drug Discov Today,* 11**,** 97-109.

JAENISCH, R. & BIRD, A. 2003. Epigenetic regulation of gene expression: how the genome integrates intrinsic and environmental signals. *Nat Genet,* 33 Suppl**,** 245-54.

JEMAL, A., BRAY, F., CENTER, M. M., FERLAY, J., WARD, E. & FORMAN, D. 2011. Global cancer statistics. *CA Cancer J Clin,* 61**,** 69-90.

JENUWEIN, T. & ALLIS, C. D. 2001. Translating the histone code. *Science,* 293**,** 1074-80.

JIANG, C. & PUGH, B. F. 2009. Nucleosome positioning and gene regulation: advances through genomics. *Nat Rev Genet,* 10**,** 161-72.

KUMAR, R., HORIKOSHI, N., SINGH, M., GUPTA, A., MISRA, H. S., ALBUQUERQUE, K., HUNT, C. R. & PANDITA, T. K. 2012. Chromatin modifications and the DNA damage response to ionizing radiation. *Front Oncol,* 2**,** 214.

LUGER, K., MÄDER, A. W., RICHMOND, R. K., SARGENT, D. F. & RICHMOND, T. J. 1997. Crystal structure of the nucleosome core particle at 2.8 A resolution. *Nature,* 389**,** 251-60.

MAI, A. & ALTUCCI, L. 2009. Epi-drugs to fight cancer: from chemistry to cancer treatment, the road ahead. *Int J Biochem Cell Biol,* 41**,** 199-213.

MANN, B. S., JOHNSON, J. R., COHEN, M. H., JUSTICE, R. & PAZDUR, R. 2007. FDA approval summary: vorinostat for treatment of advanced primary cutaneous T-cell lymphoma. *Oncologist,* 12**,** 1247-52.

MARKS, P. A. & XU, W. S. 2009. Histone deacetylase inhibitors: Potential in cancer therapy. *J Cell Biochem,* 107**,** 600-8.

MOLYNEUX, E. M., ROCHFORD, R., GRIFFIN, B., NEWTON, R., JACKSON, G., MENON, G., HARRISON, C. J., ISRAELS, T. & BAILEY, S. 2012. Burkitt's lymphoma. *Lancet,* 379**,** 1234-44.

MURRAY, K. 1964. The occurrence of epsilon-N-methyl lysine in histones. *Biochemistry,* 3**,** 10-5.

NAKAO, M. 2001. Epigenetics: interaction of DNA methylation and chromatin. *Gene,* 278**,** 25-31.

NGALAMIKA, O., ZHANG, Y., YIN, H., ZHAO, M., GERSHWIN, M. E. & LU, Q. 2012. Epigenetics, autoimmunity and hematologic malignancies: a comprehensive review. *J Autoimmun,* 39**,** 451-65.

NIGHTINGALE, K. P., GENDREIZIG, S., WHITE, D. A., BRADBURY, C., HOLLFELDER, F. & TURNER, B. M. 2007. Cross-talk between histone modifications in response to histone deacetylase inhibitors: MLL4 links histone H3 acetylation and histone H3K4 methylation. *J Biol Chem,* 282**,** 4408-16.

NIGHTINGALE, K. P., O'NEILL, L. P. & TURNER, B. M. 2006. Histone modifications: signalling receptors and potential elements of a heritable epigenetic code. *Curr Opin Genet Dev,* 16**,** 125-36.

PEEDICAYIL, J. 2006. Epigenetic therapy--a new development in pharmacology. *Indian J Med Res,* 123**,** 17-24.

PHILLIPS, D. M. 1963. The presence of acetyl groups of histones. *Biochem J,* 87**,** 258-63.

QUINTÁS-CARDAMA, A., SANTOS, F. P. & GARCIA-MANERO, G. 2011. Histone deacetylase inhibitors for the treatment of myelodysplastic syndrome and acute myeloid leukemia. *Leukemia,* 25**,** 226-35.

ROOPRA, A., DINGLEDINE, R. & HSIEH, J. 2012. Epigenetics and epilepsy. *Epilepsia,* 53 Suppl 9**,** 2-10.

ROZEN, S. & SKALETSKY, H. 2000. Primer3 on the WWW for general users and for biologist programmers. *Methods Mol Biol,* 132**,** 365-86.

SHAN, Z., FENG-NIAN, R., JIE, G. & TING, Z. 2012. Effects of valproic acid on proliferation, apoptosis, angiogenesis and metastasis of ovarian cancer in vitro and in vivo. *Asian Pac J Cancer Prev,* 13**,** 3977-82.

STERNER, D. E. & BERGER, S. L. 2000. Acetylation of histones and transcription-related factors. *Microbiol Mol Biol Rev,* 64**,** 435-59.

TABISH, H. & MULHERKAR, R. 2012. Lymphoblastoid cell lines: a continuous in vitro source of cells to study carcinogen sensitivity and DNA repair *Int J Mo1 Cell,* 1**,** 75-87.

TANG, J., YAN, H. & ZHUANG, S. 2013. Histone deacetylases as targets for treatment of multiple diseases. *Clin Sci (Lond),* 124**,** 651-62.

TURNER, B. M. 1993. Decoding the nucleosome. *Cell,* 75**,** 5-8.

TURNER, B. M., BIRLEY, A. J. & LAVENDER, J. 1992. Histone H4 isoforms acetylated at specific lysine residues define individual chromosomes and chromatin domains in Drosophila polytene nuclei. *Cell,* 69**,** 375-84.

TÓTH, K., BÖHM, V., SELLMANN, C., DANNER, M., HANNE, J., BERG, M., BARZ, I., GANSEN, A. & LANGOWSKI, J. 2013. Histone- and DNA sequence-dependent stability of nucleosomes studied by single-pair FRET. *Cytometry A*.

WEITZMAN, J. 2012. Epigenetics in health and disease. *Joint Bone Spine,* 79**,** 565.

YE, J., COULOURIS, G., ZARETSKAYA, I., CUTCUTACHE, I., ROZEN, S. & MADDEN, T. L. 2012. Primer-BLAST: a tool to design target-specific primers for polymerase chain reaction. *BMC Bioinformatics,* 13**,** 134.

YI, J., ZHANG, L., TANG, B., HAN, W., ZHOU, Y., CHEN, Z., JIA, D. & JIANG, H. 2013. Sodium valproate alleviates neurodegeneration in SCA3/MJD via suppressing apoptosis and rescuing the hypoacetylation levels of histone H3 and H4. *PLoS One,* 8**,** e54792.

ZENTNER, G. E. & HENIKOFF, S. 2013. Regulation of nucleosome dynamics by histone modifications. *Nat Struct Mol Biol,* 20**,** 259-66.

ZHANG, C., RICHON, V., NI, X., TALPUR, R. & DUVIC, M. 2005. Selective induction of apoptosis by histone deacetylase inhibitor SAHA in cutaneous T-cell lymphoma cells: relevance to mechanism of therapeutic action. *J Invest Dermatol,* 125**,** 1045-52.